A Comprehensive Method and System for the Design and Deployment of Wireless Data Networks

Roger R. Skidmore

Dissertation submitted to the Faculty of the
Virginia Polytechnic Institute and State University
in partial fulfillment of the requirements for the degree of

Doctor of Philosophy
in
Electrical Engineering

Dr. Theodore S. Rappaport, Co-Chair
Dr. Leonard R. Ferrari, Co-Chair
Dr. Brian D. Woerner
Dr. A. Lynn Abbott
Dr. Naren Ramakrishnan

April 25, 2003
Blacksburg, Virginia

Keywords: Wireless, Radiowave, Propagation, Networks

A Comprehensive Method and System for the Design and Deployment of Wireless Data Networks

Roger R. Skidmore

Co-Chairs: Dr. Theodore S. Rappaport *, Dr. Leonard R. Ferrari
Dr. Brian D. Woerner, Dr. A. Lynn Abbott, Dr. Naren Ramakrishnan

The Bradley Department of Electrical Engineering, University of Virginia Tech
* *University of Texas, Austin*

Increasingly, wireless subscribers are demanding reliable data capabilities from wireless networks. The ability of wireless network engineers and Information Technology (IT) professionals to rapidly design, deploy, and maintain wireless communication systems that can provide strong, reliable data service is severely hampered by a lack of adequate systems and methods for simulating the performance of such networks a priori. Unlike older generation wireless systems that could be readily deployed on the basis of strong received signal strength and simple circuit-switched channel allocation protocols, modern and emerging wireless data networks are more noise and interference limited and rely on packet-based protocols. A heavier emphasis is needed on predicting and simulating throughput, bit error rate, frame error rate, user priority classes, and overall network capacity. This research provides wireless network engineers and IT professionals with a comprehensive system and method for the simulation and design of wireless communication systems that combines site-specific databases, equipment-specific distribution system modeling, and advanced ray tracing propagation analysis to directly predict throughput, frame error rate (FER), and other critical performance parameters for emerging wireless data networks.

Acknowledgements

The work presented herein was made possible by the personal contributions of a variety of individuals to whom I am greatly indebted. Dr. Ted Rappaport has been an excellent advisor and a good friend throughout this effort. Without his advice and support, this project would never have succeeded. His high expectations have shown me exactly what I am capable of doing when I set my mind to it. I will also be forever indebted to all of the faculty and staff of the Mobile and Portable Radio Research Group (MPRG) at Virginia Tech.

My committee members, Dr. Ferrari, Dr. Abbott, Dr. Woerner, and Dr. Ramakrishnan, have shown great patience in working with me as I have been absent from Blacksburg for much of this work. They have always kept an open door and a smile to greet me, and their insight and guidance has proven of great benefit to my research. Many, many thanks to each of you!

I would also like to extend my sincere gratitude to John Rocovich, the Bradley Fellowship, and the Virginia Tech Board of Visitors for supporting the Wireless Valley Industrial Scholars Fellowship. My participation in the Wireless Valley Industrial Scholars Fellowship program enabled me to pursue this research while working and building Wireless Valley Communications. All the work contained herein was accomplished at Wireless Valley Communications, Inc. To all of my co-workers at Wireless Valley, thank for your belief in me and support of my work. Your enthusiasm has kept me going through more than one late night.

To the love of my life, Susan, thank you so much for your love and patience. My mother and father have always stood behind me and supported me. Thank you both so very much! Finally, to my Lord and Savior, Jesus Christ, I reserve the highest of all praise, in whose life I find purpose and the strength to carry on.

Contents

List of Figures

List of Tables

Chapter 1

Introduction

1.1 Overview

Portable, wireless communication devices are proliferating throughout the world. As of the year 2003, over 150 million people in the United States use a wireless communication device, and the use of portable wireless communications devices is growing at 20 percent per year [182, 50]. Widespread access to the Internet has provided the average consumer with the ability to access information and communicate using data in ways previously impossible. The proliferation of wireless communication devices has brought with it a desire to access the Internet and exchange data wirelessly [141]. Recently, the demand for wireless data services has risen dramatically, and the number of wireless local area networks (WLANs) being deployed in the United States and around the world will increase substantially over the next several years [50, 150].

In short, the quantity of wireless communication systems being designed and deployed worldwide is rising substantially. However, existing techniques used to design and deploy wireless communication systems are insufficient for the latest and emerging wireless technologies. Unfortunately, many indoor wireless networks today are designed using trial-and-error techniques that are time consuming and lead to over-engineered, costly networks [141]. Most indoor building environments do not have readily available maps that can be used for site-specific wireless network design as are common for outdoor environments. For outdoor

wireless network design, the availability of and access to highly detailed information regarding the physical environment has dramatically improved over the past several years. Site-specific information, and particularly satellite imagery, has reached remarkable levels of detail and resolution. However, most outdoor wireless network design applications still rely on predictive techniques and site-specific database technology that pre-date emerging wireless standards by more than a decade [141]. The research presented in this thesis proposes new techniques which better model the performance of wireless data communication systems. These new techniques utilize site-specific environmental information, efficient predictive algorithms that demonstrate improved accuracy over prior techniques, and are fully capable of representing the performance of the latest wireless data technologies.

The research presented in this thesis was performed at and is owned by Wireless Valley Communications, Inc. The research herein was made possible by support from the Wireless Valley Industrial Scholars Fellowship program, which allowed students at Virginia Tech who also worked full-time in industry to pursue advanced degrees while doing research off-campus. Research presented in [165], which was kept unpublished for a period of three years beginning in 1997, is dramatically expanded upon by this thesis. The genesis of this work, presented in [165], was exclusively licensed from Virginia Tech and Virginia Tech Intellectual Properties, augmented with new inventions, and commercialized in subsequent years by Wireless Valley Communications, Inc. As of early 2003, over 200 companies world-wide have licensed Wireless Valley software. The research presented in this thesis describes the novel approaches of a new class of design, measurement, optimization, and management software applications. This research is a subset of a much larger body of intellectual property owned by Wireless Valley Communications, Inc. More than 30 patents are pending in the United States and internationally, in part due to the research presented in this thesis. As of April 2003, four patents, [167], [142], [143], and [144], have been awarded to Wireless Valley.

One of the key results of this research is the development of computer aided design (CAD) methods that allow for the rapid, repeatable design, simulation, and installation of wireless networks inside and around buildings. This research is the first to allow multi-user network design based on the ability to determine expected throughput, bit error rate (BER), packet error rate (PER), and/or frame error rate (FER) using site-specific databases of the physical environment and modern propagation prediction techniques. The specific protocol details of wireless standards are accounted for, as such details directly relate to the performance of a

wireless system in different environments and under various conditions.

This research includes the study of new techniques for representing and manipulating the physical environment in a site-specific computer model that combines both indoor and outdoor locales. Advanced radio wave propagation models and post-processing mechanisms are analyzed in detail, and novel techniques for predicting radio wave propagation are presented. In addition, specific combinations of equipment types, placements, interconnections, and configurations that can directly influence the performance, design, and cost of a network are also accounted for in this research. By combining radio wave propagation and the particulars of the wireless network distribution system within a highly detailed site-specific model of the environment, this research discloses techniques for determining the throughput, bit error rate, packet error rate, and/or frame error rate for any wireless data network.

Presented in Chapter 1 are fundamental, background details that must be thoroughly understood and appreciated in order to develop the desired methods and techniques. A novel method for generating site-specific computer models of any environment is proposed in Chapter 2. Advanced ray tracing techniques, including a novel data analysis technique, are described in Chapter 3. A novel technique for the automatic determination of equipment position and configuration in and around buildings is presented in Chapter 4. Finally, methods for correlating received signal strength intensity (RSSI), signal-to-interference ratio (SIR), signal-to-noise ratio (SNR), delay spread, mobile receiver velocity, total propagation distance, and/or other parameters with throughput, bit error rate, packet error rate, and/or frame error rate are introduced in Chapter 5.

1.2 Wireless Technologies

Wireless communication technology has progressed greatly over the past twenty years. The first wireless phone networks, or *cellular networks*, began to appear in the early 1980s. These analog wireless networks used frequency-separated channels to carry voice conversations, and, by modern standards, were very spectrally inefficient [15, 141]. Large towers or tall building rooftops were the primary locations for equipment placement in order to provide coverage. The Advanced Mobile Phone System (AMPS) wireless standard deployed within the United States is exemplary of the *First Generation* wireless communication networks.

The design constraints associated with the deployment of first generation wireless phone networks generally revolved around issues of coverage. Issues of capacity were also critical, but tended to take second priority to the initial problem of guaranteeing a certain level of received signal strength intensity (RSSI) by a mobile user.

Beginning in the early and mid-1990s, digital cellular and personal communication system (PCS) networks began to appear. These *Second Generation* networks are generally characterized by digital technology that provided improved spectral efficiency, improved interference rejection, superior quality, and higher data rates compared to first generation networks due to their reliance on digital technology. Such digital networks rely upon either Time Division Multiple Access (TDMA) or Code Division Multiple Access (CDMA) techniques. The Global System Mobile (GSM) and IS-95a CDMA standards are exemplary of such second generation networks (commonly referred to as *2G* technologies). The design constraints associated with second generation system deployments are more complex due to the more advanced system architecture, larger number of competing service providers, and increased subscriber base. The principal design issue remained guaranteeing a certain level of RSSI and capacity, but was complicated by issues of interference. These *2G* networks provided improved capacity compared to earlier technologies, and the (typically) higher frequencies led to decreased coverage areas and many more, smaller tower and building sites.

The deployment of *Third Generation* wireless systems has been delayed due to the worldwide economic recession in the telecommunications industry beginning in 2001. This has resulted in the appearance of interim technologies and systems. These interim technologies provide limited data transfer capabilities, such as text messaging, and provide service providers with an upgrade path to true third generation systems. Such networks, typically referred to as *2.5 Generation*, or *2.5G*, systems, are exemplified by the General Packet Radio Services (GPRS), and Enhanced Data rates for Global Evolution (EDGE) standards, which are seeing widespread success in Europe. In the United States, both AT&T Wireless and Cingular announced in 2003 their decision to upgrade their networks to GSM, GPRS, and EDGE.

Whereas the goal of second generation technologies was to provide cellular subscribers with a higher degree of satisfaction in the voice quality of their conversations relative to the first generation networks, the goal of *Third Generation* technologies is to provide subscribers with the ability to send and receive data in addition to basic voice information. Wideband

CDMA (W-CDMA) and CDMA2000 are exemplary of third generation network technologies beginning deployment today. In many instances, EDGE, listed above as a 2.5G technology, is referred to as a 3G technology as well.

Figure 1.1 provides a diagram showing the relationships between various cellular and PCS wireless communication system technologies, and the paths enabling transitions between the different generations of wireless phone technologies. Note that 2G wireless systems provide user data rates of less than 65 kbps, whereas 3G wireless systems promise 2 Mbps.

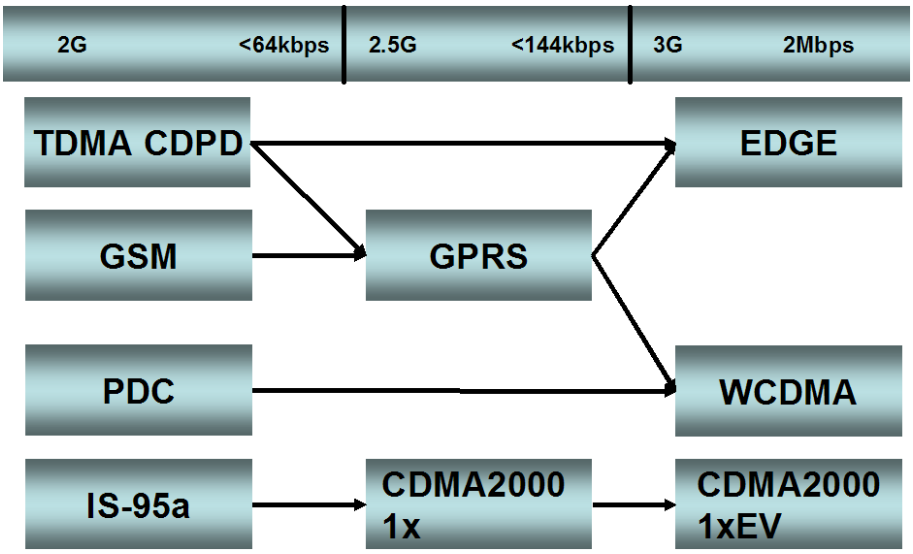

Figure 1.1: Typical migration paths from (left to right) of several second generation (2G) wireless technologies to third generation (3G) wireless technologies. Per user data rates for each technology are also given.

The explosive growth of the Internet and World Wide Web has provided people throughout the world with access to vast amounts of information. This has led to a desire to access information such as e-mail wirelessly. As a result, the emerging third generation technologies are focused on the ability to send and receive data quickly while supporting a large number of simultaneous users. Typically, the average subscriber requires high data rates when inside buildings, such as when sitting at a desk. Thus, the need to provide reliable access to wireless data communication networks not only around, but also inside of buildings is critical to the success of emerging wireless data technologies.

In contrast with cellular, PCS, and other wireless voice technologies that historically targeted mobile users in their cars or out of doors, wireless local area network (WLAN) technologies have emerged that primarily target providing wireless data services to users inside buildings. Recently, the IEEE 802.11a and IEEE 802.11b WLAN standards were adopted, with the IEEE 802.11g WLAN standard soon to follow [141]. This has led to a dramatic increase in the deployment of wireless LAN systems [50, 150]. Wireless LANs share many of the same design constraints as third generation wireless phone systems, such as the data transfer speed and total system capacity. Local Multipoint Distribution Systems (LMDS) and such technologies as Bluetooth are also exemplary of next generation wireless technologies. These next generation systems still need an adequate level of RSSI within the desired service area, but also face requirements for certain levels of capacity, interference, data throughput rates, and security.

1.3 Wireless Communication System Infrastructure

Historically, cellular and PCS wireless networks have targeted subscribers in outdoor environments. The first and second generation wireless voice networks are exemplified by hardware and distribution infrastructure installed on towers or building rooftops. Before wireless communication devices became common, the wired telephone infrastructure present in most buildings in the United States provided the de facto communication mechanism; thus, the first wireless service providers chose instead to target the mobile user out-of-doors as their target consumer. Now that wireless communication devices are prevalent, and with the advent of the Internet and the prevalence and demand for data, the demand for ubiquitous wireless service both inside and outside is increasing rapidly.

In deploying wireless communication systems, a variety of different approaches have emerged. These approaches are typically distinguishable by the type of hardware components that comprise the wireless communication system. That is, the type of equipment used in deploying the wireless communication system can be categorized. It is beneficial to introduce the concept of a *base station* and a *repeater*. A base station is a wireless transceiver that is capable of independently generating, transmitting, and receiving radio signals [141]. A repeater is a radio signal amplifier that is capable of receiving, amplifying, and then re-transmitting

received radio signals [141]. Base stations, because of their ability to generate new radio signals, are beneficial in wireless networks because they provide new wireless channels that a subscriber may utilize, which allows more subscribers to simultaneously communicate via the wireless network and thus creates additional network capacity. However, for many wireless technologies (e.g., GSM), the use of base stations requires careful channel planning to limit interference that new base stations can cause on existing networks [141]. Repeaters do not increase network capacity due to their inability to generate new radio signals [141]. However, repeaters are generally less expensive than base stations, and can be easier to design and deploy due to lessened concerns regarding channel planning and interference.

The hardware components that form a wireless communication system are generally referred to as a *distribution system*, as the components *distribute* the radio signal to desired locations. The use of a distribution system is desirable when the cost of base stations and/or repeaters is prohibitively high, as a distribution system enables a wireless network designer to minimize the number of base stations and/or repeaters being used. That is, rather than populate an environment with a number of individual base stations and/or repeaters, a wireless network designer can instead make use of a much smaller number of base stations and/or repeaters and utilize distribution systems to distribute a radio signal throughout the environment and achieve the same service area. The design of wireless communication systems, whether inside a building, on a tower, or on a rooftop, involves the decision of what equipment to purchase, where to place equipment, and how to configure it in order to meet all of the design criteria imposed by the customer. There are currently three different types of distribution systems for emerging in-building wireless networks: *passive*, *active*, and *hybrid*. Each is described in further detail below. In addition, although a WLAN access point can be viewed as a special type of passive distribution system, the typical deployment methodology for WLANs is unique and is discussed in its own section.

1.3.1 Passive Distribution Systems

Passive distribution systems are so named because they contain no devices other than a base station or repeater that require power. Passive distribution systems are characterized by coaxial cabling, simple connectors and splitters, and antennas, and are the most common distribution technology in use today [163]. Passive distribution systems are considered

inexpensive to install and maintain, but are limited in their ability to support next generation technologies without significant redesign due to the increasing signal loss through the distribution network as the radio signal frequency increases [161]. In designing passive distribution systems, special attention needs to be given to the losses through the distribution system to ensure sufficient radio signal strength reaches each antenna. Figure 1.2 shows a block diagram of a typical passive distribution system.

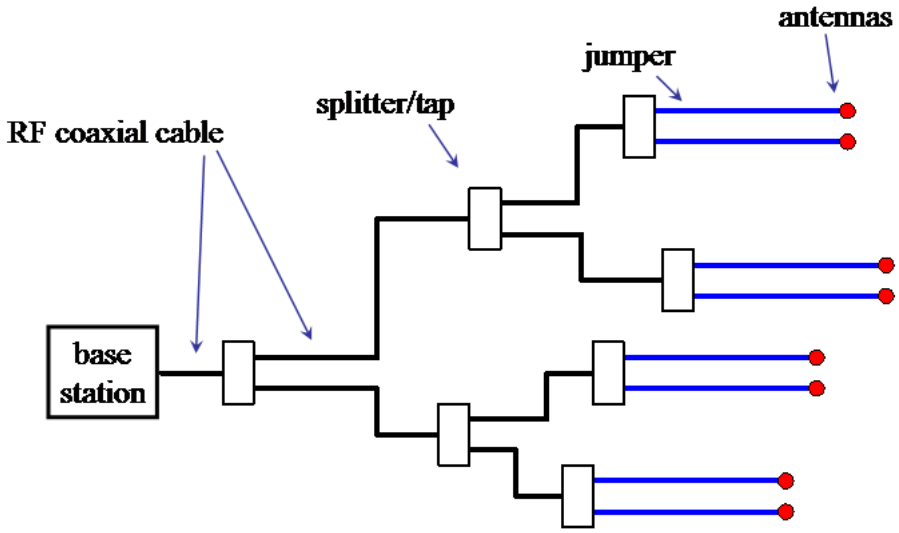

Figure 1.2: Block diagram detailing the logical layout of a typical Passive Distribution System.

1.3.2 Active Distribution Systems

Active distribution systems are so named because they contain components that require power in order to function. They are characterized by the use of inline radio frequency (RF) amplifiers. As of April 2003, RF amplifiers are considered expensive, and the extra cost required to provide power to the amplifiers may be prohibitive as well. Active distribution systems are popular inside large buildings and tunnels, where long stretches of lossy cable combined with a typically low-power base station or repeater creates prohibitively low RF signal power at each antenna, which can be readily solved through the use of inline RF amplifiers to boost the RF signal power. Special attention needs to be given to the gains

and losses through the various components of the system. Particular attention needs to be made to select equipment for use in active distribution systems that provides for sufficient noise rejection and/or dynamic range. For example, placing a high-gain RF amplifier close to an antenna may result in an excessively strong RF signal that can saturate or even damage mobile devices. Careful planning of the forward link (i.e., base station/repeater to mobile) and reverse link (i.e., mobile to base station/repeater) RF signal gains is required. Finally, the use of inline RF amplifiers can result in undesirable intermodulation effects through the inadvertent amplification of interfering or problematic RF frequencies. Figure 1.3 shows a block diagram of a typical active distribution system.

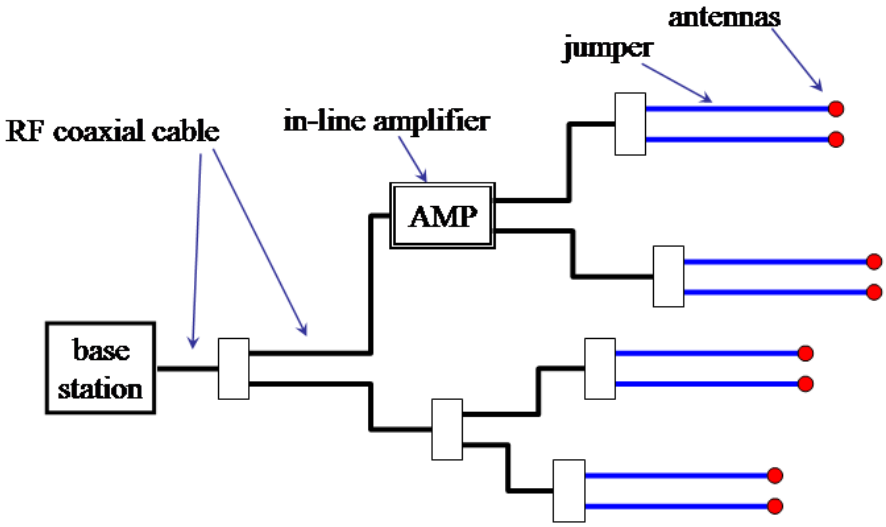

Figure 1.3: Block diagram detailing the logical layout of a typical Active Distribution System.

1.3.3 Hybrid Distribution Systems

Hybrid distribution systems are a special subclass of active distribution systems. Hybrid distribution systems contain fiber optic or baseband cabling with specialized components to convert the radio signal between RF, optical, and/or baseband formats. A typical configuration involves a base station that sends and receives optical signals via dark fiber. The dark fiber cable could stretch for several kilometers with little impact on signal quality due to the extreme low-loss inherent in fiber optic cabling. The dark fiber connects to an optical-to-RF

converter device (typically referred to as a *hub*). The hub converts the optical signal into an RF signal, and then locally distributes the RF signal via coaxial cables and antennae.

Hybrid distribution systems provide more flexibility in supporting future generations of wireless technologies by offering the potential for greater bandwidth and through the use of more advanced and "intelligent" hardware components. Examples of hybrid distribution systems include the Litenna® from Foxcom Wireless, and LGCell® from LGC Wireless. Such systems tend to be easier to design than passive or active distribution systems, as the gains and losses through the system are typically fixed and do not change with the length of cable runs [163]. Figure 1.4 shows a block diagram of a typical hybrid distribution system.

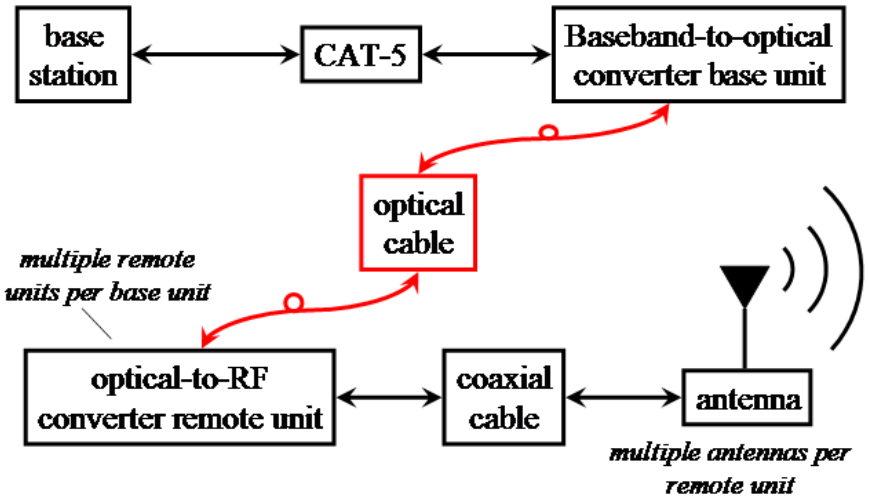

Figure 1.4: Block diagram detailing the logical layout of a typical Hybrid Distribution System.

1.3.4 Wireless Local Area Network Distribution Systems

Wireless LAN systems are generally viewed as being an indoor wireless service. Most wireless LANs utilize multiple, independent base stations with co-located antennae that plug into standard Ethernet ports to distribute signal [72]. These are commonly referred to as *access points* [72]. Unlike cellular and PCS technologies that typically require the installation of new infrastructure to serve as the distribution system, wireless LAN systems can generally exploit

existing Ethernet cabling within a building to serve as the primary distribution system. The most common deployment of wireless LAN systems today is as simple extensions to existing wired Ethernets [150]. The building or campus housing the wireless LAN typically already has an existing cabling network that is used for the existing wired computer network (e.g., a CAT-5 cable network). The existing cabling network distributes wireless Internet connectivity throughout the building or campus. The design of wireless LAN systems is somewhat simplified as there is no need to worry about gains and losses through a distribution network. Each WLAN access point acts a router linking the existing wired Ethernet backbone with mobile users sending and receiving data packets via RF signals.

1.4 Current Methods for Deploying Wireless Systems

The past two decades have seen the emergence of several approaches to designing wireless communication systems. Many of these approaches rely upon the experience and knowledge of the designer. As the use of wireless devices increases in and around buildings, relying on designer experience to design and maintain new wireless networks is a hindrance for several reasons. First, the quantity of new wireless systems needed in and around buildings requires a rapid and repeatable design methodology rather than a reliance on the experience of one or two individuals. Second, the latest generation of wireless networks are in their infancy and have yet to be mass deployed, which means there are few engineers or Information Technology (IT) professionals with experience designing and maintaining such systems. Wireless LANs in particular suffer from a lack of experienced designers and network architects. The IT professionals currently maintaining the wired data networks for corporations worldwide have little to no experience with wireless technology and are ill-prepared for the task of building out a wireless network. Third, the design criteria and constraints placed on the latest generation of wireless systems, such as maximizing capacity and service area while minimizing interference, are far more complex than the design criteria specified for prior generation systems. Before beginning to analyze new methods and techniques for designing and analyzing wireless communication networks, it is important to understand how the wireless industry has built-out infrastructure thus far and what current techniques exist for doing so.

1.4.1 Deploying Outdoor Wireless Systems

The deployment of first and second generation wireless communication systems in the United States has been marked by the construction of a nationwide network of wireless communication equipment mounted on towers. Each tower system, typically referred to as a *cell site*, is intended to provide service to mobile subscribers within a certain geographic region. As subscribers move between geographic areas, referred to as *roaming*, wireless equipment on different towers communicate with the mobile to coordinate the conversation. When the signal of the mobile switches from one cell site to another a *hand-off* is said to have occurred. Figure 1.5 provides an example of a network of cell sites.

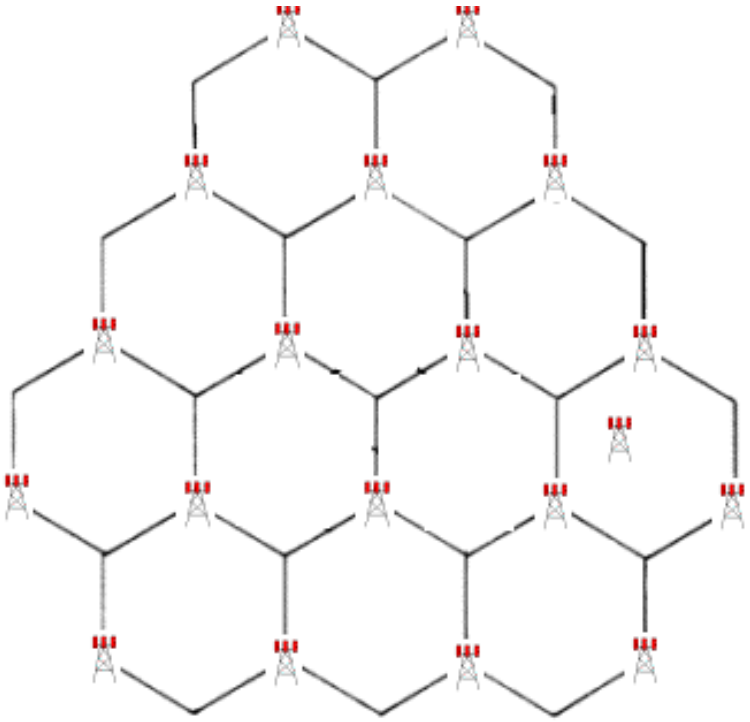

Figure 1.5: Network of macrocellular towers.

As the number of service subscribers increases, more cell sites need to be added that provide service to smaller areas [141]. This process of *cell-splitting*, or subdividing the coverage area of the original cell site by adding additional, smaller cell sites to provide service to a subset of the original coverage area, is a well-known technique for increasing the capacity of a wireless communication network [141]. Figure 1.6 displays this graphically.

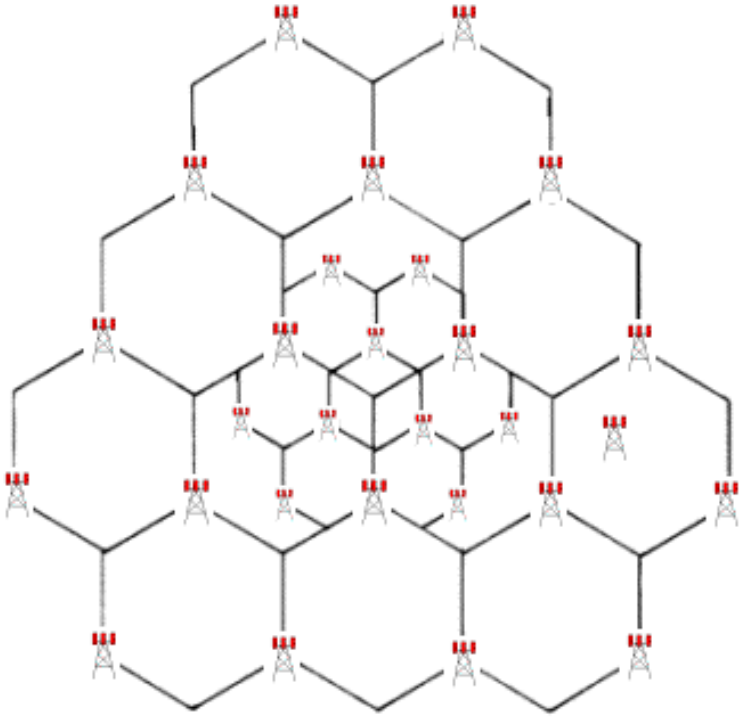

Figure 1.6: Capacity in a wireless network can be increased through *cell-splitting*, which replaces a single macrocellular tower site with numerous, smaller tower sites known as *microcells*. The microcell towers are intended to cover the same area as the original macrocellular tower, but boost the overall capacity of the network through frequency reuse. Both macrocells and microcells are typically easy to find as most are located on towers or building rooftops.

The design of large scale, or *macrocellular*, wireless communication systems is generally accomplished through the use of software engineering applications. Such software applications provide the means of predicting the performance of wireless communication systems by working with a computer representation of the physical region in which a wireless communication system is to be deployed. A computer representation of a physical environment is commonly referred to as a *site-specific model* or *site-specific database* [165]. The site-specific model contains information about the physical environment. The software then applies some form of radio wave propagation prediction algorithm that takes into account the physical environment and the specifics of the wireless communication system being designed. The results of the prediction are displayed in some manner that a human observer can interpret. Figure

1.7 displays the graphical output of a popular commercial macrocellular prediction product used to predict wireless coverage on a map.

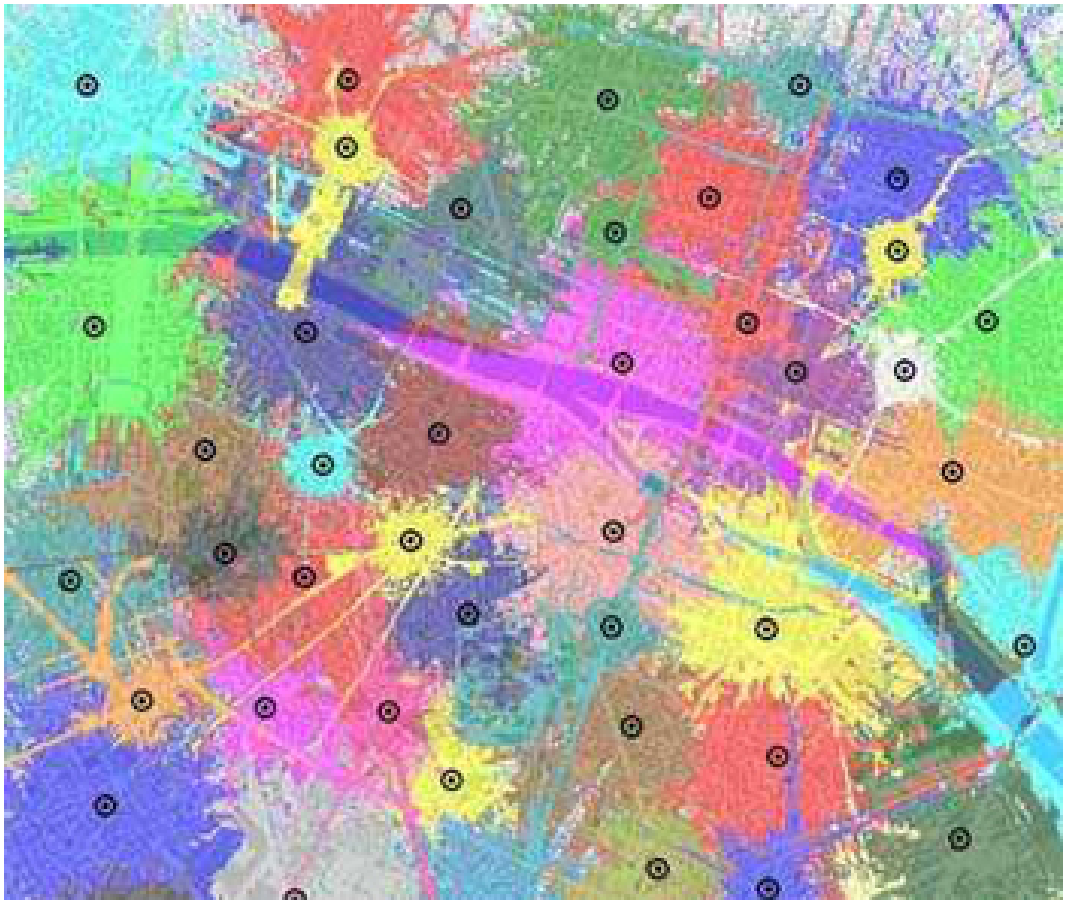

Figure 1.7: Coverage plot of a macrocellular network from the Agilent Wizard® product.

The use of software applications is recognized industry-wide as the most efficient approach to the design of large-scale wireless communication systems. There are dozens of predictive techniques and algorithms utilized in the macrocell design software applications now available. Most are empirical in nature, having been derived from the results of large measurement campaigns combined with knowledge of the fundamental principals of radio wave propagation [20, 70, 116, 129, 186]. All of the techniques make very limited use of site-specific information regarding the physical environment to make estimations of the performance of wireless communication systems within a given region. Most of the macrocellular predictive techniques were developed to accommodate site-specific information with a resolution far

worse than what is currently available. There exists a substantial body of research relating to the prediction of radio wave propagation in macrocellular environments, including [1, 20, 22, 51, 57, 70, 92, 108, 116, 129, 130, 135, 136, 137, 138, 139, 140, 170, 177, 186]. Examples of macrocellular design applications common today include PlaNET®, available from Marconi, and Wizard®, available from Agilent.

1.4.1.1 Deploying Microcellular Wireless Systems

In order to balance the needs of an ever increasing subscriber base and the bandwidth demands of emerging wireless technologies, the size of wireless cell sites have become dramatically smaller over time. *Microcells* are similar to macrocells, but have lower power and a smaller service radius. Microcells tend to be deployed in urban areas, where subscriber density is highest. Typical locations for microcell equipment include building rooftops, water towers, billboards, and on the sides of buildings. Figure 1.8 provides an example of a performance prediction for a microcellular wireless communication system from a popular commercial predictive product.

Unfortunately, the predictive techniques used to determine the performance of macrocellular wireless communication systems are not suitable for the design of systems with smaller coverage areas [15]. Most macrocellular predictive techniques are based upon empirical studies whose validity does not hold when applied to smaller-scale, more highly detailed environments [15]. Instead, more advanced predictive techniques, mostly deterministic in nature, have been developed that provide more reliable estimates of microcell system performance [44, 47]. However, deterministic prediction techniques require site-specific information of much higher resolution than that used in macrocell wireless system performance prediction [159]. The site-specific information used in predicting macrocell wireless system performance is not of sufficient resolution to accurately depict the small-scale fluctuations in the physical environment, such as locations of buildings, elevations, and surface material consistencies, which can have a dramatic effect on microcellular system performance [5]. Until recently, it was very difficult to acquire site-specific models of the physical environment of sufficient resolution to predict microcellular system performance accurately; however, today highly accurate and detailed imagery and geographic information is readily available [79]. In fact, televised coverage of the military action in Iraq in 2003 displayed first-hand the amazing

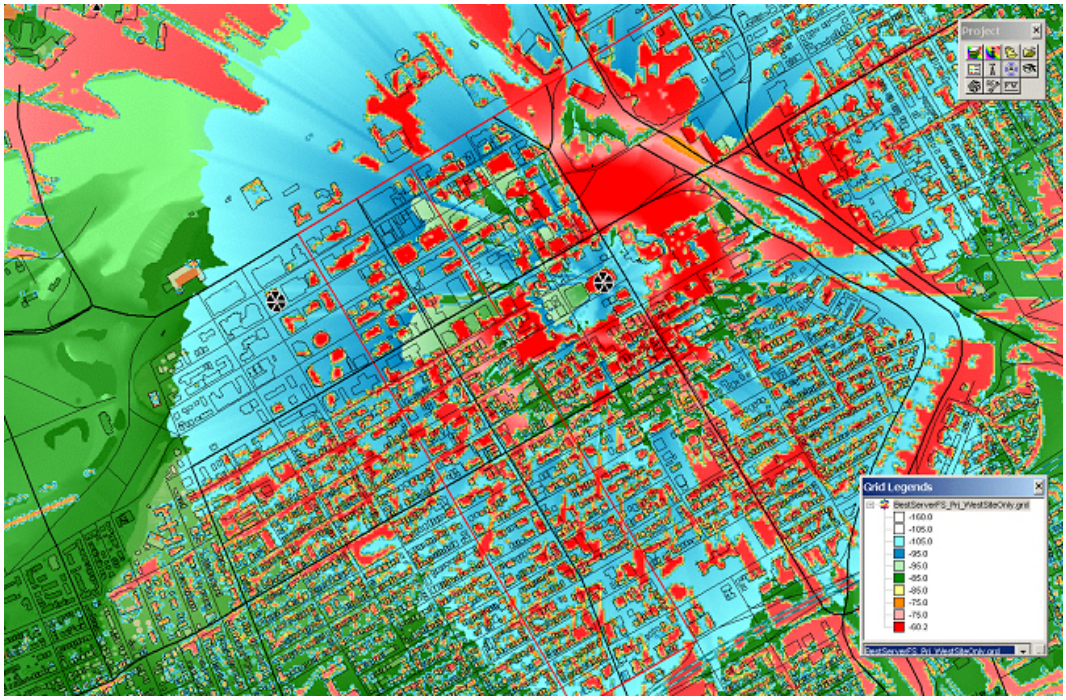

Figure 1.8: Coverage plot of a microcellular network from the Marconi decibelPlanner® product.

resolution of satellite imagery now available. There exists a substantial body of research relating to the prediction of radio wave propagation in microcellular environments, including [8, 44, 47, 52, 69, 96, 100, 102, 125, 135, 136, 137, 138, 139, 140, 149, 152, 155, 160, 169, 175]. Examples of microcellular design applications commonly used today include SignalPro® from Comarco, decibelPlanner® from Marconi, and *SitePlanner*® from Wireless Valley® Communications, Inc.

1.4.2 Deploying Indoor Wireless Systems

Until recently, wireless service providers relied primarily upon outdoor cell sites to provide service in and around buildings. A number of studies have been performed to analyze radio wave penetration into buildings due to both macrocells and microcells and for various technologies [3, 45, 49, 64, 125, 178, 179, 187]. However, recently wireless service providers have begun to deploy wireless communication equipment inside of buildings that are specifically

designed to provide service strictly to those within the building. There are various reasons for this. Such indoor wireless systems shift subscribers from the outdoor system onto the in-building system through the spectrum containment provided by low-power indoor systems, thus freeing resources on the outdoor network, increasing the overall network capacity and providing for higher data rates to subscribers. In addition, as wireless LANs increase in popularity, more building owners, facility managers, and tenants are installing IEEE 802.11b networks in their buildings. Figure 1.9 provides an example of a performance prediction for an indoor wireless communication system from *SitePlanner*®, a popular commercial predictive product available from Wireless Valley Communications, Inc.

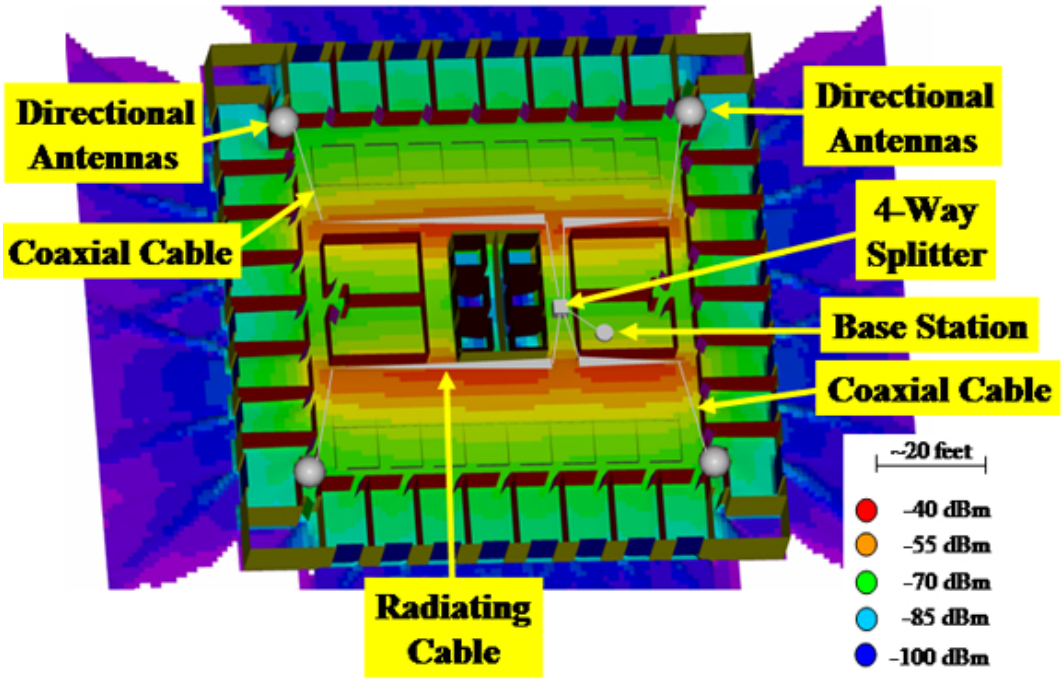

Figure 1.9: Coverage plot of an indoor wireless local area network (WLAN) from the Wireless Valley *SitePlanner*® product.

Until recently, most indoor wireless systems today were designed without the aid of predictive software. Instead, the indoor network design relied upon the time-consuming collection of extensive measurement data and trial-and-error to determine equipment placements and configurations. Early indoor networks tended to be over-engineered at excessive

cost, and could generate significant interference on outdoor systems due to signal leakage from the building. However, considerable research has been carried out to analyze radio wave propagation within buildings, and this research has produced highly accurate, site-specific predictive techniques [141]. There exists a substantial body of research relating to the prediction of radio wave propagation within in-building environments, including [7, 29, 31, 45, 61, 73, 75, 80, 87, 112, 120, 123, 126, 157, 164, 165, 172, 184]. The recent advent of software such as *SitePlanner*® that provides powerful simulation, design, and optimization capabilities is gradually changing the deployment of indoor wireless networks from a method of exhaustive, repetitive measurement collection and trial-and-error to one of rapid, efficient performance prediction and simulation.

1.4.3 Requirements of Emerging Technologies

Using predictive and modeling software applications to assist in the design of wireless communication system has proven invaluable in improving the efficiency and reducing the cost of wireless network deployments throughout the history of wireless communications [141]. The ability to predict the performance of a wireless communication network at a particular location provides designers with an excellent opportunity to analyze trade-offs in equipment selection, placement, and configuration prior to installation. Emerging wireless communication technologies require more complex modeling techniques than those developed and used to date. New wireless technologies have additional design constraints such as data throughput rates that need to be considered, and which current predictive techniques provided in the literature cannot satisfy. This thesis provides a solution that allows rapid simulation, design, and optimization of emerging wireless data networks.

Chapter 2

Databases for Wireless Network Design

2.1 Introduction

This chapter focuses on the various methods and technologies for modeling the physical environment in a site-specific manner. The *physical environment* consists of indoor, outdoor, and/or underground features, or any combination thereof. The elevation and type of the terrain, vegetation, meteorological effects, buildings and other manmade obstructions, and living beings themselves, and the location, quantity, and the relative motion of these objects make up the physical environment. A representation of the physical environment or some subset thereof within a computer forms a model of the environment, and when such a model is of a particular region or area (e.g., downtown Chicago, the Sears Tower building, etc.), it is referred to as a *site-specific model*. Such site-specific models are generally stored in some form of computer database or file that may be queried for information or displayed in some manner on a computer display, and are particularly useful in the realm of wireless communication system design and deployment.

The first step in accurately predicting the performance of a wireless communication system is producing a detailed, site-specific model of the environment in which the wireless system is to be utilized [163]. Although predictive techniques have emerged which rely on statistically

generated radio channels to produce effective results, such techniques cannot accurately predict with any degree of certainty the performance of a specific wireless communication system at a particular location of interest [162, 168]. To accurately predict the propagation of radio waves, a site-specific model of the physical environment is necessary [5, 8, 80, 129, 149, 165, 141]. Note that certain features (such as metal walls) have more significance on prediction accuracy than others (such as clear glass windows) [141].

Over the past two decades, many techniques and mechanisms have emerged to model and represent the physical environment. Today, this field is generally referred to as the study of Geographic Information Systems (GIS) [134]. Many of these mechanisms were computationally intense, difficult to implement, and/or were inappropriate for the prediction of wireless communication system performance, and until recently, the acquisition of extremely accurate information on the physical environment on a large scale was not available. However, recent advances in technology, as exemplified by satellite imagery shown during televised news coverage of the 2003 military action in Iraq, have enabled wireless communication system designers to gain access to highly detailed information about the physical environment.

2.2 Data Formats

Today, the format of data on the physical environment that one may acquire can be very broadly categorized as either *raster* or *vector* [151, 163]. Descriptions of these categories are useful for any discussion of site-specific modeling techniques.

2.2.1 Raster Data

Site-specific geographical information is most readily available in the form of digital overhead imagery. Such imagery is most easily represented as a *raster* image. A raster image provides a picture of the environment in the form of an ordered collection of *pixels* [151]. The pixels are arranged in a two-dimensional grid [71]. Each pixel is associated with a particular value, which typically manifests itself as an intensity, shading, or color [71]. When viewed as a whole, the grid of pixels with their varying colors, shades, and intensities form a pictorial representation of a physical environment that a human can easily interpret. A good example

of a raster image is the bitmap (BMP) shown in Figure 2.2, which displays a portion of downtown Chicago. The shade, intensity, and location of each pixel relative to all other pixels in the raster image of Figure 2.2 is important in the interpretation of the data as a whole. Other common raster image formats include Tagged Interchange Format (TIF) files, Targa files, and Joint Picture Exchange Group (JPEG) files.

Figure 2.1: Satellite imagery of Chicago, Illinois.

In the context of geographic information systems, raster data typically consists of an ordered arrangement, typically a grid as in the image mentioned above, of numbers. Each number (pixel) in the grid corresponds to some measurable value associated with a position in the real

Figure 2.2: Higher resolution imagery of downtown Chicago.

world. For example, the value of a pixel may represent elevation above sea level [134, 159]. Raster elevation data for downtown Chicago would provide a grid of regularly spaced values corresponding to the elevation above sea level of a particular location in Chicago. In this case, the terrain is represented as a rectangular grid whose vertices contain elevation values.

The values associated with each pixel in a raster data set are not limited to color, shading, intensity, or elevation, but may take any form. For example, the value at each pixel may correspond to the average number of people in a given location, or may provide some indication of the terrain type in a given area (e.g., concrete parking lot, grassy field, etc.). More details on specific raster data set formats and their usefulness in predicting wireless communication system performance are provided in later sections of this thesis.

2.2.2 Vector Data

Unlike raster data, *vector* data is not organized as an ordered collection of pixels. Instead, vector data provides information regarding one or more particular points in some logical space that are associated with one another in some fashion. For example, in a vector data set a line, as shown in Figure 2.3 may be represented as two points in space, where each point is an end point of the line [71, 151]. By contrast, the same line in a raster data set, as described in Section 2.2.1, may be represented as a linear array of pixels. Thus, a vector data set can convey much the same information as a raster data set, but simply does so in more compact and transportable format [71]. Common vector data set formats in use today include Drawing Exchange Format (DXF) files and Windows Metafile (WMF) files.

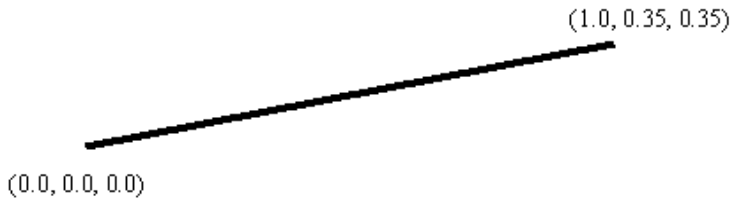

Figure 2.3: In a vector file format, a line may be represented as two ordered triplets representing a specific location in a coordinate space.

In the context of geographic information systems, vector data sets are typically used to represent objects in the physical environment, such as buildings, walls, hills, mountains, or any other definable object [159]. Three spatial coordinates (e.g., X, Y, and Z, or latitude, longitude, and elevation) are used to represent the extents of surfaces, which in turn represent physical objects in the environment [71]. It should be clear that the term *three dimensional* incorporates two dimensional views of the data, such as top down views, and an elevation or height value can be used to represent two dimensional vector data as being three dimensional as well. Thus, vector data sets typically specify the boundaries of the physical region being represented. To represent lines, circles or other compound shapes, a vector data set uses a sequence of points. For instance the line represented in Figure 2.3 is usually specified with a starting point and an end point, where each point is an X, Y, Z triplet. Polygons and basic

shapes may also be supported within vector image formats, and are typically specified as a set of points corresponding to the vertices of the polygons.

Vector data sets provide substantial benefits when compared to raster data sets [159, 151, 163]. Vector data sets are usually more economical in storage when compared to raster image formats [151]. Also, vector data sets provide a more defined representation of the physical environment. Lines or other shapes within a vector data set may easily represent obstructions and obstacles in the physical environment. This provides the ability to perform direct intersection tests between a radio wave propagating through the environment and the obstructions in the environment represented within a vector data set. This is not possible in a raster data set [163]. In addition, vector data sets provide the ability to associate values and attributes with logical entities rather than a fixed position in space. For example, the line shown in Figure 2.3 may, itself, have attributes such as color, thickness, shading, and intensity, and the endpoints of the line may convey elevation and position. The same line represented in a raster data set might only be a linear array of pixels, where each pixel much contain the duplicated attributes of color, thickness, shading, intensity, elevation, and position with no knowledge of its association with the other pixels which collectively represent the line. Thus, vector data sets are generally more easily manipulated and managed in a computer than raster data sets [71, 163]. More details on specific vector data set formats and their usefulness in predicting wireless communication system performance are provided in later sections of this thesis.

2.2.3 Combined Raster and Vector Formats

Because raster and vector data sets are fundamentally different in their approach to storing and conveying information, it is difficult to combine the two into a single data set in a meaningful manner without losing information [71, 151]. As such, formats developed to date that are capable of storing and manipulating both raster and vector data sets generally maintain the information separate from one another. If the two data sets correspond to the same physical location, the information in the separate data sets may be merged in order to derive some meaningful information. In most cases, this is to generate a visual representation that conveys certain information to a human observer. For example, Figure 2.4 shows a raster image of the town of Blacksburg, Virginia, with vector information representing the height

and physical appearance of various buildings in the same area. Both the raster and vector data sets contribute greatly to the interpretation of the data set as a whole. Thus, the two data sets taken together provide much more information than each individually could convey.

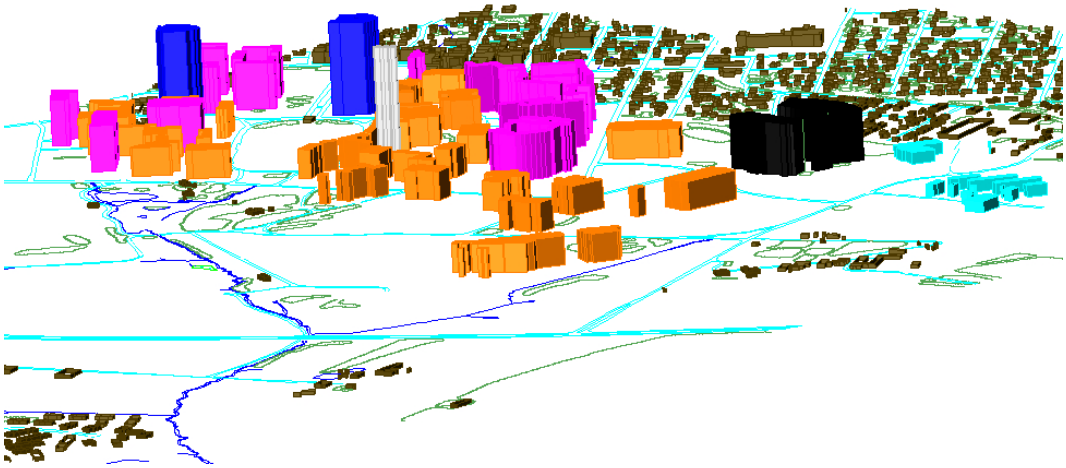

Figure 2.4: Raster image of downtown Blacksburg, Virginia, overlaid with vector data representing the relative building heights. Generated using *SitePlanner*® from Wireless Valley Communications, Inc.

2.3 Geographic Information System (GIS) Technology

GIS technology has progressed dramatically in the past two decades [134]. Today, there are dozens of sources for highly detailed, geographical information on most major cities, and such information can be provided in a variety of raster and vector data formats. The following sections outline the most common data formats and variety of information types that are useful in wireless communication system prediction.

2.3.1 Photogrammetry

High-resolution aerial photographs of geographic regions are now commonplace and readily available. Scores of companies worldwide offer this form of information, including [53], [79],

and [114]. Satellite imagery can provide very highly detailed information on any given area at virtually any scale [79]. Figure 2.2 provides a good example of a satellite image of downtown Chicago. Such raster imagery has limited usability in predicting wireless communication system performance beyond providing a visual reference for a human observer. However, several of the data formats described later are derived or created from high-resolution satellite imagery.

2.3.2 Land Use Representation

The major drawback to photogrammetry is the relative inability to utilize the raster data for anything other than displaying an image to a human observer. In order to enhance the usability of photogrammetry, the United States Geological Survey (USGS) developed the concept of *land use* [183]. The concept of land use is that any given position, identifiable by a latitude and longitude coordinate, can be associated with additional information. For example, a land use data set, indexed by latitude and longitude, can provide a grid of values that provide an index into a table listing terrain types. This provides a means of identifying characteristics about the region in and around a given latitude and longitude position that cannot be derived from an aerial image.

Land use information, also known as clutter maps, can provide details on the surface of the terrain (e.g., concrete parking lot, grassy pasture, swamp, dense forest, etc.), clutter (e.g., rural housing, urban high-rise, etc.), elevation, population density, or any other measurable quantity that can be associated with a particular position or region. The USGS has provided a standardized indexing mechanism to describe land use data [183], and all commercial macrocell predictive techniques rely on such land use information to achieve reasonable accuracy [2, 25, 115].

The drawback of land use information is that it, too, is raster in nature, and attempts to broadly categorize characteristics of a region rather than to precisely model individual obstructions that impact propagation in and around buildings on small distance scales.

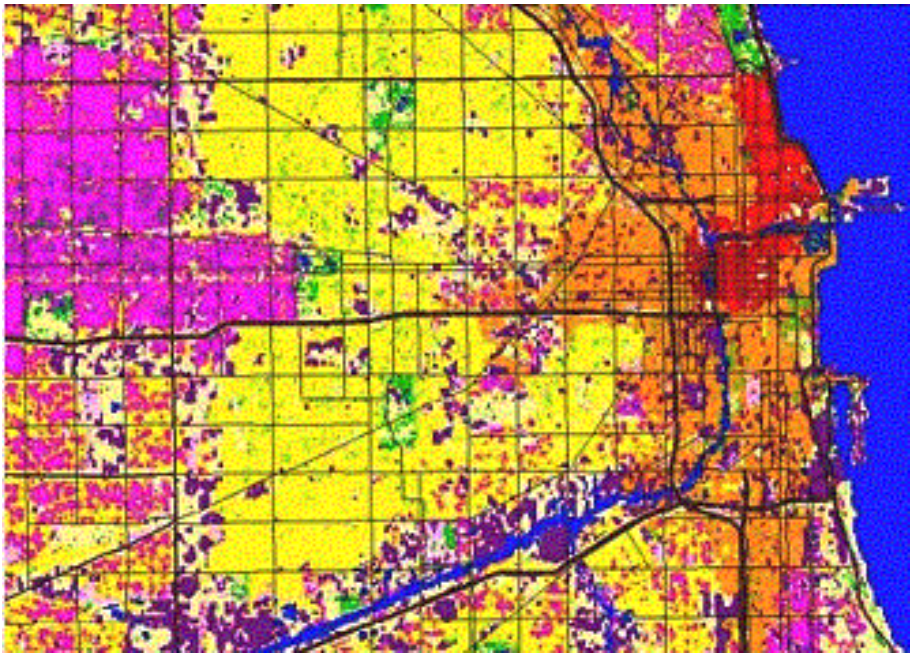

Figure 2.5: An example Land Use image, or clutter map, for the Chicago area. Each color corresponds to a specific land use category (e.g., farmland, forest, urban buildings, water, etc.). [183]

2.3.3 Digital Elevation Modeling

By considering the elevation of terrain in the area of interest, the accuracy of radio wave propagation prediction can be significantly improved [5, 128, 129]. As such, special attention needs to be given to land use data that identifies terrain elevation. Such land use formats are typically referred to as Digital Elevation Models (DEMs) [183]. DEMs typically take the form of an equally spaced grid of numbers representing elevations above sea level. The grid is indexed by latitude and longitude, and thus effectively provides a lookup of the terrain elevation at a particular location on the globe.

2.3.3.1 Types of Digital Elevation Models

There are two common variations of Digital Elevation Models (DEMs) available today. Both are typically stored in a standard, raster grid data format, indexed by latitude and longitude.

The first such DEM, a *bald earth* elevation model, represents the elevation of the terrain within a given region exclusive of vegetation, buildings, or any other manmade obstruction [79, 159]. Figure 2.6 provides a sample of a bald earth elevation model.

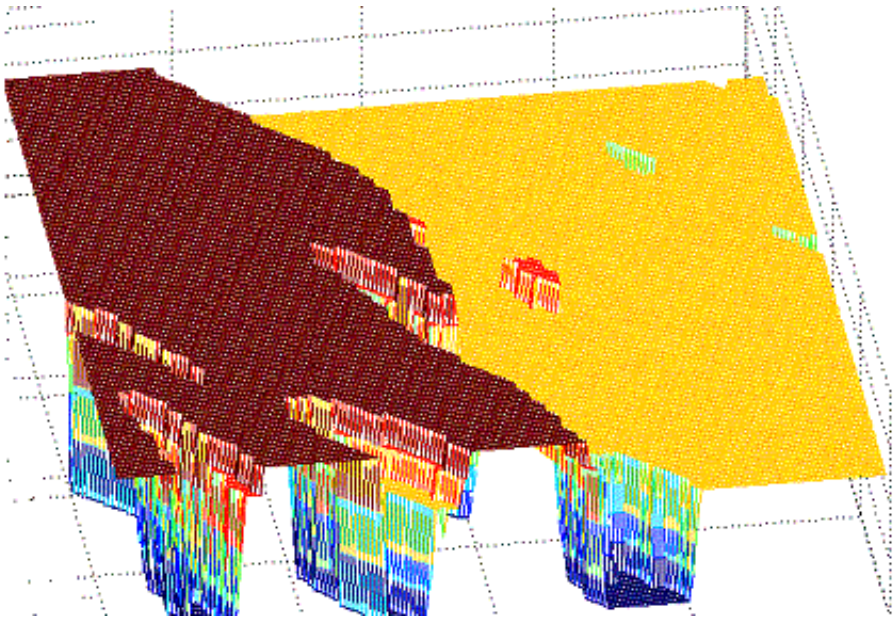

Figure 2.6: Digital Elevation Model providing elevation information for a portion of downtown Chicago. The data is the *bald earth* elevation, meaning that the elevation of the ground above sea level exclusive of buildings or vegetation is considered. [183]

The second such DEM, a *canopy* elevation model, represents the elevation of the terrain within a given region, but with the measured elevation including the tops of all foliage within the region [79, 159]. That is, a canopy DEM provides the elevation of the terrain, and considers the elevation to be the tops of any foliage located at the indexed location. Many canopy DEMs will also include buildings in their terrain elevation data. Thus, a canopy DEM will provide the elevation to the tops of any foliage or manmade obstructions or obstacles at a given position. Figure 2.7 provides a sample of a canopy elevation model.

A special file format known as the Geological Tagged Interchange File Format (GeoTIFF) is commonly used to represent DEMs. GeoTIFF is a raster image file format in which the color, shading, and intensity of the pixels comprising the image are interpreted as elevation. This provides a rather convenient way of storing and representing elevation data in a way

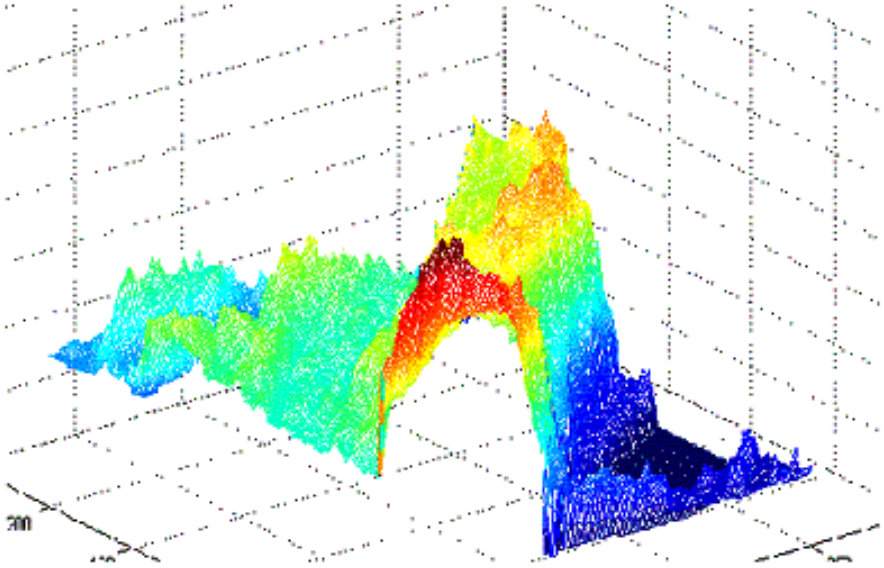

Figure 2.7: Digital Elevation Model providing elevation information for a portion of downtown Chicago. The data is the *canopy* elevation, meaning that the elevation data considers the elevation of the ground along with vegetation and buildings. [183]

that is easily interpretable by both a human observer and another computer. Figure 2.8 provides a sample GeoTIFF elevation model.

An important limitation of all DEMs is the inability to differentiate between different portions of the data. That is, the DEM format provides nothing to distinguish an elevation point due to a building from an elevation point caused by a river. Thus, an observer of DEM information cannot distinguish between the different elevated obstacles and obstructions in the environment without some other form of land use information to supply the differentiation. The most commonly available DEMs only provide information accurate to within thirty meters of an exact position and within thirty feet of the exact elevation. Recent improvements in photogrammetry technology allow DEMs to approach a resolution of one meter both in position and elevation, but such data is prohibitively expensive at the time of this writing. However, recent satellite imagery unveiled during 2003 indicates that readily available satellite imagery far exceeding previously known resolutions may soon commercially available.

Figure 2.8: An example GeoTIFF file. The color of each pixel in the file corresponds to a specific range of elevation for the terrain shown at that pixel. [183]

2.4 Buildings

Buildings and other manmade obstructions can significantly impact the performance of wireless communication systems [4, 5, 15, 141]. Whether causing shadowing or acting as reflectors and diffractors, buildings need to be included in any accurate site-specific prediction of radio wave propagation in an urban environment [5, 13]. The Digital Elevation Models (DEMs) discussed in Section 2.3.3.1 do not provide the ability to distinguish buildings from other terrain obstacles.

To counter this, many companies and organizations that provide terrain information also provide separate information on the outer physical structure of buildings that are present in a particular region [53, 79, 114]. This information is typically provided in a vector format, where lines or polygons are used to represent the outlines of buildings. Figure 2.9 shows the

same region as the aerial photograph of Figure 2.2, but in this case lines are used to trace the outlines of the buildings present in the region. The building outlines are typically identified by points in a three dimensional space, where the z-coordinate represents the relative height or elevation of the building.

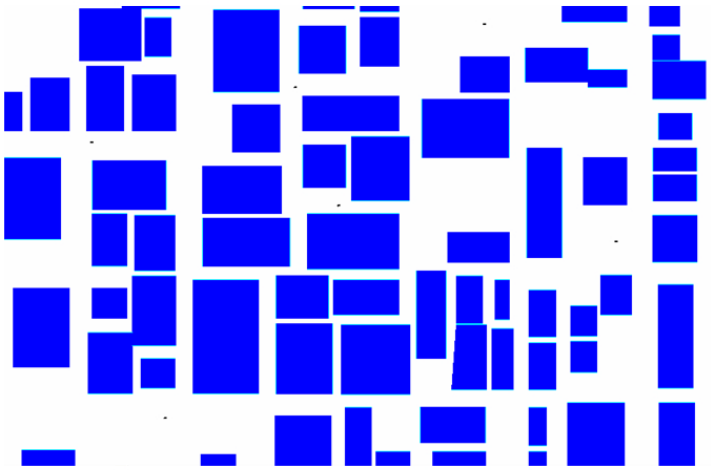

Figure 2.9: An example vector file containing building footprints for a section of downtown Chicago. Created by tracing a raster aerial photo of a portion of Chicago using *SitePlanner*® from Wireless Valley Communications, Inc.

The outlines shown in Figure 2.9 could represent either the rooftops or the footprints of buildings. Such imagery provides a representation of the outer edge of the exterior wall of the buildings in a given geographic area. This form of information is typically generated either manually, using land survey information, or through a process whereby the height of buildings is determined by analyzing the depth of shadows in aerial photographs [79]. In either case, the format of the building data takes the form of vector lines overlaid onto the original raster image [79], [159]. Although this can provide information on the position and relative size and shape of buildings, it does not provide details on the material consistency of the surfaces of the buildings or provide the ability to discern or represent the internal structure of buildings.

2.5 Surface Modeling

Radio waves will reflect off surfaces, diffract around corners, become scattered by surfaces, and penetrate surfaces through well-known, well-defined mechanisms [15, 141]. Any highly accurate site-specific simulation of wireless communication system performance requires a means of modeling the interaction of radio waves with the environment. This requires being able to determine intersections between radio waves and terrain, buildings, and other obstructions and obstacles. It is relatively straightforward to determine intersections when working with vector information such as lines and surfaces [71, 151]. However, intersection tests are not practical on raster data sets [71, 151]. Methods have emerged for transforming raster data sets into a vector format that can then be used in intersection analyses. Several of these methods are outlined in the following sections.

2.5.1 Triangular Irregular Networks

A Triangular Irregular Network (TIN) is a vector data format that is extremely useful in representing terrain features. A TIN, for the purposes of modeling terrain features, is a collection of adjoining triangular surfaces whose vertices represent the elevation of the terrain a given location. Figure 2.10 gives an example of a typical TIN.

The Triangular Irregular Network concept was developed as a simple way to represent a surface given a set of irregularly spaced points [101]. A TIN model of terrain features is vector data that consists of a non-overlapping network of planar triangular surfaces based on a network of irregularly spaced elevation points as shown in Figure 2.10 [159]. The planar face of each triangular surface in the TIN forms a representation of the surface of the terrain at that location and, in the context of radio wave propagation analysis, provides a representation of the physical environment suitable for determining intersections between radio waves and obstacles in the physical environment.

The TIN implementation can be made more efficient by placing more points in the areas of rough terrain and fewer points in smoother terrain areas [159]. The areas with relatively flat terrain can be modeled by using large triangles and rough terrain can be modeled using smaller triangles [159]. This makes the TIN model an efficient way of representing objects

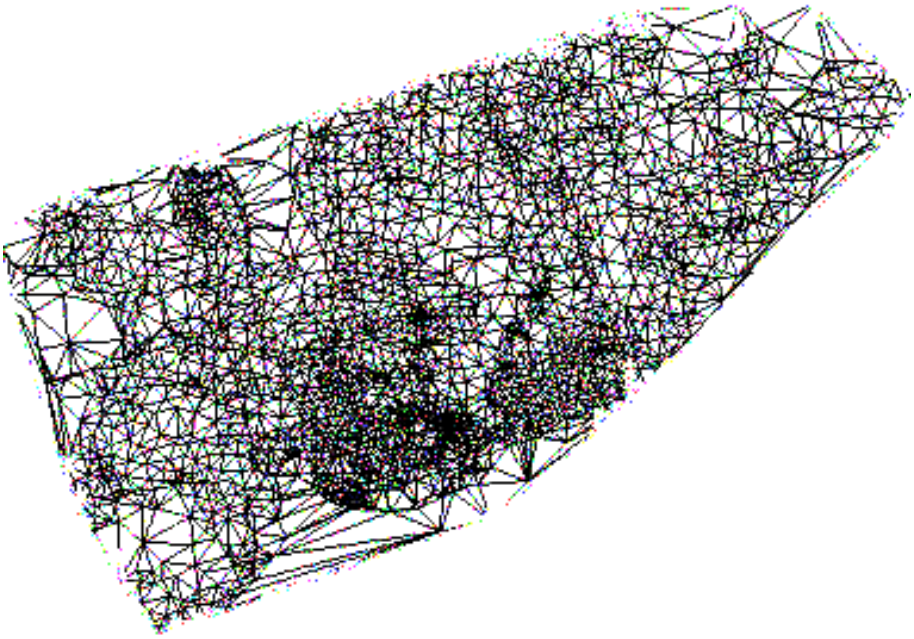

Figure 2.10: An example Triangular Irregular Network (TIN) where each vertex of each triangle represents the elevation at a particular geographic location. [159]

in the physical environment. As the number of surfaces that need to be modeled to represent the terrain decreases, the computational complexity of wireless communication system performance prediction models also decreases, as there are fewer obstacles to consider in the simulation. The application of TIN models within this research is as a convenient and efficient means of converting a raster data set, representing an outdoor physical environment, into a vector data set.

2.5.2 Representing Terrain

There are a number of different techniques for converting Digital Elevation Model (DEM) information, a raster data set, into a TIN, a vector data set. Such techniques are derivatives of a technique known as DeLaunay Triangulation, and are well documented in [27], [37], [58], [81], [101], [111], [119], [131], [159], and [151]. The most straightforward method to convert the DEM into a TIN is to connect each point in the DEM to its two nearest neighbors to form a network of triangles [151]. More optimal solutions apply smoothing and averaging

routines to reduce the number of elevation points that are considered in the TIN [159]. To decrease the number of surfaces used to model the terrain, the non-critical points of the DEM can be filtered out and discarded, leaving only the critical elevation points to be used in developing the TIN [159]. This will produce a TIN data set that accurately represents the terrain in a region with the smallest number of triangular surfaces. Figure 2.11 shows a portion of the same terrain data set from Figure 2.10 after the application of a smoothing algorithm to reduce the total number of triangular surfaces.

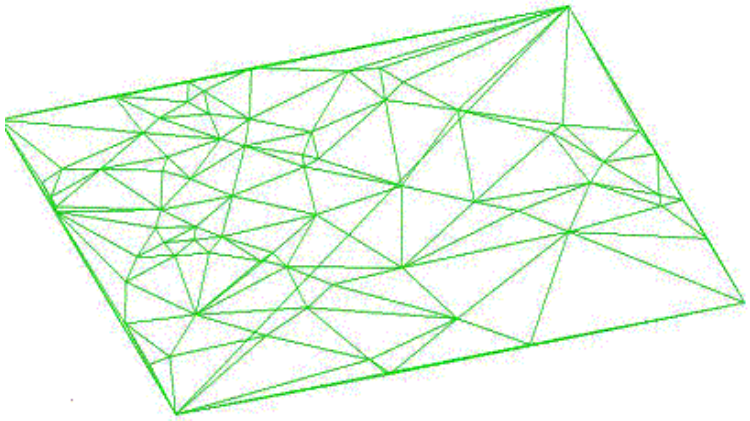

Figure 2.11: An example Triangular Irregular Network (TIN) after a smoothing algorithm has been applied to reduce the total number of triangles (surfaces) in the final data set. Such smoothing operations enable TIN data to efficiently represent terrain elevation. [145]

2.5.3 Representing Buildings

When provided with a canopy DEM containing building elevation information, the techniques of creating a TIN format discussed in Section 2.5.2 still apply. Figure 2.12 provides a TIN representation of a physical environment that includes buildings. One artifact of the conversion process is that that the sides of the buildings tend to be sloped is due to the relative accuracy of the DEM information [159]. Also note that there is no distinction between the terrain and the building structures aside from the elevation differences.

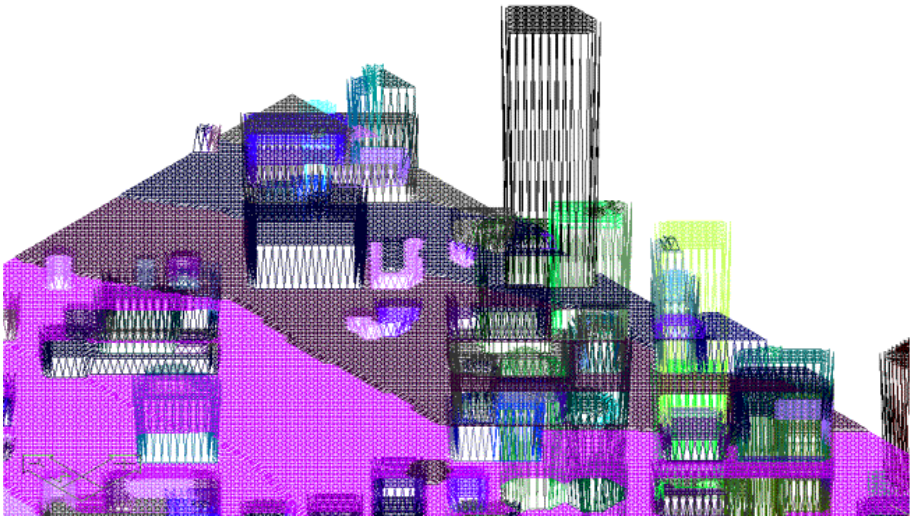

Figure 2.12: A Triangular Irregular Network vector data set representing terrain and building elevation for a portion of downtown Chicago. The vertex of each triangle represents the elevation of the ground, building, or vegetation, whichever is furthest above sea level at that location. However, there is no way to immediately distinguish whether the elevation represented is for the ground, building, or vegetation. [145]

2.5.4 Combined Terrain and Building Surface Modeling

If building information such as that described in Section 2.4 is available, it can be utilized to develop a surface model that represents both terrain and buildings without the loss of precision in representing building surfaces described in Section 2.5.3. By connecting building footprints and rooftops with planar surfaces, representations of buildings can be formed similar to those in Figure 2.13. Such building surface models are generally created manually, and stored in some form of vector file format [53, 79, 114].

Recently, a technique was developed at Wireless Valley Communications, Inc. through the Wireless Valley Industrial Scholars Fellowship program and detailed in [159] that enables both terrain and external building structural information in a canopy DEM to be modeled within a single, TIN vector data set while maintaining the ability to easily distinguish building structures from the surrounding terrain features. This technique applies well-known edge detection algorithms to a canopy DEM. Recall from Section 2.3.3.1 that a canopy DEM contains both terrain and building elevation information. Applying an edge detection algorithm

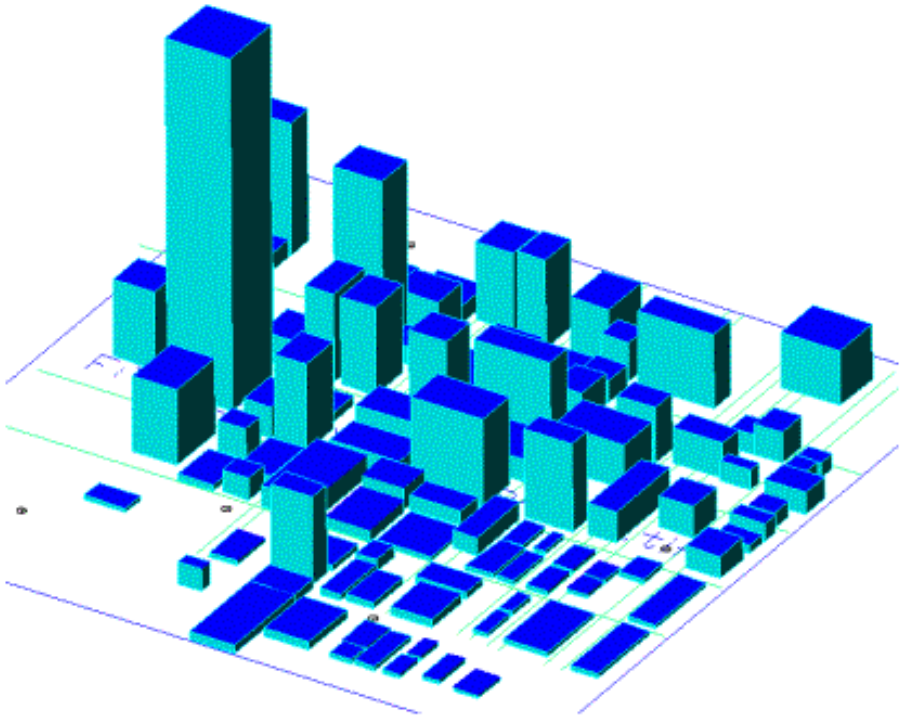

Figure 2.13: Vector data set representing the surfaces of buildings in the downtown Chicago area. Such data provides building position and height information, but does not include terrain elevation. [145]

along with an assumption that rapid changes in elevation will tend to signify the walls of a building, the technique will identify building footprints and rooftops. Thus, given a single canopy DEM data set for a region, the application of the technique will generate building surface information in a form identical to that given in Section 2.4.

Such building surface information can be merged with terrain surface information to form an accurate, site-specific elevation model for a given region [159]. Building surface information such as shown in Figure 2.13 can be merged with a TIN surface representation of the terrain in the same region. This was formerly not practical, as the TIN representation of any surface is not easily edited or altered [151]. Due to research work performed at Wireless Valley Communications, Inc., such combining is now possible without danger of gaps or inconsistencies between the building and terrain information [159]. Figure 2.14 provides an example of such a merged data set.

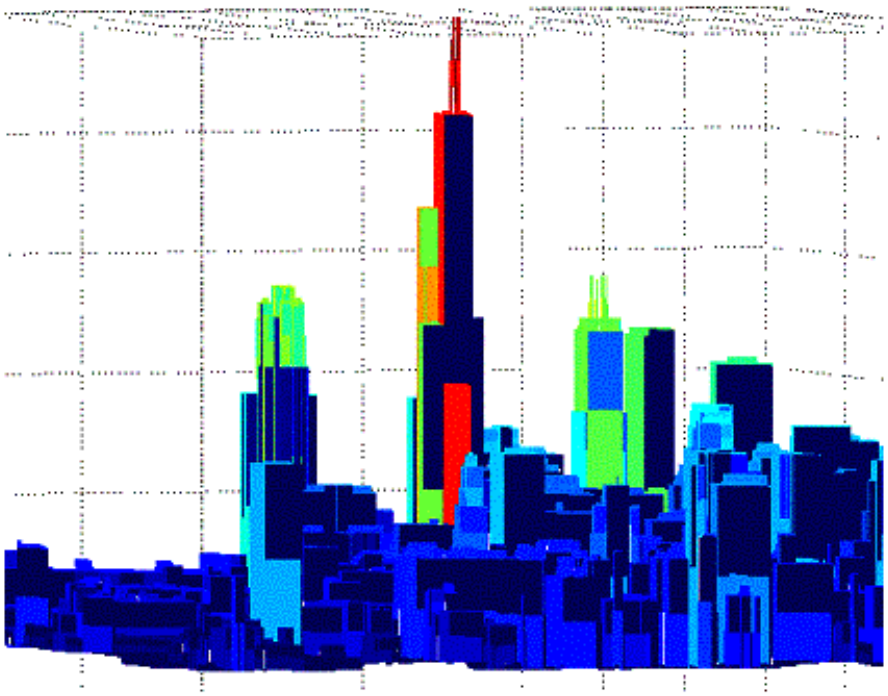

Figure 2.14: Merged Triangular Irregular Network (TIN) data representing terrain and vegetation elevation with vector building surface information. Such data combines to form a highly accurate representation of the physical environments, and is an efficient manner to model and represent urban areas. [145]

The vector format of the combined terrain and building information provides several advantages over the purely raster data representation. The vector representation of the data enables attributes such as material type, roughness, reflectivity, permittivity, aesthetic characteristics, or any other information to be easily associated with or embedded within each surface. Thus, the surfaces representing the various building structures can be easily distinguished from surfaces representing terrain obstacles in the vector format, which is not possible in the aforementioned raster formats [159]. This provides the ability to much more accurately represent the environment and achieve better results when attempting to simulate the performance of wireless communication systems in a region modeled in such a manner.

2.6 Indoor Environments

As with the outdoor environment, the ability to quickly and easily model indoor physical environments is critical in order to accurately predict the performance of a wireless communication system within buildings. Unfortunately, the quantity of research and industrial development regarding the modeling of indoor physical environments is much more limited [163]. Also, unlike the outdoor environment where aerial or satellite imagery is readily available, information on the structure of indoor environments is much more limited for wireless applications. In many cases, the interior physical structure of buildings may be private or restricted information, and may change over time. Building owners or tenants may add, remove, or change the layout of walls, cubicles, and furniture, and techniques for predicting the performance of wireless communication systems within such environments are needed that are either resistant to such changes or which enable the computer model of the environment to be easily edited and kept up-to-date as the building environment changes.

2.6.1 Raster Representations of the Internal Building Structure

The most readily available information regarding the physical layout of a building is in the form of a picture of the floor plan [163]. Pictures such as fire exit maps are raster data sets that provide an image of the building layout that a human observer can easily interpret. Many data formats exist for visually representing building floor plans in such a manner, including Windows bitmaps (BMP), Tagged Interchange Format (TIF) files, Targa files, and Joint Picture Exchange Group (JPEG) files [163]. Such data is typically provided as a separate raster image per building floor. None of these data formats provide information regarding the orientation of building obstructions in a manner that is easily interpreted by computer software, and provide no information on the material consistency or height of the building obstructions. Thus, other than providing information on relative positions and distances within the building structure, such raster imagery alone is of little use in the context of radio wave propagation prediction [165, 163]. Figure 2.15 provides an example of an image of the layout of a building floor.

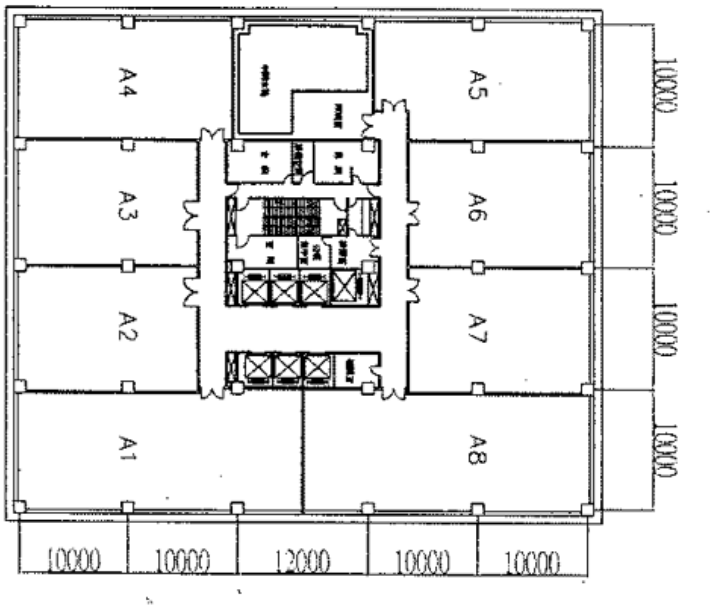

Figure 2.15: A raster image representing a building blueprint.

2.6.2 Two Dimensional Vector Representations of Internal Building Structure

Over the past several years, the use of computer aided design (CAD) programs such as AutoCAD® to design new buildings has increased greatly [10]. This has led to an increase in the availability of building layout information in a vector format. As of the time of this writing, the overwhelming majority of this information provides little or no data on the relative height and material consistency of the various building walls and other internal obstructions. Also, as with the raster building imagery described in Section 2.6.1, such vector building layout information is typically provided as a separate file per building floor. Figure 2.16 provides an example of a vector representation of a building floor.

2.6.3 Vector Representations of Internal Building Structures

As mentioned in Section 2.5, the use of surfaces to represent physical obstructions is advantageous to the prediction of wireless communication system performance. Research performed

Figure 2.16: A Computer Aided Design (CAD) vector file of a building blueprint.

by at Wireless Valley Communications investigated and proposed methods for representing internal building structures as two dimensional lines and/or three dimensional surfaces [126, 127, 164, 165]. This research was advanced significantly and eventually commercialized at Wireless Valley Communications, Inc., into a pioneering software engineering application known as *SitePlanner*®. *SitePlanner* is the only commercial software engineering application developed specifically to design wireless communication systems within an indoor or campus environment, and represents the state-of-the-art in terms of modeling indoor and campus environments in a site-specific manner. *SitePlanner* is now considered an industry standard in the area of wireless communication system design, measurement, and optimization, and is in use within over 200 companies around the world, and has seen over 30 patents filed.

SitePlanner utilizes a two or three dimensional vector format to represent the physical environment [163]. This format enables a realistic representation of the physical building environment that is easily interpretable by either a computer software application or human observer. Surfaces are used to represent physical obstructions within the buildings, such as walls, doors, windows, ceilings, elevators, furniture, or any other physical object. Each surface has additional information associated with or embedded within it to identify attributes such as material consistency and aesthetic appearance [143]. Figure 2.17 provides an example of a *SitePlanner* representation of a building.

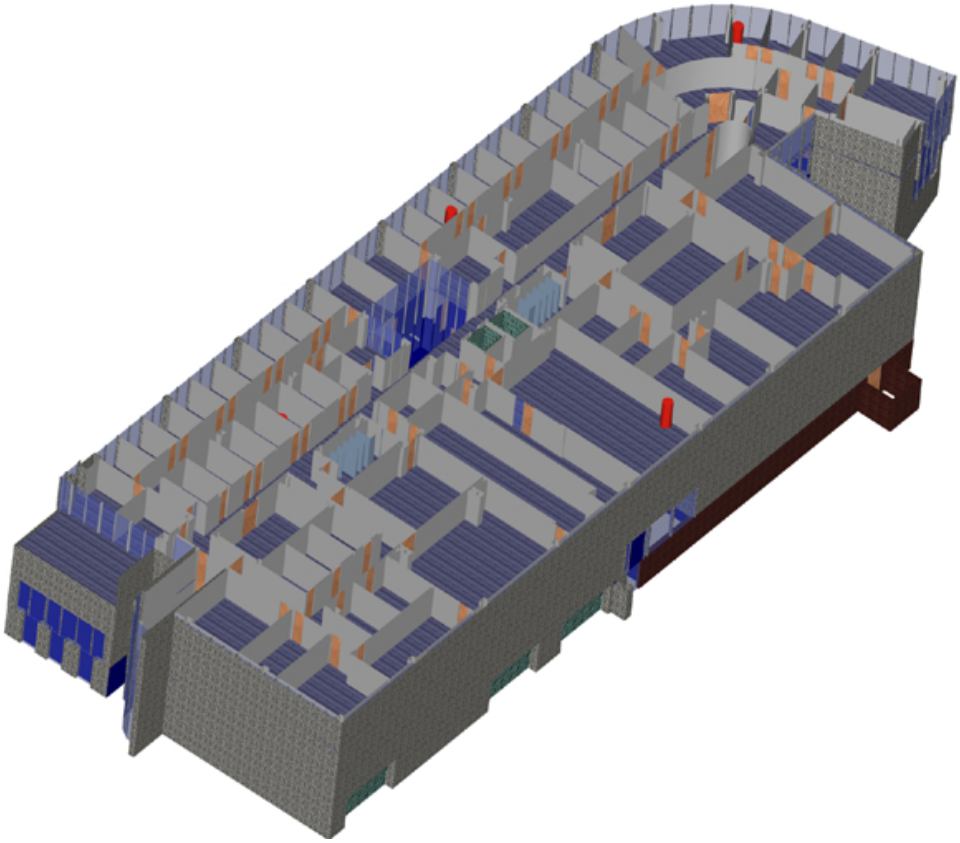

Figure 2.17: Three-dimensional model of a building floor plan constructed using Wireless Valley's *SitePlanner*® product. Each partition contains embedded information regarding electromagnetic and aesthetic characteristics.

SitePlanner provides the means to convert either raster or vector building floor plan information, as detailed in Sections 2.6.1 and 2.6.2, into a two or three dimensional representation of internal and external building structures using surfaces [163]. For raster images of building floor plans, *SitePlanner* provides the ability to manually trace the image, overlaying two or three dimensional surfaces to represent the walls and other building obstructions. For vector images, *SitePlanner* can manipulate the existing vector data, such as lines and arcs, to generate surfaces that represent the walls and other building obstructions. Multiple floors are aligned with one another in two or three dimensions to generate an accurate approximation of a multistory building. Multiple buildings may then be aligned with one another to generate accurate approximations of a campus environment on undulating terrain. Figure

2.17 provides an example of a multistory building, and Figure 2.4 provides an example of a campus environment, both modeled using *SitePlanner*.

2.7 Integrated Indoor and Outdoor Site-Specific Models

In order to fulfill the goals of this research and the inevitable need of the wireless industry, a repeatable method for generating and representing both terrain information and building structures was necessary. This was accomplished by combining the methods of Sections 2.5.4 and 2.6.3. The solution combines both methods into a single, repeatable process for simultaneously modeling indoor and outdoor regions. The implementation in software takes the form of additional functionality embedded within the *SitePlanner* software product available from Wireless Valley Communications, Inc. Software algorithms have been implemented that automate many of the steps described previously to acquire a site-specific model of a physical space. This process consists of three steps: 1) create a vector model of the external building environment, 2) create a vector model of the internal building environment, and 3) merge the internal and external building environment models. The basic method is outlined in Figure 2.18.

2.7.1 Modeling the External Building Environment

First, applying the advanced TIN conversion techniques described in Section 2.5.4, a canopy DEM is converted into a collection of triangular surfaces representing the fluctuation elevation of buildings and terrain as shown in Figure 2.14. Because the techniques outlined in [145] provide for the automatic determination of building surfaces separately from the surrounding terrain and foliage, the triangular surfaces representing building types can be identified and segregated. Using techniques described in Section 2.6.3, each surface has additional information associated with or embedded with it to identify attributes such as material consistency and aesthetic appearance [143]. Hence, each building surface can be identified as being of type "BUILDING", allowing for easy categorization later. Figure 2.19 provides an example of a converted canopy DEM displayed in *SitePlanner* wherein building

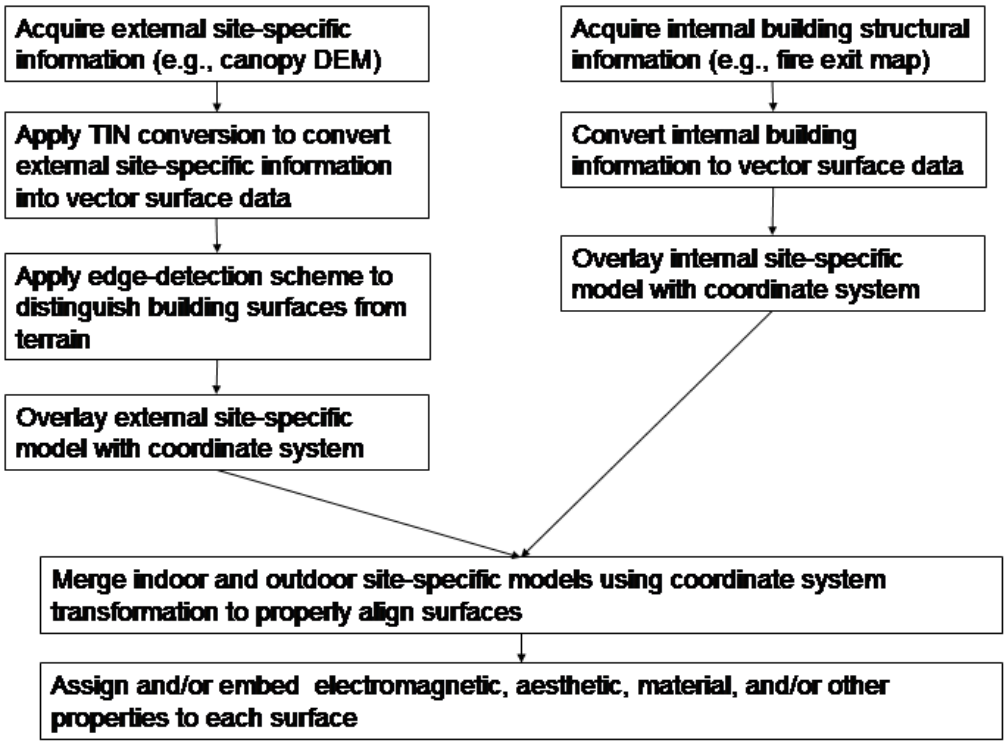

Figure 2.18: Basic method for creating merged indoor-outdoor site-specific models.

surfaces are colored to differentiate them from terrain.

If the canopy DEM contains associated latitude-longitude coordinate information regarding the extents of the region it represents, this information may be used by *SitePlanner*® to automatically overlay the resulting site-specific model with a coordinate system based on latitude, longitude, and elevation. If coordinate information of this type is not readily available, it may be entered manually by the user through use of the dialog box shown in Figure 2.20.

Note that although a latitude, longitude, elevation coordinate system is used, any coordinate system based on an ordered doublet or triplet will suffice. Once a coordinate system of some type is in place, it becomes possible to identify distinct positions within the site-specific model using one or more ordered triplets, or doublets with implied or default elevation or height values.

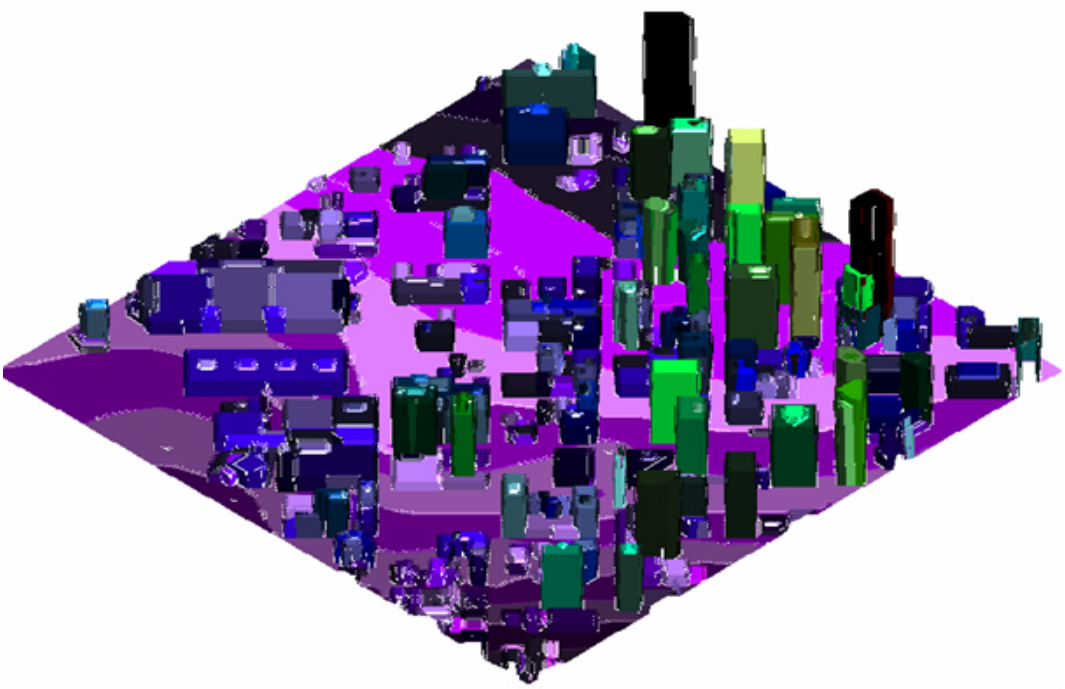

Figure 2.19: Three-dimensional model of a portion of downtown Denver created using Wireless Valley's *SitePlanner*® product. Building surfaces are shown in various colors to differentiate them from surrounding terrain.

If land-use (see Section 2.3.2) or similar types of geo-referenced data is available, it can now be used to correlate individual surfaces within the site-specific model with a particular type of clutter, material consistency, or any other electromagnetic or aesthetic property. For example, if information is available in a standard format such as that identified in Section 2.3.2 which identifies the terrain at location *(37.0, 180.0)* as being *CONCRETE PARKING LOT*, the triangular surface in the site-specific model of the region occupying the position *(37.0, 180.0)* may instantly be assigned electromagnetic properties (e.g., reflectivity, scattering coefficient, etc.) based on the knowledge of its material consistency. Similarly, cost or vendor-specific information of the object (used by architects) may be assigned to or embedded within the object surfaces. This cost or vendor-specific information may be contained within the original environment data, or manually created by the user at any time later.

Alternately, the user may freely select one or more surfaces within the computer model and

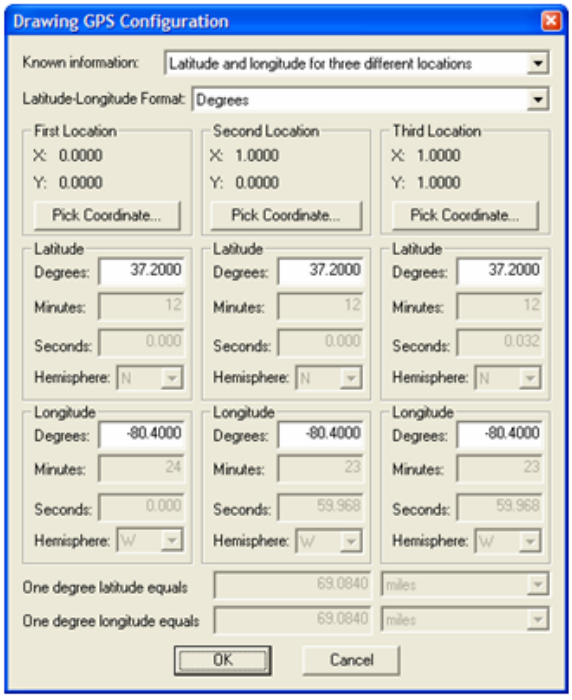

Figure 2.20: Dialog box user may activate to overlay the site-specific model with a coordinate system based on latitude, longitude, and elevation.

assign electromagnetic, aesthetic, or other properties through a series of dialog boxes. During this research, the author developed software at Wireless Valley Communications that models and represents any site-specific environment. The software maintains a fully editable database of material types, where each material type encapsulates the electromagnetic, aesthetic, and any other properties of an obstruction of the given material. For example, if a surface is assigned a material type of *TINTED WINDOW GLASS*, it shares the same properties and attributes as all other surfaces assigned that same material type. Figure 2.21 provides a screen capture showing a selection dialog where a user may identify material type and select one or more surfaces to assign the material type to. This information may be utilized later to determine the result of interfacing between electromagnetic waves and the various surfaces comprising the site-specific model as described in Chapter 3.

Because obstructions interact differently with electromagnetic waves of different frequencies, the database of material types maintained by the software includes the frequency-dependent

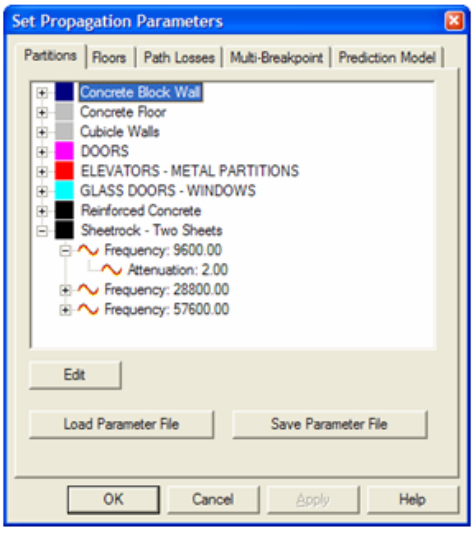

Figure 2.21: Dialog box used to manually assign electromagnetic and aesthetic properties to one or more surfaces in the site-specific model.

attributes of each material type, as well. That is, each material type category includes information on how an obstruction of that type of material will respond when it encounters a radio wave of a particular frequency [145].

2.7.2 Modeling the Internal Building Environment

Next, applying the techniques described in Section 2.6.3, a scaled two or three dimensional vector model of the internal structure of any building may be created. The resulting model will appear similar to that shown in Figure 2.17. As with the surfaces comprising the model of the external building environment, the surfaces comprising the internal building environment may also be assigned electromagnetic or aesthetic properties. The user simply selects the desired material type from a series of selection dialogs and proceeds to select one or more of the internal building surfaces in order to assign the desired material type. Figure 2.21 provides a screen capture showing a selection dialog where a user may identify material type and select one or more surfaces to assign the material type to. This information may be utilized later to determine the result of interfacing between electromagnetic waves and the

various surfaces comprising the site-specific model as described in Chapter 3.

In addition, the user may identify a *coordinate reference point*. A coordinate reference point takes the form of a selected point within the two or three dimensional model of the building structure. The user identifies a particular point in the internal building model and then identifies an ordered doublet or triplet that represents the equivalent location within the external building model of Section 2.7.1. The identification of this coordinate reference point provides for a translation matrix to be formed that describes the transformation between the coordinate systems of the indoor and outdoor building environments. For example, given (x_i, y_i, z_i) as the coordinate reference point for the indoor site-specific model, and (x_o, y_o, z_o) as the coordinate reference point identified for the corresponding outdoor building environment, the resulting coordinate translation matrix to convert each coordinate in the indoor model to its corresponding coordinate in the outdoor model is given in Equation 2.1.

$$\begin{bmatrix} x_t \\ y_t \\ z_t \\ 1 \end{bmatrix} = \begin{bmatrix} 1 & 0 & 0 & x_o - x_i \\ 0 & 1 & 0 & y_o - y_i \\ 0 & 0 & 1 & z_o - z_i \\ 0 & 0 & 0 & 1 \end{bmatrix} x \begin{bmatrix} x_i \\ y_i \\ z_i \\ 1 \end{bmatrix} \tag{2.1}$$

In Equation 2.1, (x_i, y_i, z_i) is the coordinate reference point for the indoor site-specific model, (x_o, y_o, z_o) is the coordinate reference point identified for the corresponding outdoor building environment, and (x_t, y_t, z_t) is the transformed coordinate from the indoor to the outdoor environments.

2.7.3 Merging the Internal and External Building Environments

This first step in the process, Section 2.7.1, results in three-dimensional representation of an outdoor environment comprised of a set of surfaces, no two of which overlap. Positions within the two- or three-dimensional model are referenced through ordered doublets or triplets, generally of the form *(latitude, longitude, elevation or height)*. The second step in the process, Section 2.7.2, results in a set of surfaces which collectively represent the internal and external physical structure of a particular building, properly scaled and with a coordinate reference point specified for the drawing that positions the building relative to the external

environment model created in Section 2.7.1.

The software implements the ability to combine the internal and external site-specific environment models. This is done using the coordinate transformation relationship defined by the coordinate reference point identified in Section 2.7.2. Each surface within the internal building model is translated into the coordinate system of the external building model and properly positioned. When applied to all structures of the internal building model, the result is that the internal structure of the building is now fully represented within the external model of the surrounding buildings and terrain. Once merged with the internal building model, the original external walls for the building that existed previously in the external building model may be discarded as they are generally extraneous information at this point. Figure 2.22 depicts the resulting merged indoor-outdoor model.

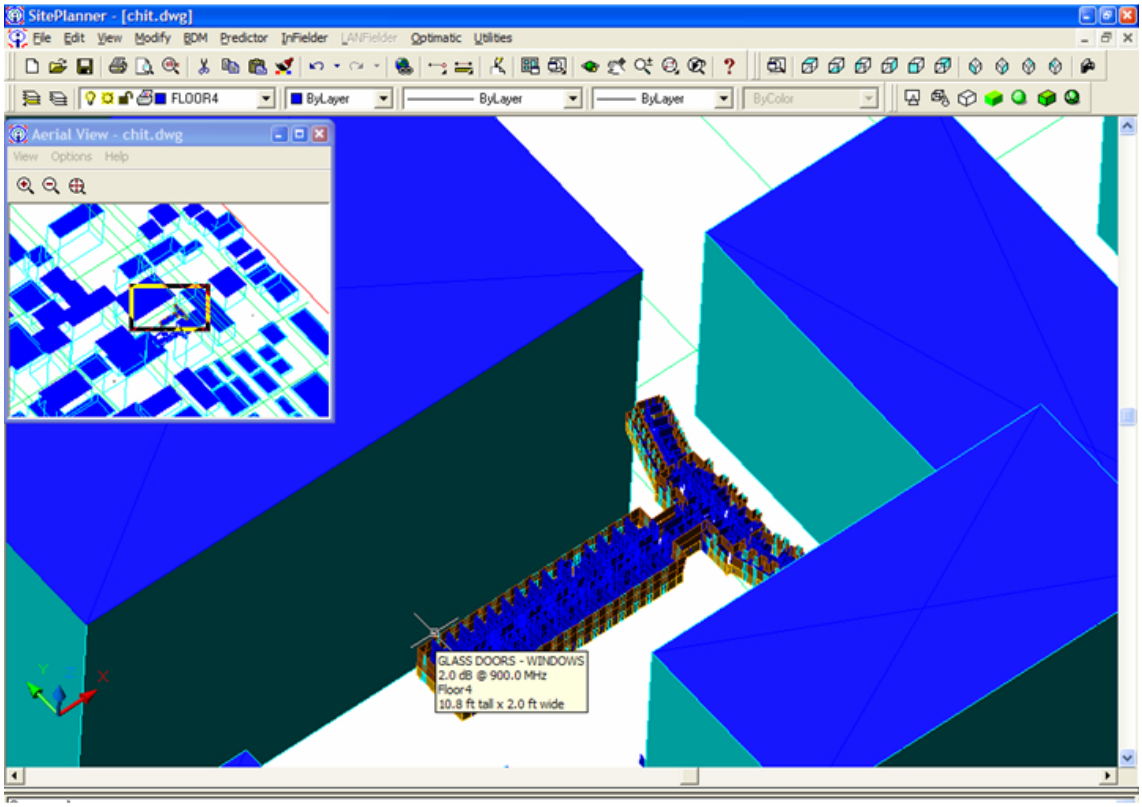

Figure 2.22: Merged indoor-outdoor site-specific representation of a building environment created using *SitePlanner*®.

This is a revolutionary approach to modeling site-specific representations of physical environments and will allow unprecedented prediction and management capabilities going forward. These aforementioned approaches are patent pending by Wireless Valley Communications, Inc.

2.8 Conclusion

A revolutionary, repeatable method has been defined for creating a merged indoor-outdoor site-specific representation of any physical environment. The single site-specific representation of the physical environment contains both internal and external building structural and terrain features. This enables universal prediction and visualization of wireless network performance and infrastructure layout between indoor and outdoor environments on any scale. The resulting merged indoor-outdoor models of the building environment may be utilized in radio wave propagation analyses of any scale and scope, from macrocellular to indoor, and for maintenance and management purposes in addition to design. This chapter represents a significant advance in the ability to model and simulate not only wireless network performance, but also proposes a technique for integrating location-specific data sets of varying formats into an integrated site-specific model of any environment.

Chapter 3

Site-Specific Prediction Techniques

3.1 Introduction

This chapter focuses on the various methods and technologies for predicting radio-wave propagation within a site-specific environment. A huge demand exists in the wireless industry for the development of accurate radio-wave propagation techniques [141]. Large-scale path loss models that predict average log-normally distributed signal level as a function of propagation distance have, to date, been the dominant type of site-specific predictive techniques. However, as the resolution and availability of site-specific information improves, as discussed in Chapter 2, and as the bandwidth of wireless communication systems increases, the application of higher resolution, deterministic prediction techniques becomes more attractive. Deterministic methods can provide channel parameters such as delay spread, angle-of-arrival, channel impulse response, fading characteristics, and other invaluable information that is otherwise only available through exhausting measurement collection [141]. The field of site-specific propagation prediction, much like the field of wideband wireless data communications, is still relatively immature. This chapter begins by discussing some of the history behind deterministic propagation analysis and culminates by focusing on the state-of-the-art techniques developed and used in this thesis.

3.2 Distance Dependent Prediction Models

Distance dependent models derive from the path loss equation given in Equation 3.1 [156, 141]. Path loss is the measure of power loss between a transmitter and receiver relative to a known reference path loss at a distance d_0.

$$PL(d_0) = P_T - P_R + G_T + G_R + 20\log(\frac{\lambda}{4\pi}) \tag{3.1}$$

In Equation 3.1, $PL(d_0)$ represents the path loss at the reference distance d_0 where d_0 is typically 1.0 meter or some other close-in reference distance that is closer than all other distances of interest (but still far enough to be in the far-field of the transmitting antenna), λ is the wavelength in meters, G_T and G_R are transmitter and receiver antenna gains in dB respectively, and P_T and P_R are the transmitter and receiver powers in dBm respectively. Equation 3.1 solves for path loss with respect to a one meter free space reference.

An assumption that is generally made is that the average dB path loss with respect to a known path loss reference value (typically assumed to be at one meter free space for indoor and low power transmitters or small antennas) linearly increases as a function of the logarithmic transmitter-receiver (TR) separation distance. The slope of this increase is characterized by the *path loss exponent* n in Equation 3.2 [141]:

$$\bar{PL}(d) = 10n\log(\frac{d}{d_0}) \tag{3.2}$$

where $\bar{PL}$ is the average path loss, d is the separation distance between transmitter and receiver in meters and d_0 is the path loss reference distance (typically assumed to be one meter for indoor and low power transmitters with small antennas). Thus, Equation 3.3 provides a general path loss model [141, 156, 165]:

$$PL(d)[dB] = PL(d_0) + \bar{PL}(d) + X_\sigma \tag{3.3}$$

where $PL(d)$ is the path loss in dB and X_σ represents a log-normal shadowing random variable in dB having a standard deviation of σ.

Variations to Equation 3.3 have emerged which leverage the variability of the path loss exponent n from environment to environment. For example, in a grocery store a path loss exponent of $n = 1.8$ (or 18 dB loss per decade of distance) may produce an accurate result, while a path loss exponent of $n = 3.0$ (or 30 dB loss per decade of distance) may produce optimal results in a hospital [141, 165].

3.3 Partition-Based Prediction Models

Partition-based predictive models were pioneered by researchers in the Mobile and Portable Radio Research Group (MPRG) at Virginia Tech, and are heavily used today in the design of indoor wireless communication systems [48, 156, 165, 163]. A major contributing factor to the success of partition-based predictive models is their relative simplicity combined with the ability to easily fine-tune their accuracy given measurement data [48, 141]. Partition-based predictive models combine the use of path loss exponent(s) with knowledge of the principle obstructions in the physical environment to roughly gauge path loss, and thus predict, with reasonable accuracy, the coverage area or interference for a given wireless communication system. All partition-based models are derivatives of the distance dependent models discussed in Section 3.2 [141]. Equation 3.4 provides the basic partition-based model [141, 156, 165].

$$\bar{PL}(d)[dB] = \bar{PL}(d_0) + 10n \log\left(\frac{d}{d_0}\right) + FAF + \sum_{i=0}^{M} PAF_i. \tag{3.4}$$

In Equation 3.4, n is the path loss exponent, FAF is the Floor Attenuation Factor (an attenuation factor in dB that represents signal loss as a radio wave propagates across the floors of a building), and PAF represents the Partition Attenuation Factor (losses in dB that are summed as the signal propagates through M specific obstructions). To apply Partition-based predictive models, a designer must simply draw a straight path between transmitter and receiver, determine the intervening obstructions and their respective attenuation factors (the PAF), determine the applicable floor attenuation factor (the FAF) if any, and apply the path loss exponent. The straight line path connecting transmitter and receiver is referred to as the *primary path*, and so partition-based models are sometimes referred to as *primary*

ray tracing models [141]. Alternately, in Equation 3.4, the floor attenuation factor FAF may be replaced by a path loss exponent that varies by the floor separation between transmitter and receiver, as shown in Equation 3.5 [141, 156, 165].

$$\bar{PL}(d)[dB] = \bar{PL}(d_0) + 10n_{MF}\log(\frac{d}{d_0}) + \sum_{i=0}^{M} PAF_i \tag{3.5}$$

These models and their derivatives are currently at the heart of the predictive engine in *SitePlanner*, a wireless communication system design software application available from Wireless Valley Communications, Inc., which was the result of research performed by the author early in his research [165, 163]. Figure 3.1 shows sample predictive output from *SitePlanner* produced using partition-based path loss models. Such models are highly advantageous to wireless system designers due to the relative ease and quickness by which they can be applied, and due to ease with which they may be fine tuned when provided with measurement data [165, 163]. However, these models alone do not provide all of the detailed information regarding network throughput that future wideband wireless networks will require.

3.4 Ray Tracing Prediction Models

3.4.1 Introduction

Deterministic radio wave propagation techniques involving *ray tracing* methods offer unprecedented accuracy for predicting wireless communication system performance [47, 14, 31, 157, 175]. Ray tracing models are capable of estimating the complete spatial-temporal impulse response for any given receiver location. Information of that type would otherwise only be available through complex and often exhausting measurement collection. Ray tracing enables the ability to predict RMS delay spread, power delay profiles, mobile fading, angle-of-arrival, time dispersion, and any other channel characteristic. Such channel characteristics will be vital information for wireless engineers tasked with designing future wideband wireless communication systems.

However, even with advances in computing capabilities, use of ray tracing models is not

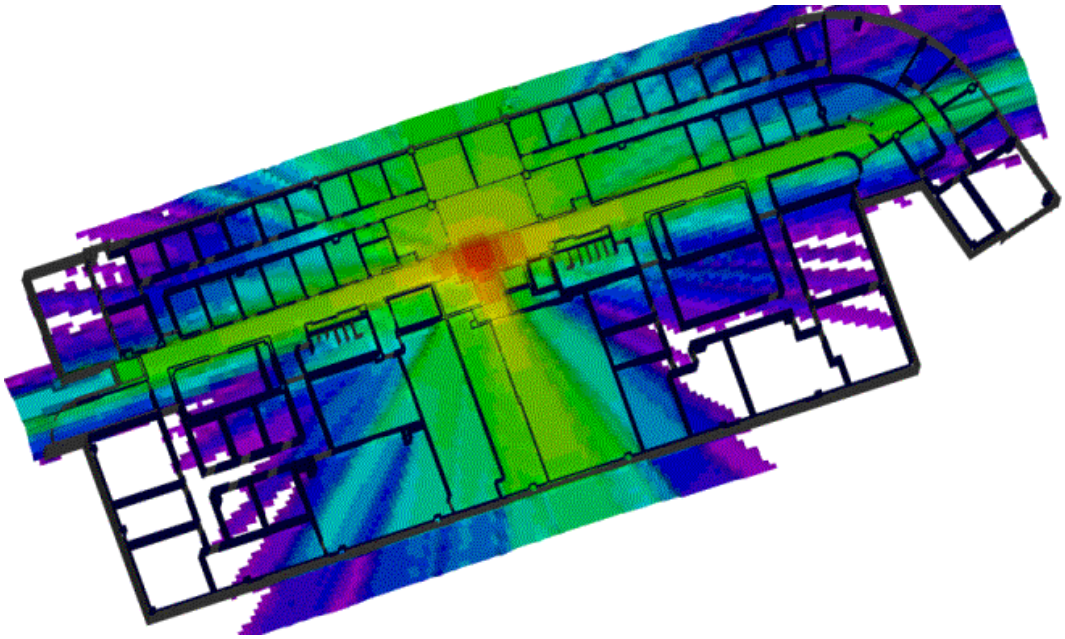

Figure 3.1: Predicted signal strength within the fourth floor of Durham Hall on the Virginia Tech campus given a test transmitter on the same floor. Predictions were performed using partition-based path loss models within *SitePlanner*®from Wireless Valley Communications, Inc.

yet widespread among wireless engineers. It is instead relegated to research labs and other non-commercial venues. This is due, in part, to various problems that continue to make ray-tracing models impractical. First, ray tracing is computationally intensive even by the computing standards of today. Secondly, there is a decided lack of highly detailed, readily available site-specific information of sufficient resolution for ray tracing models to be applied optimally. Third, there are no efficient techniques for calibrating ray tracing algorithms given measurement information; therefore, if the results of the ray-tracing algorithm do not closely match the measured data, a wireless designer has little to assist in adjusting the parameters of the algorithm to compensate.

The basic premise of ray tracing is to discretize electromagnetic waves emanating from a transmitter into a finite set of rays. These rays project outwards in straight lines from the transmitter. The rays trace a path through the physical environment, and attempt to mimic the actual path followed by electromagnetic waves. As the rays traverse through the

physical environment, each physical obstruction encountered directly affects the trajectory of each ray. For example, a ray that intersects a wall may reflect off, diffract around the wall, penetrate through the wall, and/or be scattered by the wall. By tracing the paths all the rays take through the environment, an approximation of how transmitter power is distributed throughout the environment can be formed.

Errors in ray tracing algorithms typically occur in one of three areas. The resolution and accuracy of the computer model of the environment on which a ray tracing algorithm is to be applied impacts the accuracy of the ray tracing algorithm [5, 8]. The geometrical optics theory that ray tracing algorithms are derived from do not precisely represent the behavior of radio waves, and thus some error is introduced as a result [47]. A third possible source of error in ray tracing algorithms is concerned with path-finding. In some instances, the ray tracing algorithm may fail to accurately represent the true radiation path of the signal [47]. These errors are discussed in more detail in later sections of this chapter.

3.4.2 Modeling the Physical Environment for Ray Tracing

In order for a ray-tracing algorithm to function well, a detailed, accurate model of the desired physical environment must be created and maintained in some form of computer database. Ray tracing algorithms require that the placement, orientation, and structure of all relevant obstructions of the physical environment be specified. Deterministic propagation modeling requires environment detail such as surface roughness, dielectric material properties, and small-scale geometry for all relevant objects in the environment, although certain parameters may be estimated or set to default values. The definition of a *relevant obstruction* may vary depending on the concerns of the wireless engineer or the specific technology involved, but generally an object should be considered relevant for the purposes of ray tracing if the existence of the object in the environment significantly affects the propagation of radio waves through the environment. This leads to simplifications of the ray-tracing algorithms, and may introduce errors into the result [5, 47]. The method outlined in Chapter 2 provides a repeatable process for creating a site-specific model of any environment suitable for ray tracing analysis. The resulting site-specific models consist of a set of surfaces, each surface having been assigned or embedded with dielectric material properties.

3.4.3 Geometrical Optics

An exact solution to any radio wave propagation problem would involve the application of Maxwell's equations. Maxwell's equations define electromagnetic wave propagation, and any exact answer would require solving these partial differential equations. The Helmholtz wave equation, given in Equation 3.6, applies to electromagnetic waves propagating in a simple, isotropic, homogenous medium.

$$\nabla^2 \vec{E} + \omega^2 \epsilon \mu \vec{E} = 0 \tag{3.6}$$

In Equation 3.6, $\vec{E}$ is the electric field vector, ϵ is the permittivity, μ is the permeability, and ω is the radian frequency ($2\pi f$).

Solving Equation 3.6 deterministically becomes extraordinarily difficult for all but the simplest environments. The technique of ray tracing attempts to approximate the solution to the Helmholtz wave equation. Ray tracing is derived from applying high frequency approximations to geometrical optics. Effectively, ray tracing attempts to mimic electromagnetic wave behavior as the frequency become very large [24].

In Equation 3.7, the wave function ψ defines scalar wave propagation.

$$\nabla^2 \psi + k^2 n^2 \psi = 0 \tag{3.7}$$

In Equation 3.7, ψ is the scalar wave function, n is the index of refraction, and k is the wave number $\frac{2\pi}{\lambda}$. A solution to the wave function, ψ, is presented in [63] and shown in Equation 3.8.

$$\psi = Ae^{-jkS} \tag{3.8}$$

In Equation 3.8, k is the wave number $\frac{2\pi}{\lambda}$, A is the wave amplitude as a function of position, and S is the trajectory and phase as a function of position [63].

Substituting Equation 3.8 into Equation 3.7 leads to both Equation 3.9 and 3.10 [47].

$$|\nabla S| \approx n \text{ when } \frac{\nabla^2 A}{Ak^2} \ll n^2 \tag{3.9}$$

$$\nabla^2 S + \frac{2\nabla S \cdot \nabla A}{A} = 0 \tag{3.10}$$

As mentioned above, ray tracing attempts to approximate the solution to the wave equation by combining high frequency assumptions with geometrical optics. By constraining the $\frac{\nabla^2 A}{Ak^2}$ term in Equation 3.9, which is a gauge of how much an electromagnetic wave will bend outside of the geometrical optics prediction (i.e., essentially a diffraction factor), to having a small value, this lends validity to the assumption of high frequency [47]. With this assumption, Equation 3.9, sometimes referred to as the *Eikonal Equation*, is an important approximation. As the frequency grows higher, the wave number k increases and the diffraction factor $\frac{\nabla^2 A}{Ak^2}$ term in Equation 3.9 decreases as a result. Therefore, diffraction effects become less significant as the frequency increases [141].

In addition, S in Equation 3.9 represents multiple layers of electromagnetic wave fronts propagating away from the transmit point. Instead of attempting to represent the wave fronts propagating through space, it is easier to represent the surface of each wave front by single rays that pass perpendicularly through the surfaces of S. Each ray then, by traversing along the same gradient set by S, represents the propagating electromagnetic wave through space. As most terrestrial radio wave propagation is in a free-space medium, the index of refraction, n, may be assumed constant [63]. That is, the rays follow straight line paths as they pass through the environment [24].

Equation 3.10 defines the electromagnetic field amplitude along the path as a function of the distance traveled. This effectively defines the ability to determine path loss incurred as the electromagnetic wave propagates through free space. This then enables the combination of Equations 3.10 and 3.9 into Equation 3.11, a general expression of the electric field of a ray as function of distance R traveled, radius of curvature ρ_1 and ρ_2 (the principle radii which characterize the curvature of the wave front), and the electric field phasor $\vec{E}_0$ at the field origin [47]:

$$\vec{E}(R) = \vec{E}_0 e^{(-jkR)} \sqrt{\frac{\rho_1 \rho_2}{(\rho_1 + R)(\rho_2 + R)}} \tag{3.11}$$

If ρ_1 is equal to ρ_2, as occurs when all of the surfaces in the environment are planar (i.e., non-curved surfaces), and if only reflection is considered, then Equation 3.11 reduces to Equation 3.12.

$$\vec{E}(R) = \vec{E}_0 e^{(-jkR)} \frac{\rho_0}{(\rho_0 + R)} \tag{3.12}$$

In Equation 3.12, ρ_0 is the initial radius of curvature in any direction. Equation 3.12 relates the electric field of any ray to the total distance the ray has propagated.

Reflective-based ray tracing was considered for this thesis. Figure 3.2 depicts the interaction between rays transmitted from a transmitter and surfaces within the site-specific environment. In Figure 3.2, the ray transmitted from the transmitter intersects with a surface. As a result, the ray both penetrates through the surface and reflects off of the surface. The resulting angles θ_i (the angle of incidence), θ_r (the angle of reflection), and θ_t (the angle of transmission) are identical.

As described in Chapter 2, the surface in the site-specific model may have electromagnetic parameters associated or embedded within it. These parameters may include such things as an attenuation factor, reflection coefficient, absorption factor, or any other parameter. These parameters are used by the predictive engine to determine the amount of electric field strength lost by the ray as a result of either penetrating through or reflecting off of any given surface. The user may be able to override these parameters for any given simulation in a variety of ways. For example, the user may identify that for each surface a ray intersects, the resulting reflection incurs a 3 dB loss in the strength of the ray. Through this mechanism, the electric field strength of any ray at any point within a site-specific model of an environment can be determined with accounts for the total propagation distance of the ray and the interaction between the ray and obstructions within the environment.

3.4.3.1 Geometrical Theory of Diffraction

The Geometrical Theory of Diffraction is commonly used in wireless communications to approximate the interaction between electromagnetic waves and the edges of planar surfaces. Diffraction is an important aspect of ray tracing, particularly in urban areas where building edges and rooftops form sharp edges that radio waves can bend around and over. The

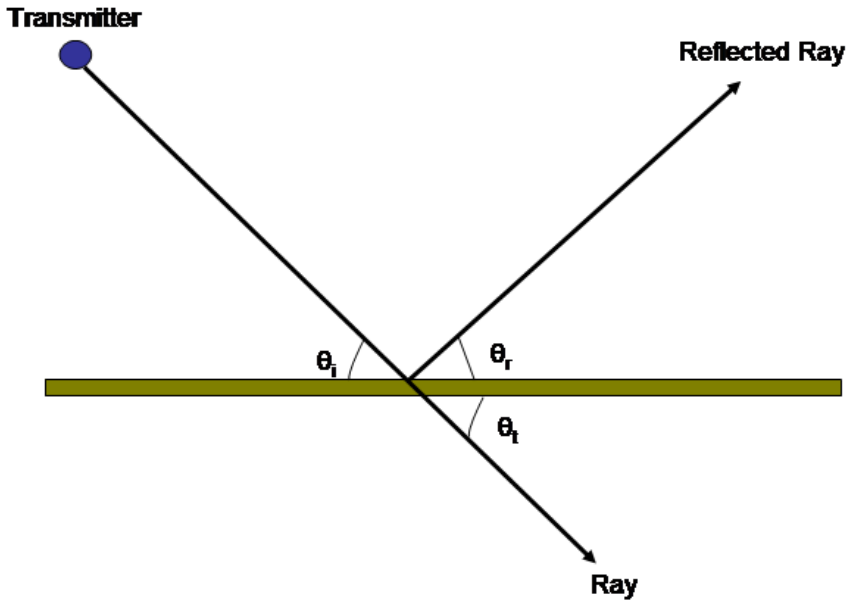

Figure 3.2: Representation of a transmitted electromagnetic wave (represented by a ray) intersecting with a surface. The ray both penetrates through and reflects off the surface.

likelihood of diffraction decreases as the frequency of the radio wave increases [89]. This effectively means that as a wireless communication system operates at higher frequencies, the impact of diffraction on the propagation of the signal decreases. Equation 3.13 provides the general form of the equation for determining the electromagnetic field strength of a diffracted ray [85].

$$E^d(s) = E^i D e^{(-jks)} \sqrt{\frac{\rho_0}{s(\rho_0 + s)}} \tag{3.13}$$

In Equation 3.13, E^d is the diffracted electric field vector, E^i is the incident electric field vector, s is the distance from the diffracting surface, D is the diffraction coefficient, ρ_0 is the radius of curvature along the diffracting edge of the surface, and k is the wave number ($\frac{2\pi}{\lambda}$).

Values for the diffraction coefficient in Equation 3.13 vary depending on the obstruction geometry and dielectric properties and may, in the context of the site-specific model detailed in Chapter 2 be embedded within or associated with any surface [85, 89]. Although not discussed later in this thesis, diffraction is another mechanism of radio wave propagation that could be explored within the context of this research.

3.4.4 Ray Tracing Methods

Two ray-tracing techniques are popular in the wireless communications industry. The *method of images* applies image theory to determine radiation paths. The second method is referred to as *brute-force ray tracing* or *ray launching* and relies on launching a finite number of rays from a transmit point to estimate radiation paths through the environment. The ray launching method of ray tracing has given rise to two subvariants: *ray shooting* and *tube shooting*. Other ray-tracing methods, such as *radiosity* and *finite element* techniques, although not as popular in wireless communications, have been applied successfully in other technology areas [24], [71]. However, both radiosity and finite element solution techniques grow computationally burdensome very quickly as the size and complexity of the site-specific environmental model increases [24], [71]. Although certainly valid techniques that can apply well in the context of this research, neither radiosity nor finite element solutions are discussed in this thesis.

3.4.4.1 Method of Images

Ray tracing algorithms that use the method of images place artificial sources in the environment that model reflections from the flat surfaces contained within the computer model of the physical environment [29, 59, 73, 175]. One advantage to the method of images is that the application of image theory ensures that exact radiation paths are determined [47]. One disadvantage to the theory of images is that the time required to map all of the images increases exponentially as the total number of surface elements present in the computer model of the environment increases [54]. Each additional surface incorporated into the computer model doubles the number of images that need to be considered [54]. Although this effect can be countered by discarding images that do not have a field of view to other surfaces, the

method of images still exhibits a strong dependence on database complexity and becomes less feasible when considering three-dimensional representations of environments such as cities where thousands of surfaces may be involved [47]. Although certainly a valid technique that can apply well in the context of this research, radiosity is not discussed further in this thesis.

3.4.4.2 Ray Launching

The technique of ray launching is very popular as a ray tracing method. The concept is relatively simple - project rays outwards from the transmit point and trace their trajectory as they reflect, diffract, and penetrate through the various surfaces in the environment. Field strength at receiver locations is determined on the basis of the various rays that intersect with the receiver or pass nearby. The computation time of ray launching algorithms is more closely tied to the number of rays launched from the transmitter than from the number of surfaces within the site-specific environment model [5].

It is advantageous to evenly distribute rays around a unit sphere centered about the transmitter from which the rays are launched [47]. One method for closely approximating this situation is to make use of a *geodesic sphere*. A geodesic sphere is a geometric figure achieved by tessellating the faces of a 20-sided regular polyhedron (an icosahedron) and extrapolating the intersection points to the surface of an encapsulating sphere. The tessellation of the icosahedron takes the form of subdividing each face of the icosahedron into equilateral triangles. The number of equilateral triangles that occur along the edge of each icosahedron face is referred to as the *tessellation frequency*. By launching rays from the center of the icosahedron through the vertices of each of these triangles, the launched rays will have nearly equivalent angular spacing around the entire sphere. The number of vertices of the formed triangles, and thus the maximum number of rays launched, can be determined through Equation 3.14.

$$V = 10N^2 + 2 \tag{3.14}$$

In Equation 3.14, V is the number Geodesic vertices generated given the tessellation frequency N. Figure 3.3 graphically represents the generation of a geodesic sphere having tessellation frequency of 6 [47].

Each ray launched using the Geodesic sphere method will be surrounded by exactly six

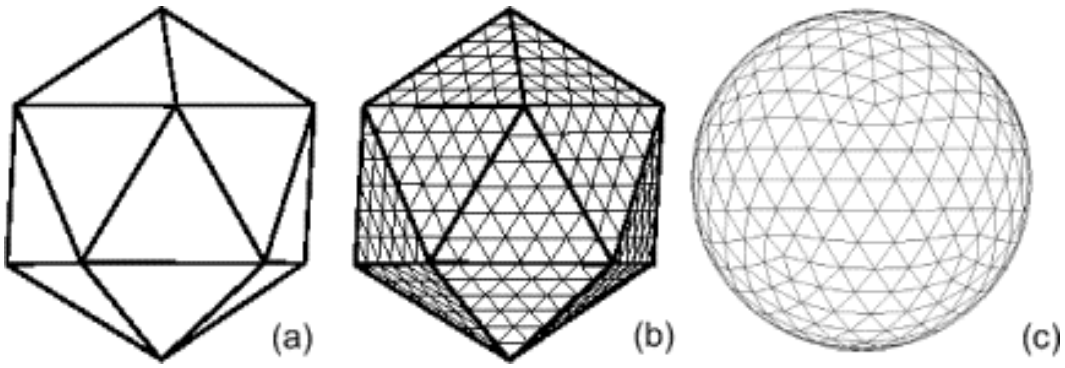

Figure 3.3: The icosahedron (20-sided polyhedron) shown in (a) is tessellated with equilateral triangles (b). The number of equilateral triangles is a function of the tessellation frequency. In this case, the tessellation frequency is 6, meaning that six triangles are formed along each edge of each face of the icosahedron. The final resulting geodesic sphere is shown in (c) [47].

neighboring rays in a hexagonal pattern. An average discrepancy of twenty percent exists between the minimum and maximum angular separations on any given Geodesic sphere [47]. Increasing the tessellation frequency will reduce the overall average angular separation between rays at the cost of additional rays being launched. The average angular separation between rays launched from a Geodesic sphere can be determined from the tessellation frequency as shown in Equation 3.15.

$$\bar{\alpha} \approx \frac{69.0^o}{N} = \frac{218.0^o}{\sqrt{M}} \tag{3.15}$$

In Equation 3.15, N is the tessellation frequency and M is the number of rays launched [47].

3.4.4.2.1 Tube Shooting Tube shooting is a ray tracing technique wherein each ray carries information regarding adjacent rays launched from the transmitter. The rays then outline an area (*tube*) as they propagate through the environment. The advantage of this technique is that the power at reception points is determined by the intersection of the receiver with the tube area rather than an individual ray [30]. However, the dependency between adjacent rays and the problems that arise when the adjacent rays take different paths through the computer model adds complexity to the algorithm [47].

3.4.4.2.2 Ray Shooting Ray shooting is basic, brute force ray tracing. Individual rays are launched from transmitters and propagate through the modeled environment entirely independent of the other rays. Rays that pass arbitrarily close to a receiver actually determine the field strength at the receiver. The relative simplicity of ray shooting lends itself very well to potential performance improvements. For this reason, the ray shooting method was selected for analysis within this thesis.

A reflection-based ray shooting method was implemented in software that encompasses all of the information presented thus far in this chapter. Figure 3.4 shows sample predictive output from *SitePlanner* produced using ray shooting models. Compare Figures 3.1 and 3.4, as both are representing the same propagation environment using two different radio wave propagation prediction models.

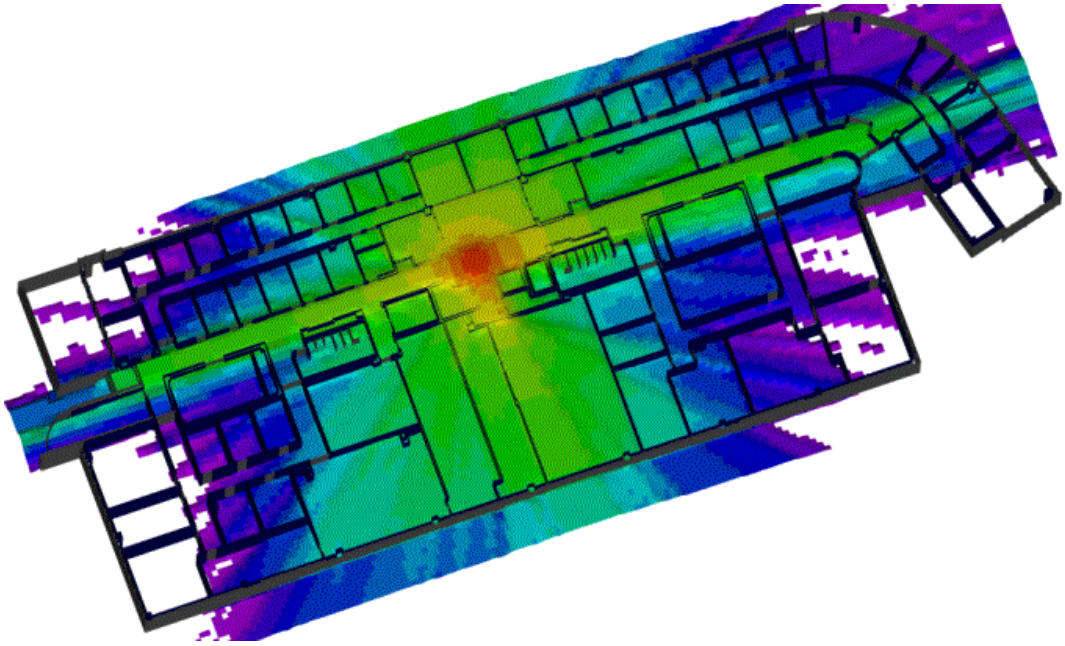

Figure 3.4: Predicted signal strength within the fourth floor of Durham Hall on the Virginia Tech campus given a test transmitter on the same floor. Predictions were performed using ray-shooting models within *SitePlanner*®from Wireless Valley Communications, Inc.

3.4.4.2.3 Reception Sphere As launched rays propagate outward from the transmitter, they spread out in space. To avoid the possibility of inadvertently missing a desired receiver

location as a result of this spreading, the receiver may be enclosed in a *reception sphere*. A reception sphere is a variable size spherical region centered about a receiver location. The size of the reception sphere is proportional to the unfolded path length of an incoming ray [155]. The goal of the reception sphere is to guarantee that a ray from each wave front is collected at the receiver location. Figure 3.5 shows a simplified example of a reception sphere being used in a ray launching model.

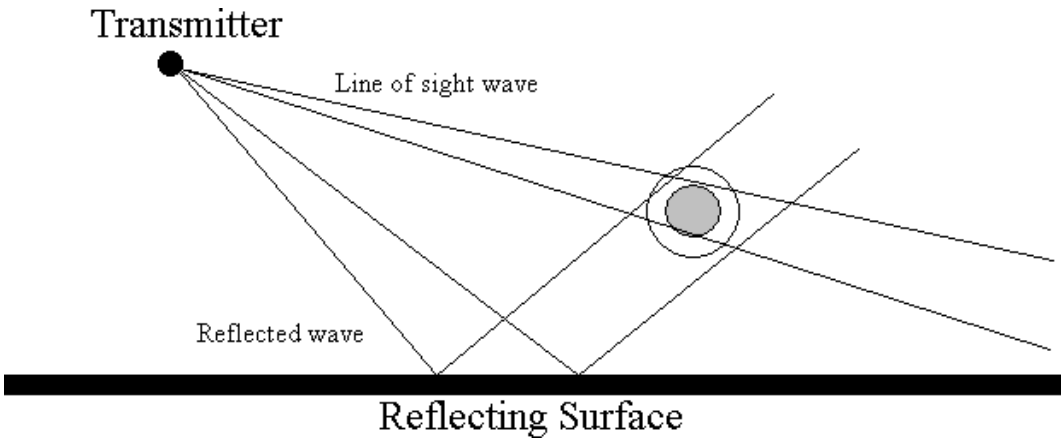

Figure 3.5: Reception spheres are sized proportional to the unfolded path length of incoming rays. For the line of sight (LOS) rays, the receiver reception sphere is smaller than for the reflected rays [44]

Ideally, exactly one ray is collected from each wave front. However, in practice it is not uncommon for two rays from the same wave front to be erroneously collected by a reception sphere simply due to the application of the reception sphere concept [47]. The accumulation of more than one ray per wave front by a reception sphere leads to a +3 (for incoherent summing) to +6 (for coherent summing) dB error in signal power at the receiver, and the contribution of the wave front will have effectively been double counted [47].

3.4.4.2.4 Distributed Wave Fronts Research pioneered by the Mobile and Portable Radio Research Group at Virginia Tech resolved the issue of double counting with the reception sphere method discussed in Section 3.4.4.2.3. The use of distributed wave fronts eliminates the problems of reception spheres by applying a three-dimensional weighting of the contribution of nearby rays to the total received power at a receiver location [47]. For

a given receiver location, the rays that pass nearby are identified and a three-dimensional weighting function is then applied to each ray in order to determine the contribution each ray makes to the total received power. This technique is detailed in [47]. It is a very useful in the context of this thesis to enhance the achievable accuracy of ray launching methods.

3.5 Ray Tracing Implementation

Due to its relative simplicity, robustness, and perceived opportunity for improved efficiency and optimization, the ray shooting method of ray tracing described in Section 3.4.4.2.2 was selected and implemented in software during the course of this research. The geodesic sphere ray launching method described in Section 3.4.4.2 was implemented in software. Referring to Figure 3.6 there is shown a screen capture of predicted ray tracing results. The prediction shown in Figure 3.6 displays both average RSSI and the power delay profile at the given point represented by the mouse cursor. In addition, angle of arrival at the given point may also be displayed, as angle of arrival information may be critical to system performance.

An analysis of the accuracy of the ray tracing simulation discussed within this thesis is presented in Section 3.8. Several enhancements were utilized to improve the initial performance of the ray shooting process. A *bounding volume hierarchy* (BVH) was utilized to reduce the number of intersection tests required during simulation. The BVH implemented is described briefly in Section 3.6. The necessity and importance of the reception sphere is one weakness of the ray shooting method, but a solution is proposed in Section 3.7. Because the ray tracing engine is fully capable of predicting the power delay profile and angle of arrival information at any point within the site-specific model, the research presented in this thesis also represents a superset of the functionality of the SIRCIM®and SMRCIM®channel modeling software applications developed by the Mobile and Portable Radio Research Group at Virginia Tech. SIRCIM and SMRCIM are statistical channel modeling software that provided for the prediction of power delay profile and angle of arrival data, but in a non-site-specific manner. This research advances that technology by providing for the prediction of channel statistics such as power delay profiles and angles of arrival in a site-specific manner.

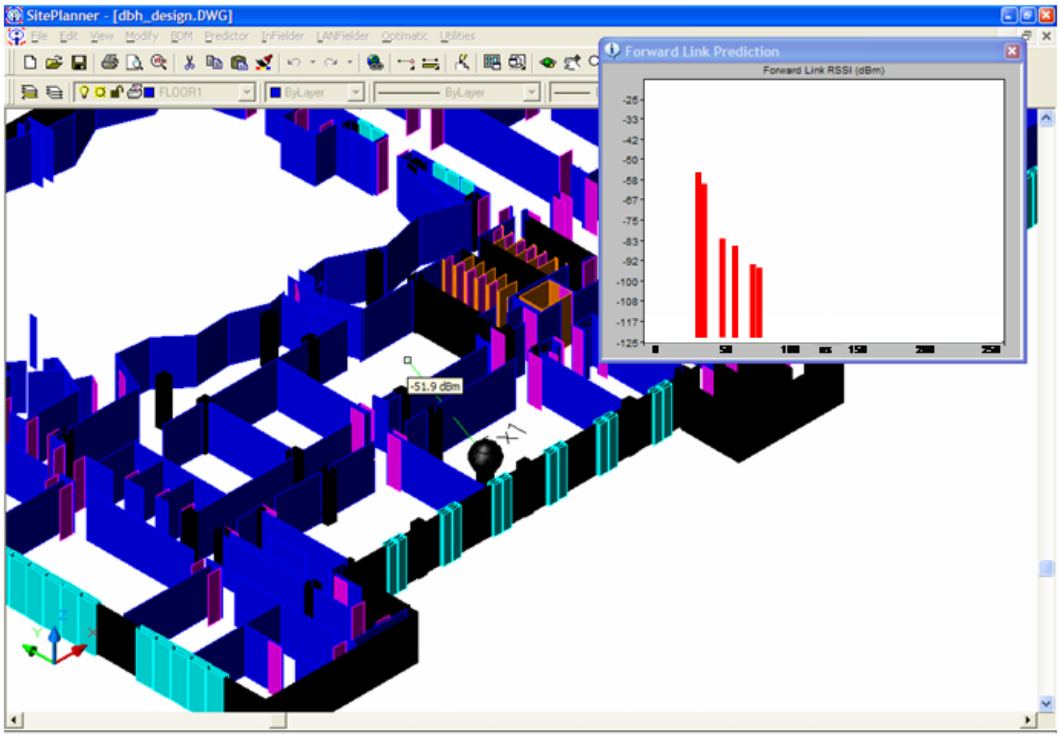

Figure 3.6: Predicted power delay profile at the given position within the site-specific model. The displayed power delay profile updates as the mouse cursor position changes.

3.6 Bounding Volume Hierarchy

The primary factor contributing to the total simulation time for the ray shooting method is the number of intersections tests performed between rays and the obstructions in the environment [47]. The simplest solution to reducing simulation time is to reduce the number of intersection tests. This can be achieved through the use of a bounding volume hierarchy.

Bounding volume hierarchies are cascaded virtual containers enclosing one or more surfaces within the site-specific model [151]. Before an intersection test is performed on a given surface, an intersection test is first performed upon the bounding volume container within which it resides. If a ray intersects a bounding volume container, additional intersection tests are then performed upon the entities within the container. Thus, large numbers of surfaces can be ignored based solely upon the single failed intersection test with the bounding volume container encapsulating the surfaces [151].

For the purposes of this research, an *irregular spherical bounding volume hierarchy* has been implemented. A spherical bounding volume hierarchy uses spheres as the chosen container [151]. The use of spheres reduces the complexity of the intersection test performed on the container itself. If the bounding volume container object were, for example, a cube, tests would be required on each face to determine whether a given ray intersects with the cube. By utilizing spherical bounding volume containers, the intersection test is simplified to merely determining if distance between the closest point on the ray to the center of the sphere is less than or equal to the radius of the sphere [151].

An irregular bounding volume hierarchy refers to the use of non-uniform bounding volume containers. That is, the construction of the bounding volume hierarchy is based upon the total number of entities encapsulated by the bounding spheres, rather than the physical region [151]. The algorithm used to construct the irregular spherical volume hierarchy is based upon limiting the number of surfaces contained by a single bounding sphere to a certain threshold.

The basic process implemented during this research for constructing an irregular spherical bounding volume hierarchy is presented in Figure 3.7.

The process of constructing an irregular spherical bounding volume hierarchy begins by enclosing the entire site-specific model in a single bounding sphere. If the total number of contained surfaces is greater than the chosen threshold, the total region encapsulated by the containing sphere is split into eight equally sized volumes, and each volume is then enclosed within a cube. The extents of the cube define the extents of surface entities contained by the cube. Surfaces that cross the boundaries of bounding cubes are split to form two separate surfaces, each having identical material characteristics. A spherical bounding volume is then created, constrained such that its position and maximum extents minimally enclose the cube. The process of dividing the total enclosed volume continues until a bounding sphere is constructed that encloses less than the threshold number of surfaces. Bounding spheres encapsulate smaller bounding spheres, creating a cascaded hierarchy of bounding spheres. Bounding spheres that enclose no surfaces are discarded and not considered during the prediction of radio wave propagation.

Figure 3.8 presents a simple representation of an irregular spherical bounding volume hierarchy when viewed from a top-down perspective. The present invention allows for the

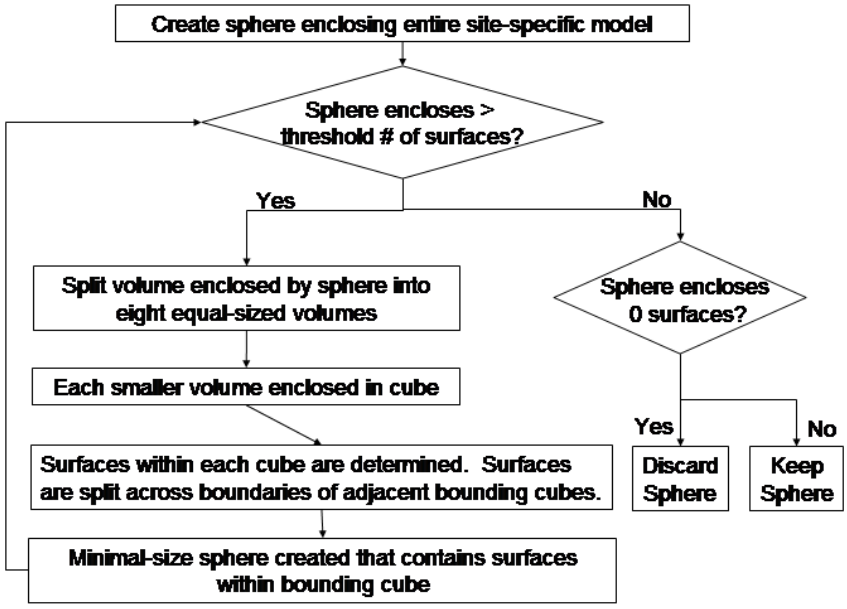

Figure 3.7: Process for creating an irregular spherical bounding volume hierarchy.

automatic construction and use of bounding volume hierarchies of the type presented without any required intervention or input from the user.

3.7 Reception Planes

One weakness of the ray shooting algorithm is the necessity of the reception sphere to determine when an electromagnetic wave has reached a receiver. As described in Section 3.4.4.2.3, the size of the reception sphere needs to increase as the total propagation distance of the ray increases due to the angular spread of the rays. If an intersection between a ray and a reception sphere is detected, the ray is assumed to have struck the receiver at the center of the sphere [155]. This inherently increases the computational complexity of the ray shooting algorithm, as the variability of the reception sphere size must be calculated with each increment in the ray propagation distance.

In order to provide a means of post-processing the ray tracing results, an alternative to the

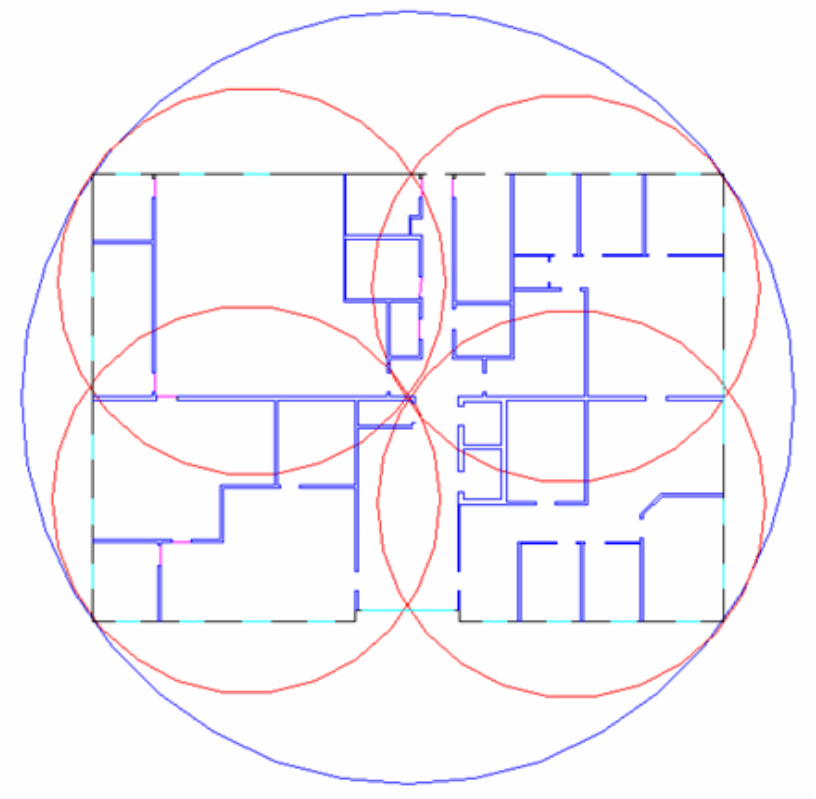

Figure 3.8: Sample irregular spherical bounding volume hierarchy.

use of reception spheres has been implemented. Instead of using variable-sized reception spheres, alternating horizontal and vertical *reception planes* are generated. Each reception plane extends to the bounds of the modeled environment. Figure 3.9 depicts two reception planes within a three-dimensional model of a building. Note that in two dimensions (for example, if the site-specific model of the environment is two dimensional), each reception place would become a reception line, but the same approach could be used.

Intersections between each ray and each reception plane are stored. At each intersection, basic information such as propagation length, received power, and previous intersection points along the ray path is stored in computer memory. The result, depicted in Figure 3.10, is a pin-cushion effect on each reception plane.

It is important to note that intersections between rays and reception spheres are performed during the simulation without thought to reception sphere size or placement of receivers,

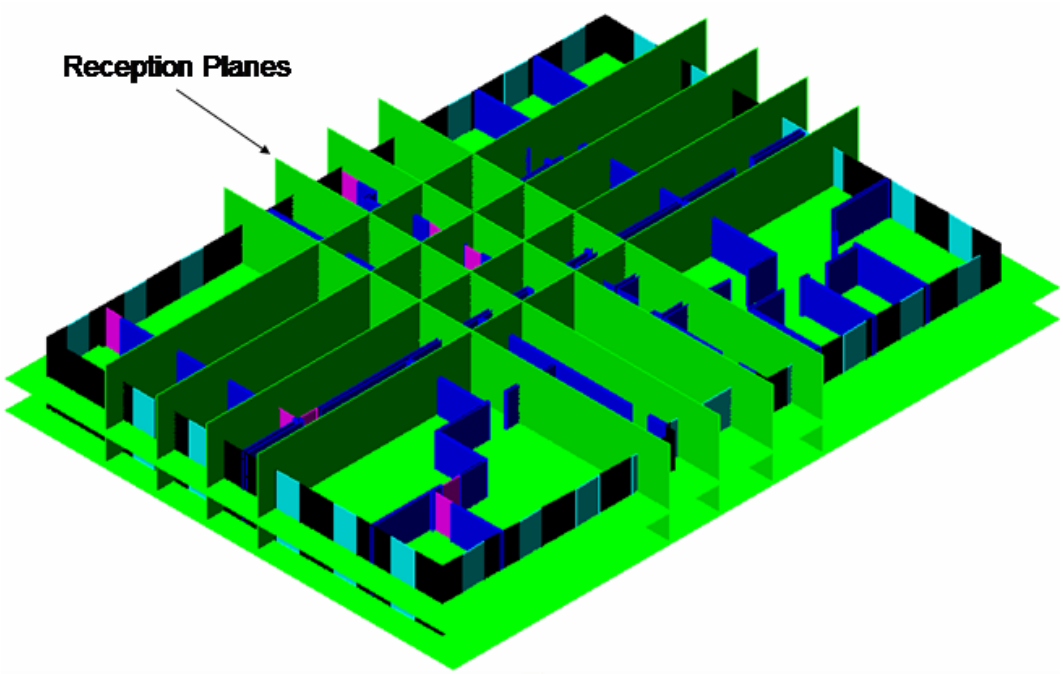

Figure 3.9: Example visual representation of reception planes within a three-dimensional model of a building. The reception planes are shown in green, overlaid onto the building model.

and is independent of the bounding volume hierarchy. It also enables the simulation to be performed without thought to the number, placement, or spacing of reception points. The number and/or spacing of receptions planes are completely definable by the user, before, after, or during the ray tracing simulation. Further analysis is needed beyond the scope of this thesis to verify the impact of varying numbers and/or spacing of reception planes in the overall accuracy of the prediction.

The second advantage to the use of reception planes is in the ability to apply varying post-processing results. As noted in Section 3.4.4.2.4, the use of various weighting algorithms can be applied to each ray in terms of its proximity to the center of a reception sphere in order to improve the accuracy of the predicted result. Through use of reception planes, ray intersections are captured and stored in an efficient manner. At any point in time following the simulation, the site-specific model can be overlaid with any number and spacing of receivers, and/or any type of weighting algorithm can be applied to achieve different

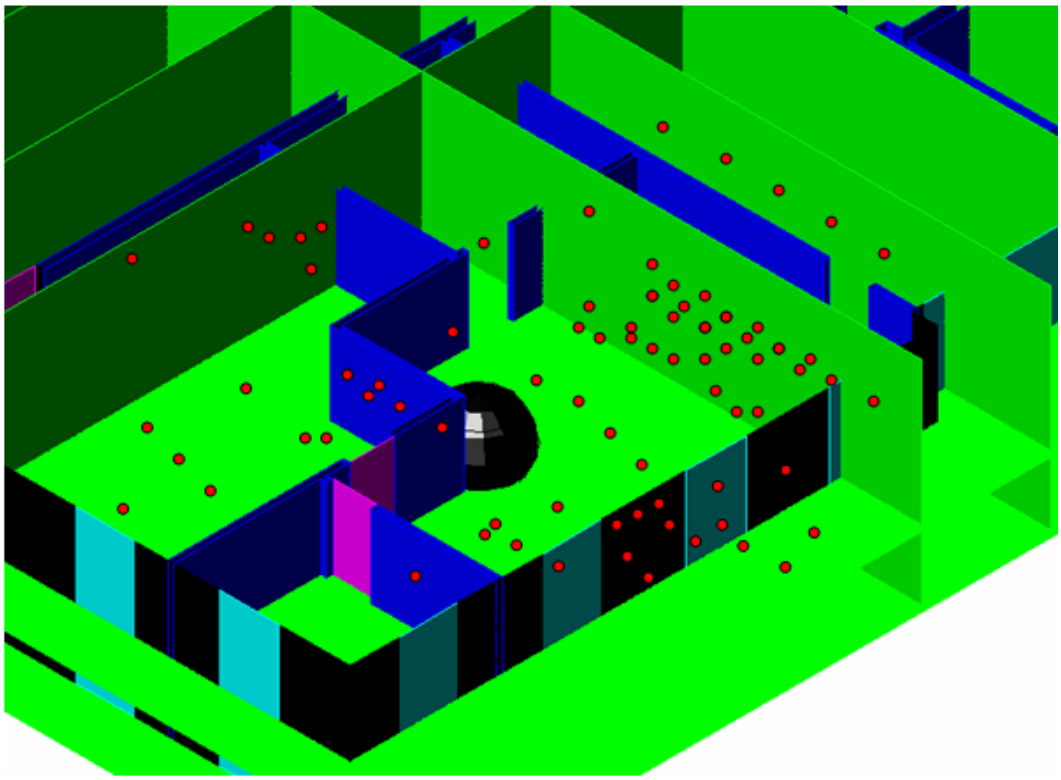

Figure 3.10: Example visual representation of reception planes within a three-dimensional model of a building with intersection points highlighted.

outcomes, without the need to repeat the ray tracing simulation. Because predicted ray intersections are captured and stored on each reception plane, variable resolution predictive results can be applied arbitrarily during the post-processing stage without the need to repeat the ray-tracing simulation.

The software enables a user to specify the resolution of the predicted result, or can automatically determine the ideal resolution based upon the number and spacing of each ray intersection on the reception plane. This enables virtual receivers to be created on-the-fly with the position of the receiver relative to the nearest reception planes used to determine the rays which intersect the receiver at that location. For example, regularly spaced rows and columns of receiver locations of arbitrary size can be created across any reception plane and the rays intersecting those receivers can be efficiently calculated in near-real time since

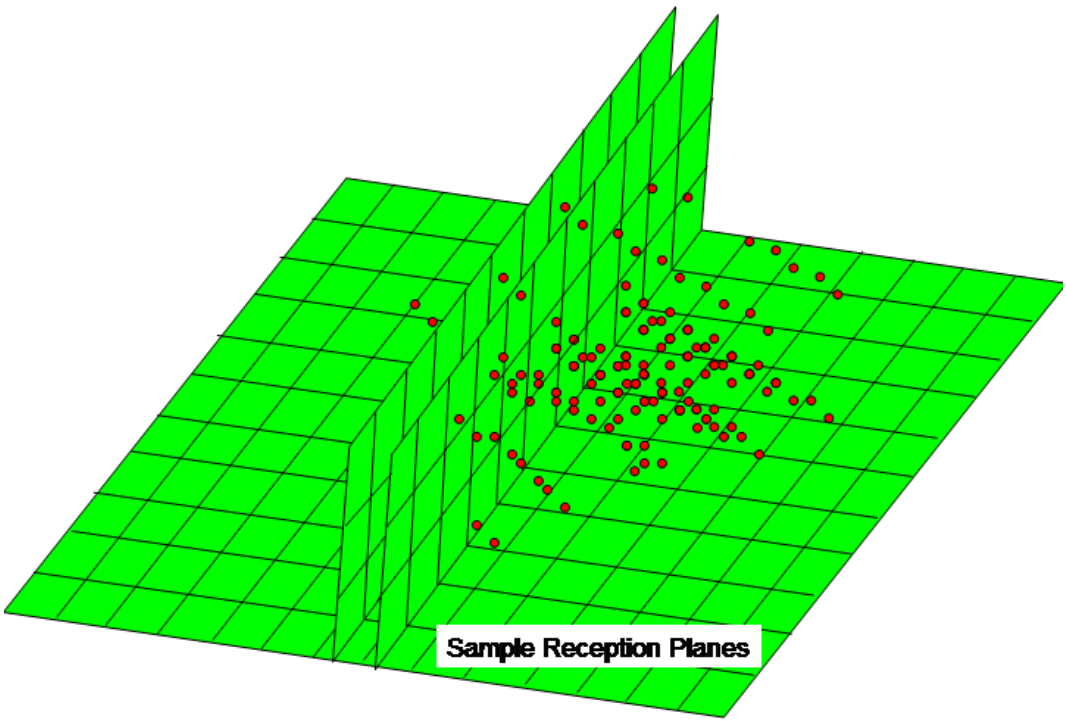

Figure 3.11: Example visual representation of a grid of receiver locations overlaid across a reception plane following simulation. This form of post-simulation processing is advantageous in analyzing and interpreting the results of the ray tracing prediction in many different ways without needing to repeat the prediction.

the only rays that need to be considered are those having already intersected the nearby reception planes. This is illustrated graphically in Figure 3.11. Note that with evenly spaced horizontal and vertical reception planes, any arbitrary point within the site-specific model can be enclosed in an arbitrarily sized cube formed by the intersections of the reception planes. This is graphically illustrated in Figure 3.12. The rays that intersect the cube and the angles of their intersection are known through analysis of the reception planes bounding the point.

The more reception planes that are utilized, the more memory required to store the predicted results. However, as of the time of this writing typical computing platforms are not limited in terms of either storage or memory, and this is not viewed as an overly restrictive factor

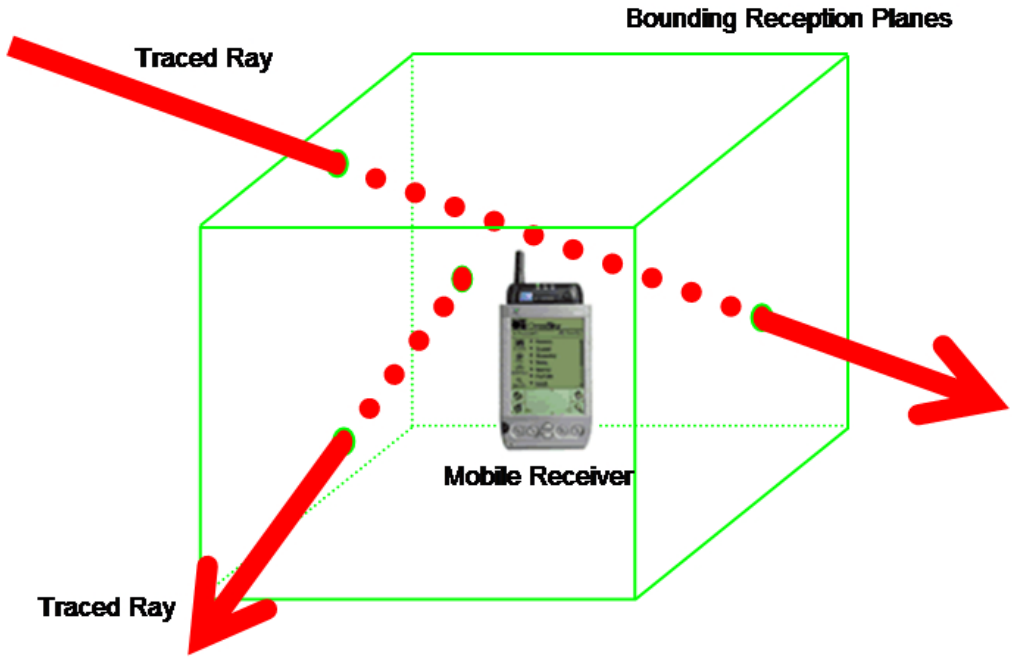

Figure 3.12: By using evenly spaced horizontal and vertical reception planes, any point in space within the site-specific model is effectively enclosed by an arbitrary sized cube. The rays intersecting the cube and the angle of arrival of the rays are effectively pre-calculated for any point as a result of the reception planes.

in the simulation.

It is hypothesized that the use of reception planes will greatly assist in the empirical tuning of ray tracing predictive accuracy. The ability to rapidly determine information regarding nearby rays at any arbitrary point in the three-dimensional site-specific model without having dramatically increased the overall simulation time is a substantial improvement over published literature.

3.8 Verification of Results

To verify the accuracy of the ray tracing predictive engine, a considerable number of measured RSSI levels were recorded and compared versus the predicted RSSI levels. A measurement campaign was carried out by Wireless Valley engineers in the School of Public Hygiene building on the Johns Hopkins University campus. This campaign was carried out using three IEEE 802.11b Cisco 340-series access points as transmitters with an additional Cisco 340 PCMCIA WLAN card in a Windows Pentium III class pen tablet personal computer. Two of the access points (identified as *Tx2_HygW3030* and *Tx3_W3014* in Figure 3.13) were positioned on the third floor, while the fourth (identified as *Tx8_4130* in Figure 3.13) was placed on the fourth floor. Measurement data was collected on the fourth floor using *LANFielder*®, a software application developed at Wireless Valley Communications that is capable of simultaneously measuring RSSI, throughput, packet error rate, rogue access points, and other crucial performance information and storing the measurements site-specifically within a computer model of a physical environment [163]. The measurement data was collected by powering on a single access point at a time, and then walking through floor four recording measurement readings using *LANFielder*. These measurement readings are indicated in Figure 3.13. Although Figure 3.13 only shows measured RSSI levels, *LANFielder* can display any of the recorded performance metrics, such as throughput and packet error rate, in a similar fashion.

A full ray tracing simulation was carried out in the software using the given site-specific building model. To convert the traced rays into a single predicted RSSI level, simple coherent summation was used rather than the distributed wave front concept discussed in Section 3.4.4.2.4, although either technique can be used effectively in the software [47]. Figure 3.14 graphically depicts the predicted ray tracing results overlaid onto both the site-specific model and the measurement data. To generate Figure 3.14, an average angular spread of one degree was used to launch rays from each of the three access points. Three reflections were allowed for each ray, and a maximum propagation distance of 200 feet for each ray. A fixed 3 dB attenuation loss per reflection was incurred on each ray. Reception places were spaced at five feet (roughly two meters). Building materials included Thin Concrete Walls (10 dB attenuation at 2.4 GHz) and Wooden Walls/Doors (1.8 dB attenuation at 2.4 GHz). The loss as RF signals penetrated from floor three to floor four was 15.3 dB at 2.4 GHz.

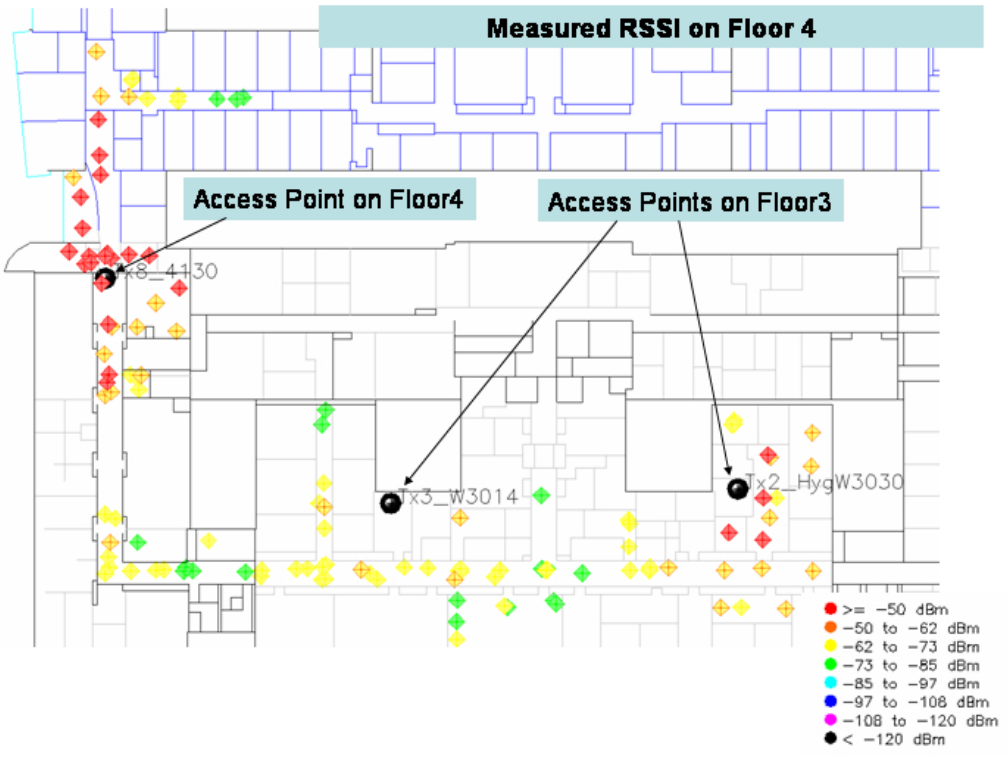

Figure 3.13: Measured IEEE 802.11b RSSI data collected on the fourth floor of an academic building on the Johns Hopkins University Campus. Two access points on the third floor and a third access point on the fourth floor were used. Measurements were site-specifically recorded using *LANFielder*®from Wireless Valley Communications. Measurement data is shown overlaid onto the site-specific model of the fourth floor.

Table 3.8 lists the mean error and standard deviation between the measured and predicted data for each access point individually.

3.9 Conclusion

A novel and unique implementation of a reflective ray shooting algorithm has been implemented. The use of reflective ray shooting is sufficient to accurately gauge wireless network

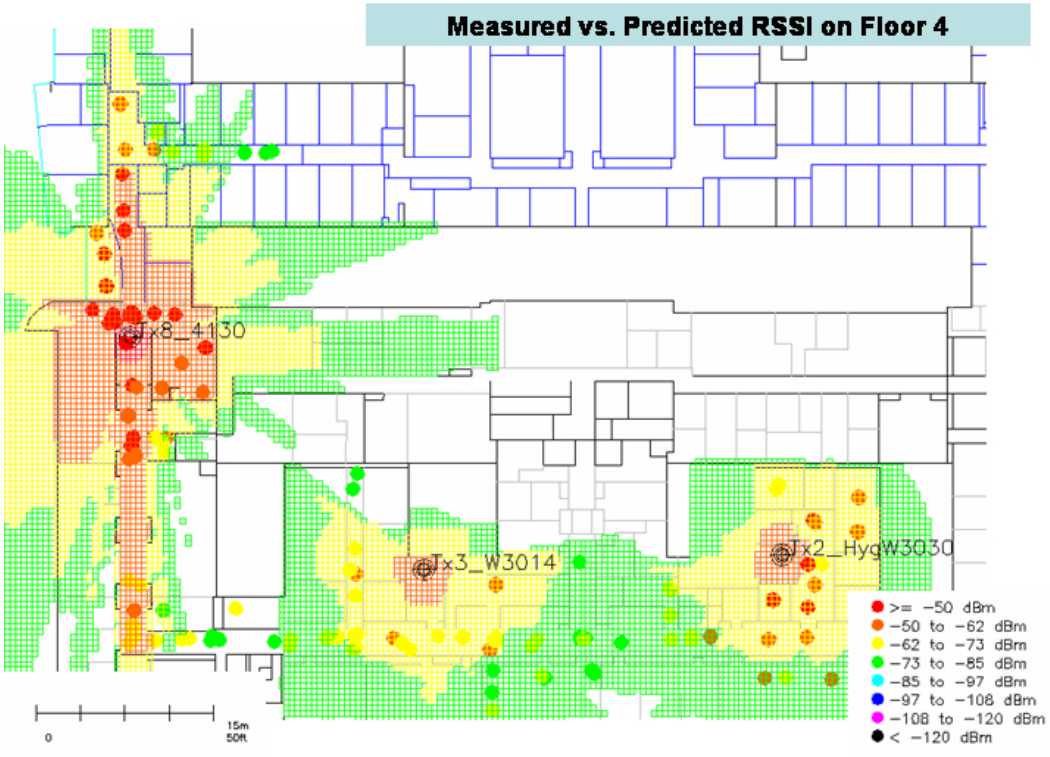

Figure 3.14: Predicted IEEE 802.11b RSSI on the fourth floor of an academic building on the Johns Hopkins University Campus using ray tracing. Two access points on the third floor and a third access point on the fourth floor are predicted. Predicted RSSI is shown overlaid onto the site-specific model of the fourth floor and along with the measurement data from Figure 3.13. $\sigma = 3.7$ dB

performance both inside and between buildings. While diffraction is not implemented within this thesis, it is well-understood, and the addition of diffraction to the algorithm will provide enhanced accuracy in urban areas where rooftop diffraction is an important consideration. The ray shooting method utilizes the concept of geodesic ray launching and irregular spherical bounding volume hierarchies to improve overall implementation performance and accuracy. The concept of reception planes is an original contribution that improves the performance of the ray shooting algorithm. Each reception planes stores ray intersections at their true point within the site-specific model. Any point within the site-specific model can be identified following the ray tracing simulation and the surrounding reception planes can be used to identify the rays that affect a receiver at the given point. Additional research is required to

Table 3.1: Measured versus predicted RSSI statistics for the ray tracing simulation shown in Figure 3.14.

Access Point	Floor	# Measurements	Mean Error (dB)	Standard Deviation (dB)
TX8_4130	4	55	1.25	3.46
TX3_W3014	3	41	2.28	2.41
TX3_HygW3030	3	22	3.99	5.52

determine the best method by which the reception plane concept put forth in this thesis will support empirical tuning of ray tracing results, which should be feasible. In addition, the research presented in this thesis improves upon the SIRCIM and SMRCIM channel modeling software concept by enabling the prediction of power delay profile and angle of arrival information to occur site-specifically, which was not possible in either SIRCIM or SMRCIM.

Chapter 4

Equipment Modeling

4.1 Introduction

One of the original contributions of this thesis, through work at Wireless Valley Communications, is the creation of an entirely new class of wireless design and simulation software that tracks and displays the location of network infrastructure. This chapter focuses on the various methods and technologies for representing individual wireless network equipment interconnection and performance. The type of equipment used, the manner in which the equipment is interconnected, and the combination of different transmitter and receiver types can directly change the simulated and actual performance of a wireless communication network. For example, using a handheld personal digital assistant (PDA) to send a file over a WLAN will generally take longer than sending the same file from a laptop. This is due to the relative computer power of the two platforms and the manner in which the Internet protocol (IP) stack is implemented on each. As another example, it has been shown that intermixing WLAN access points from one vendor with PCMCIA WLAN cards from a different vendor will result in different performance than if both access point and PCMCIA card were from the same vendor [72]. Even more obvious, different antennas made by different vendors will provide different coverage patterns, and the placement of antennas or cable lengths impacts system performance. Because of the impact of varying component layouts and configurations in a wireless system, it is important for any accurate representation of wireless network performance to account for the types of equipment being used. This chapter presents a novel

technique for representing and visualizing wireless network distribution systems developed and commercialized within *SitePlanner*®from Wireless Valley Communications, Inc.

4.2 Equipment Library

In order to implement design and simulation software capable of predicting wireless network performance that accommodates network components and their placement, a method was developed for representing equipment with the site-specific model. Most wireless network equipment can be placed in one of several categories, including by not limited to: Amplifier/Attenuator, Antenna, Base Station, Cable, Connector/Splitter, Mobile Receiver, Radiating Cable, and other components. The equipment within each category share many of the same characteristics, although specifications (such as gain, size, cost, frequency range, etc.) may vary between components within each category. In addition, there are certainly overlaps between the characteristics of equipment from different categories. Characteristics descriptive of the equipment include: manufacturer, part number, insertion loss, coupling loss, amplification/attenuation, number and modality of input connectors, number and modality of output connectors, noise figure, frequency variable effects, radiation characteristics (antennas only), and cost. In addition maintenance history is also stored and maintained.

An editable database of equipment, stored in an Extensible Markup Language (XML) format, was implemented at Wireless Valley during the course of this research. Figure 4.1 provides a screen capture of the edit dialog for a particular cable within the database.

Since equipment behaves differently depending on the frequency of the signal driving it (e.g., the loss of a cable is different at 900 MHz than at 5.85 GHz), the equipment library fully supports and accounts for frequency-dependent effects. In addition to the basic characteristics listed above, base stations and mobile receivers have additional parameters that set them apart from other pieces of equipment. Base stations and mobile receivers may be defined to have a particular set of one or more air interfaces, where an air interface provides a definitive description of the wireless standard on which the device is operating. For example, the IEEE 802.11b wireless LAN standard is a possible air interface for an access point (i.e., a base station) or mobile PCMCIA modem card (i.e., a mobile receiver) to support. A generic method representing any wireless protocol or standard was implemented in software.

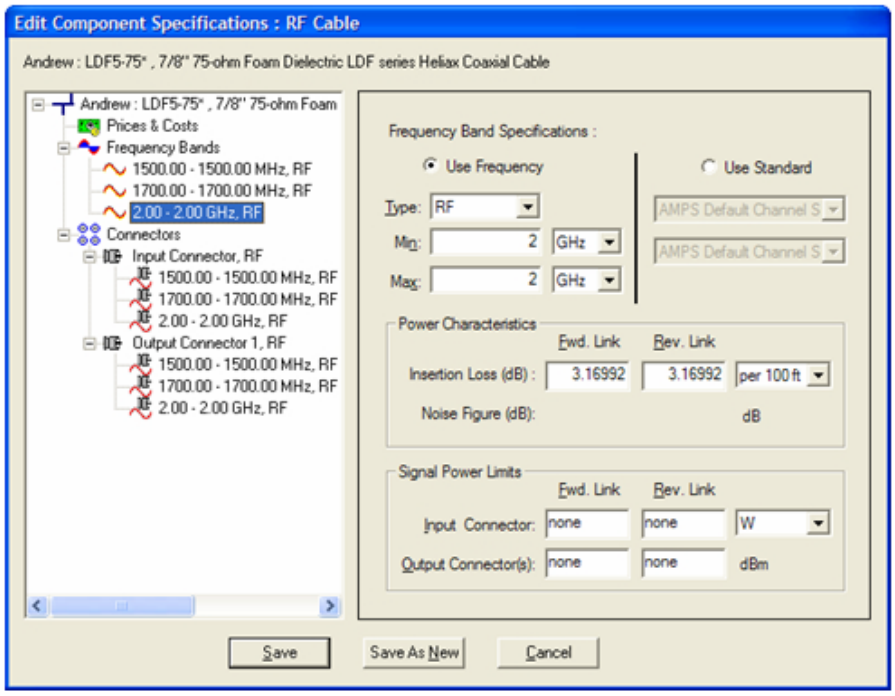

Figure 4.1: Screen capture from *SitePlanner*®from Wireless Valley Communications, Inc. showing the edit window for a cable from the equipment library.

Using this method, any air interface can be represented for the purpose of predicting wireless network performance. Parameters used to describe a wireless standard include, for example, frequencies, bandwidth, modulation scheme, and maximum throughput. Figure 4.2 shows a screen capture of a portion of the base station edit dialog.

4.3 Placing and Interconnecting Equipment

As a direct result of this research, software was implemented that enables a user to place and interconnect pieces of equipment in order to site-specifically construct a model of any wireless communications network. This is implemented by simply allowing the user to select a particular piece of equipment from the equipment library, as shown in Figure 4.3, and then identifying the location within the site-specific model of the environment where the piece of equipment is desired.

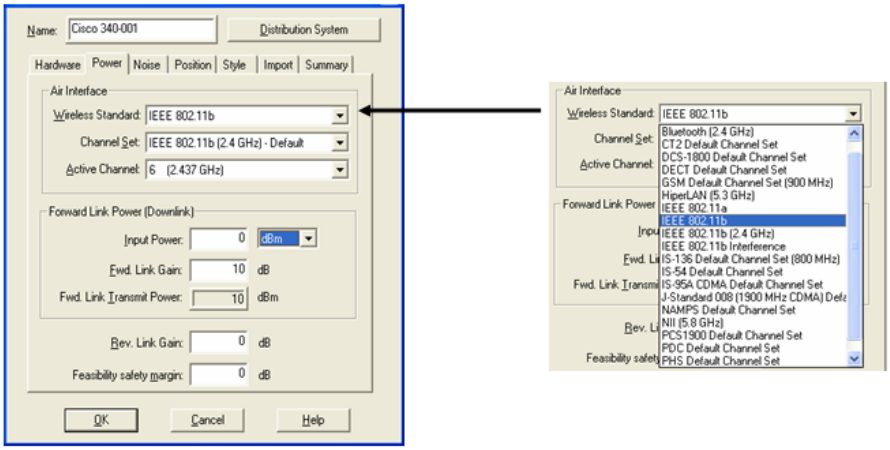

Figure 4.2: Screen capture from *SitePlanner*®from Wireless Valley Communications, Inc. showing the edit dialog for a base station. The *Wireless Standard* pull-down menu shows a pick list of possible air interface standards.

Typically, the identification of location is accomplished by simply clicking with the mouse. In Figure 4.4, a user is positioning a cable within a building by repeatedly clicking with the mouse to indicate where each bend in the cable occurs. A helpful tooltip is provided to the user indicating total length and loss through the cable.

If the selected piece of equipment has further configuration settings (e.g., an antenna can have a specific orientation), the system provides the ability to do so. For example, Figure 4.5 displays the dialog box allowing the user to specify the antenna orientation. As the cable in this example is placed within the site-specific model by the user, the software continually computes and displays the vital design data such as loss, signal strength, length, and cost, and warns the user if the cable has exceeded any manufacturer or user-specified design constraint, such as, for example, maximum cable length. The modeling of the electromagnetic behavior of all network components is vital for assuring proper simulation of a complete network and not just individual antennas as previous works have considered. The ability to interconnect wireless network equipment within a site-specific model while predicting the performance of the resulting network is a novel invention and a direct result of this research [142], [145].

The user may also indicate interconnections between different pieces of equipment. This takes the form of identifying the desired output connector of an existing piece of equipment already

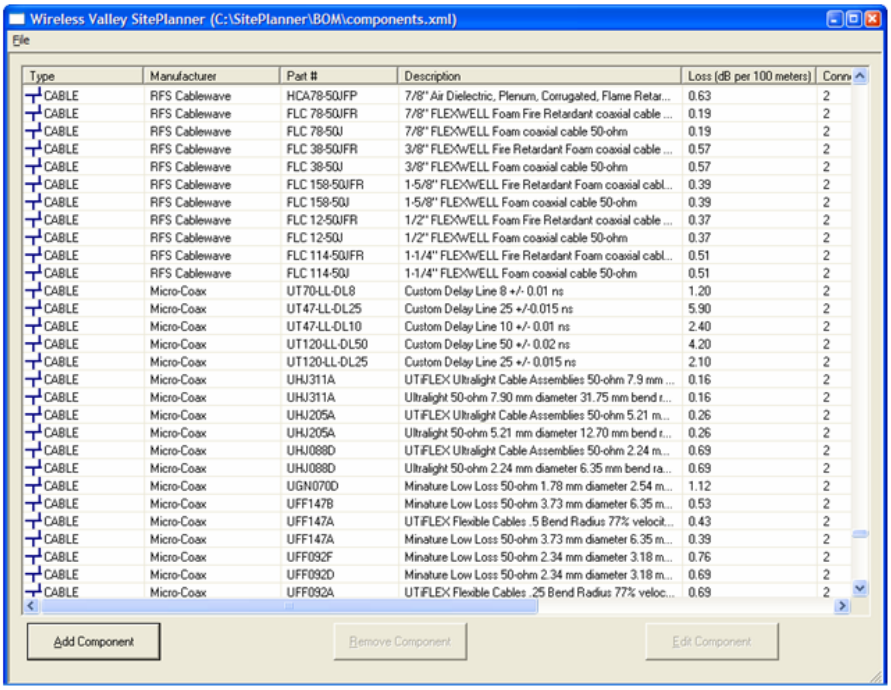

Figure 4.3: Screen capture from *SitePlanner*®from Wireless Valley Communications, Inc. showing a selection list of equipment available for placement within the site-specific model.

placed in the site-specific model. By repeating the selection, interconnection, and placement process, a detailed representation of a wireless communication network is constructed in a very rapid manner. Figure 4.6 contains a screen capture depicting logical equipment interconnections within a complex wireless network distribution system. In the background of Figure 4.6, the physical position and interconnection of the same wireless distribution system is displayed in a site-specific context.

Within the software, interconnections between individual pieces of equipment are maintained using an ordered, triply-linked, multi-child tree data structure [151]. The root of the tree is usually the base station or mobile receiver. Figure 4.7 depicts a typical tree structure used to store the interconnections between pieces of equipment in the distribution system.

Through the described process, the user may construct a complete physical and logical representation of any wireless communication network. Because each piece of equipment has detailed operating characteristics supplied within the equipment library of Section 4.2, the

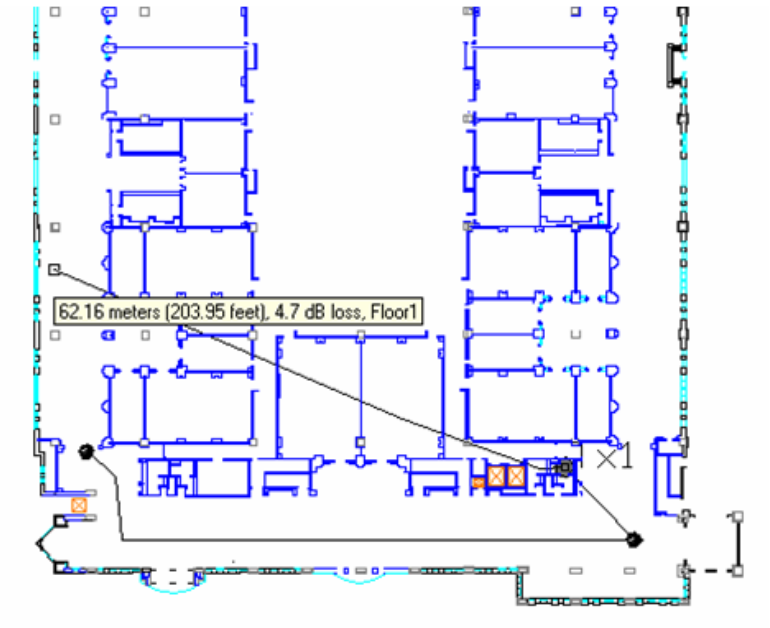

Figure 4.4: Screen capture from *SitePlanner*®from Wireless Valley Communications, Inc. showing the placement of a coaxial cable within the site-specific model.

software can determine the impact that the particular combination of equipment types and interconnections can have on overall network performance. This provides an unprecedented ability to simulate the performance of the overall wireless network [143]. The relative gains, losses, and transmission delay through the network of interconnecting equipment and overall system noise figure can be automatically calculated and incorporated into the site-specific predictions described in Chapter 3 [143], [145].

As an example of the impact the distribution network can have on overall wireless network performance, Figures 4.8 and 4.9 provide predicted performance contours for two nearly identical wireless networks. The wireless network in Figure 4.8 uses low-loss coaxial cable, while the same network in Figure 4.9 uses high-loss cable.

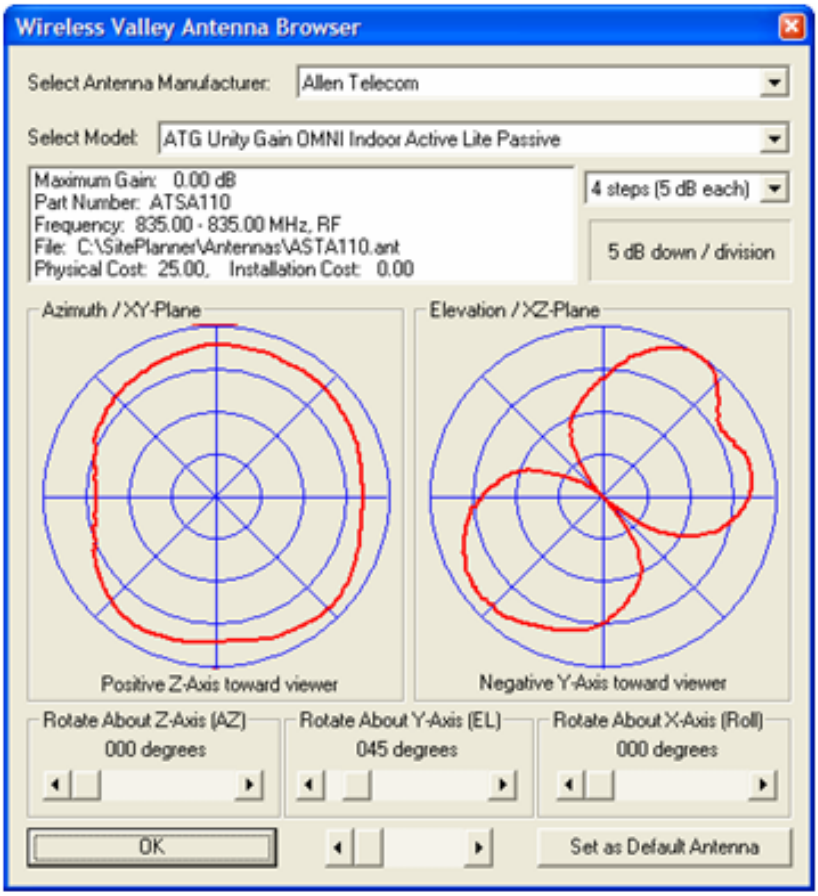

Figure 4.5: Screen capture from *SitePlanner*®from Wireless Valley Communications, Inc. showing the ability to control the orientation of an antenna.

4.4 Optimal Equipment Placement

Because of the myriad decisions involved in the design of a wireless communications network, it is advantageous if an automated method were available to determine near-optimal equipment placements in addition to extensive interactive capabilities. Prior art regarding this task has focused on either local optimization of equipment already positioned and configured, or is incapable of considering the effect of installing infrastructure on other floors of a building [160], [59]. Furthermore, no work prior to this thesis considered the effect of distribution component placement, interconnection, and/or placement. Nor did any work prior to this thesis consider the optimal selection and placement of components in a wireless

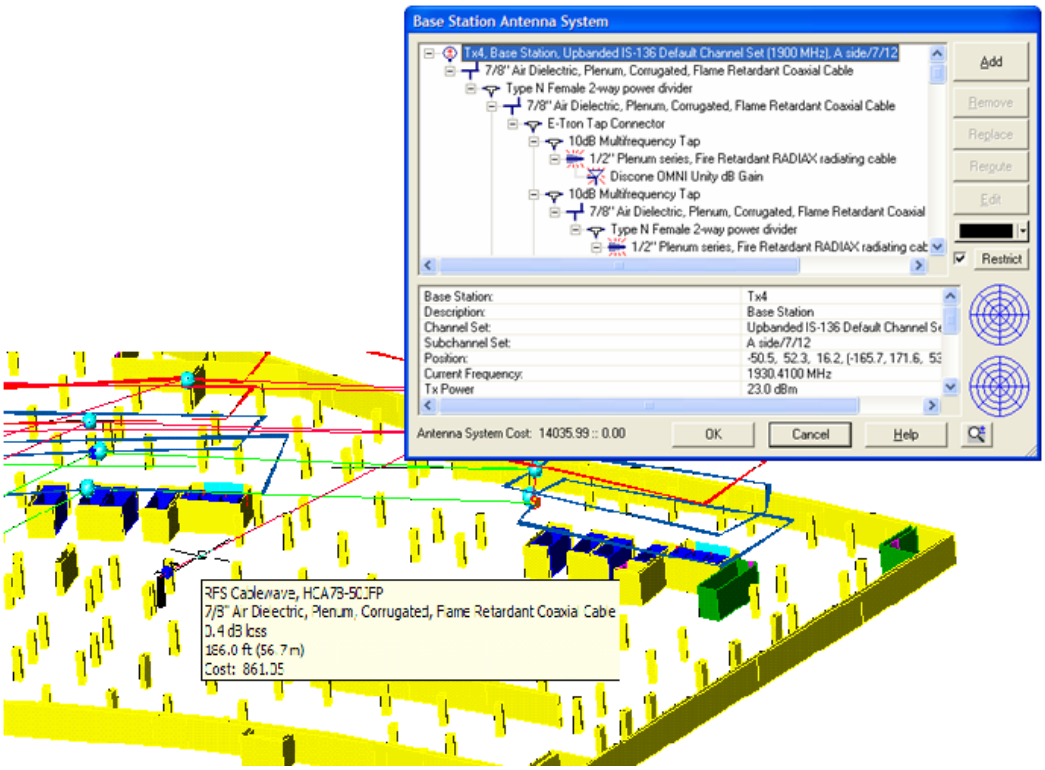

Figure 4.6: Screen capture from *SitePlanner*®from Wireless Valley Communications, Inc. the site-specific placement and interconnection of equipment alongside the logical equipment interconnections.

network. Several patents have been filed by Wireless Valley Communications, Inc., on this improvement on the state of the art. One result of this research is a fully repeatable process of determining the number, placement, and configuration of wireless communication network equipment in order to achieve a certain desired level of performance [145]. The process can be divided into a series of steps, each of which is described in the following sections.

4.4.1 Equipment Selection

In order to place bounds on the problem of automating equipment placement, the first step in the process enables the user to select the subset of equipment types to consider. As discussed in Section 4.2, one part of this research resulted in the creation of a system for representing technical, operational, cost, and maintenance characteristics of wireless network equipment

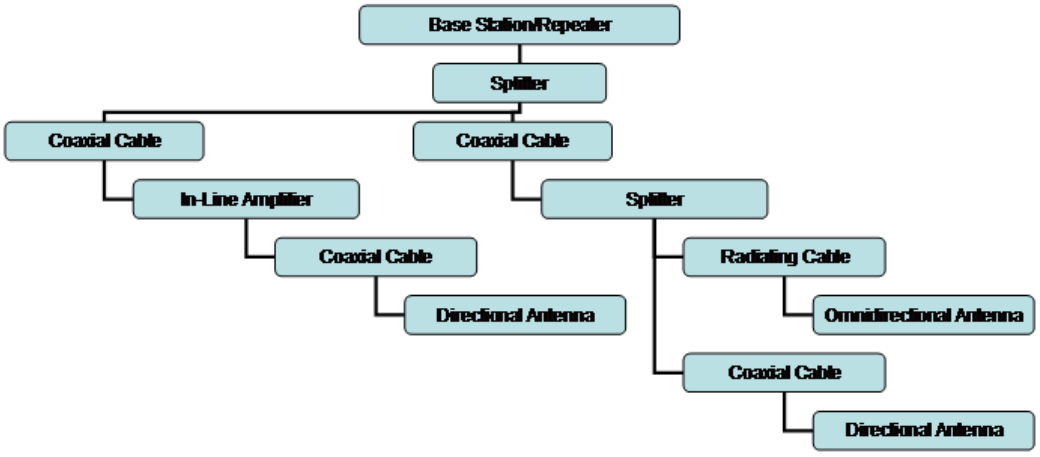

Figure 4.7: Typical tree data structure used to manage interconnections between pieces of equipment in a distribution.

in a library. The user selects one or more pieces of equipment that, when interconnected, form a complete wireless network. For example, the user may identify a particular make and model of wireless LAN access point with a specific antenna attached to it. In addition, each piece of equipment may have additional configuration settings that must be considered. For example, a wireless LAN access point may be configured to transmit and receive on a particular channel or at a particular output power setting. Figure 4.3 provides an example of a pick list the user interacts with during this step. This set of equipment and equipment configurations will be iterated during the processing loop in Section 4.4.4.

4.4.2 Valid Position Selection

By reducing the number of possible locations within the modeled physical environment at which the selected wireless network equipment can be positioned, the time required to complete the processing loop can be dramatically reduced. In the present invention developed in this thesis, the selection of valid positions takes one of two forms.

In the first form, the user actively pre-selects a set of positions within the site-specific model of the environment at which an access point or other network equipment is allowed to be placed.

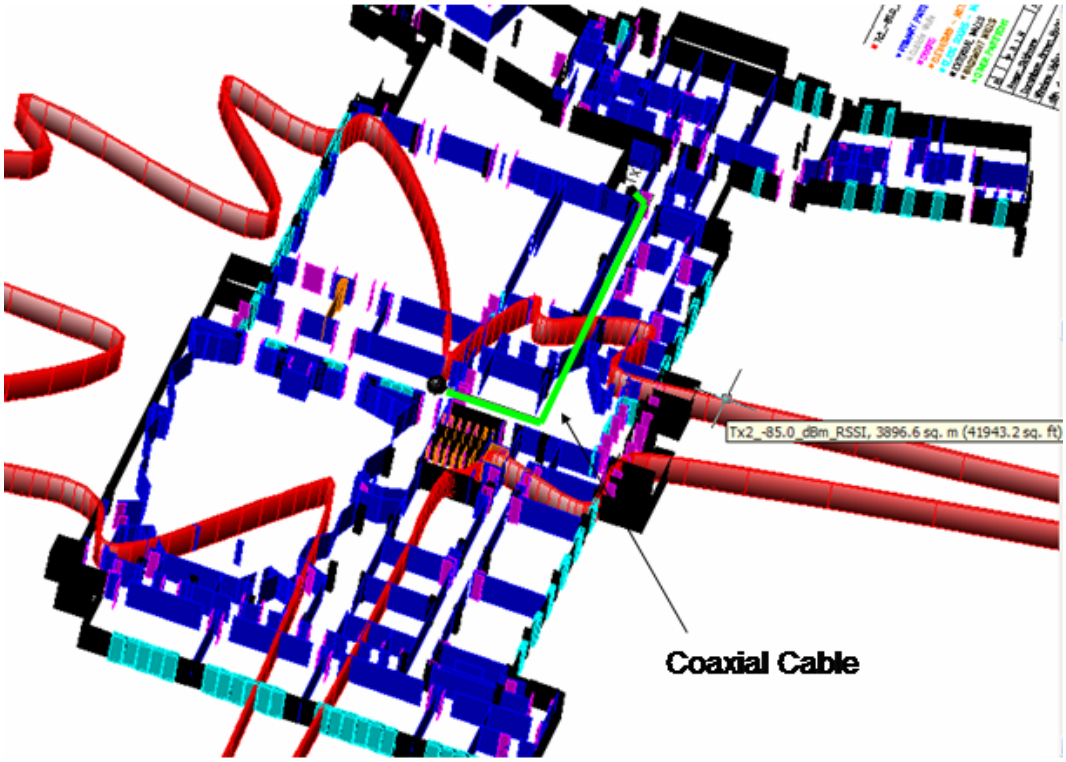

Figure 4.8: Screen capture from *SitePlanner*®from Wireless Valley Communications, Inc. showing the predicted -85 dBm RSSI boundary for the given wireless network. A low-loss coaxial cable is used.

This is typically done by using a mouse or other computer pointing device to select a point in space within the site-specific model of the environment. As points are identified by the user which have access to existing network infrastructure and/or power, or which the building owner or other authorities have identified as valid locations for network infrastructure, they are added to a set of possible equipment positions for later iteration. The process of the user actively selecting individual positions to consider for network infrastructure placement typically leads to a sparse matrix of irregular positions scattered through the site-specific model, as shown in Figure 4.10.

In the second form of the position-selection process, the physical model of the environment is overlaid with a matrix of regularly spaced positions as shown in Figure 4.11. The user may regulate the spacing between points in the grid, and a wide range of points, grids, or grid shapes may be used to discretize the modeled physical environment.

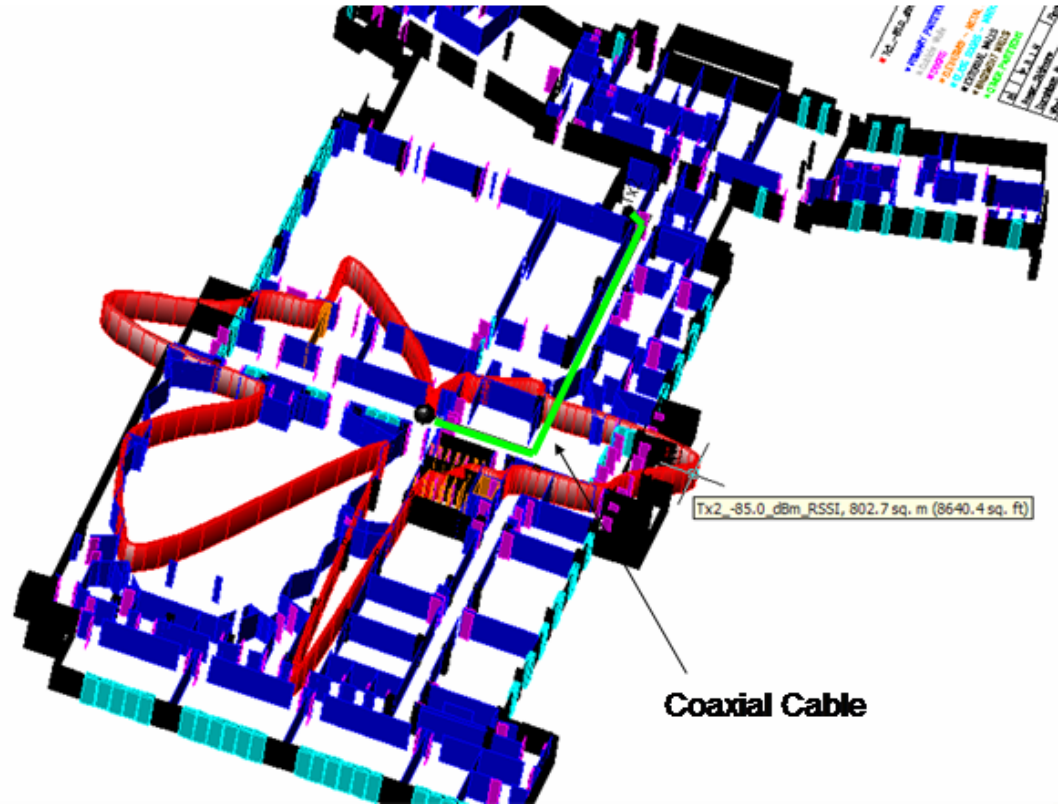

Figure 4.9: Screen capture from *SitePlanner*®from Wireless Valley Communications, Inc. showing the predicted -85 dBm RSSI boundary for the given wireless network. A high-loss coaxial cable is used, as opposed to the low-loss coaxial cable in Figure 4.8.

As this can quickly lead to a computationally infeasible solution space, the user may easily eliminate areas unsuitable for equipment placement by selecting and removing points from the grid. Figure 4.12 shows the same grid as in Figure 4.11 following the user having selected and deleted points in areas where equipment placement is not possible or desirable for whatever reason.

In addition, possible positions for network infrastructure may be identified in some form of external file read in by the software, or may be recognized by symbols or embedded information within the original site-specific information. For example, if working inside a building, the building blueprint may include symbols or text identifying the location and/or availability of cable trays, power drops, and existing network infrastructure. This information, if available, may be used by the software to identify possible or likely network infrastructure

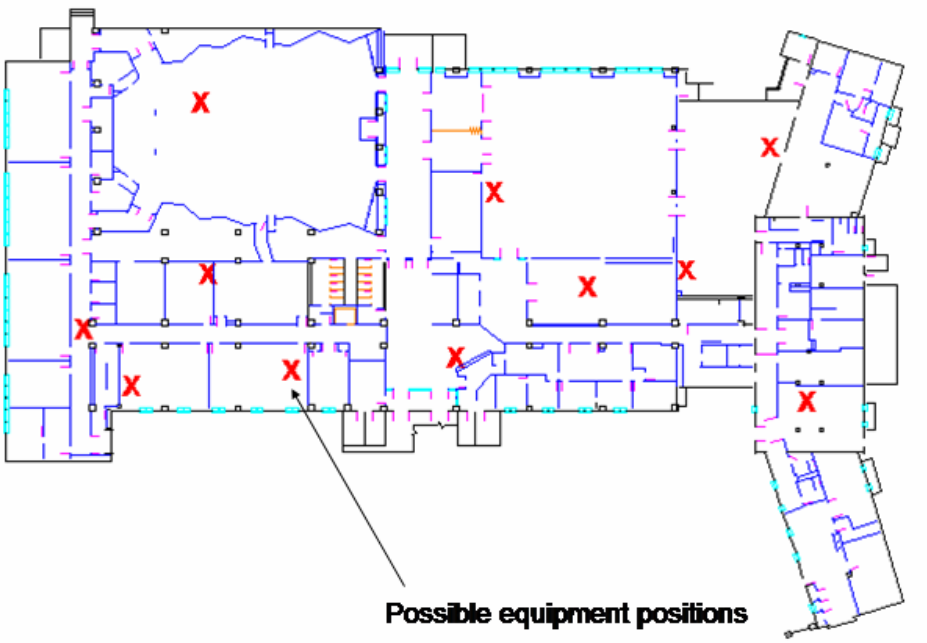

Figure 4.10: Screen capture from *SitePlanner*®from Wireless Valley Communications, Inc. showing locations within the site-specific environmental model identified by the user as suitable for possible equipment positioning.

positions.

4.4.3 Desired Performance

For any wireless network, one or more desired performance metrics can be stated as design goals. A wireless network designer then strives to achieve the proper combination of equipment placement and interconnection that bests achieves these performance goals. In order to carry out an automated method for choosing equipment and equipment locations, an indication of desired performance throughput the area of interest is necessary.

The user is prompted to indicate the regions within the site-specific model where a certain level of performance is desired. This has been implemented as the selection of one or more closed, rectangular, planar regions by clicking on opposite diagonals of the rectangular plane. A desired performance metric, such as RSSI, SIR, SNR, throughput, packet error rate, or

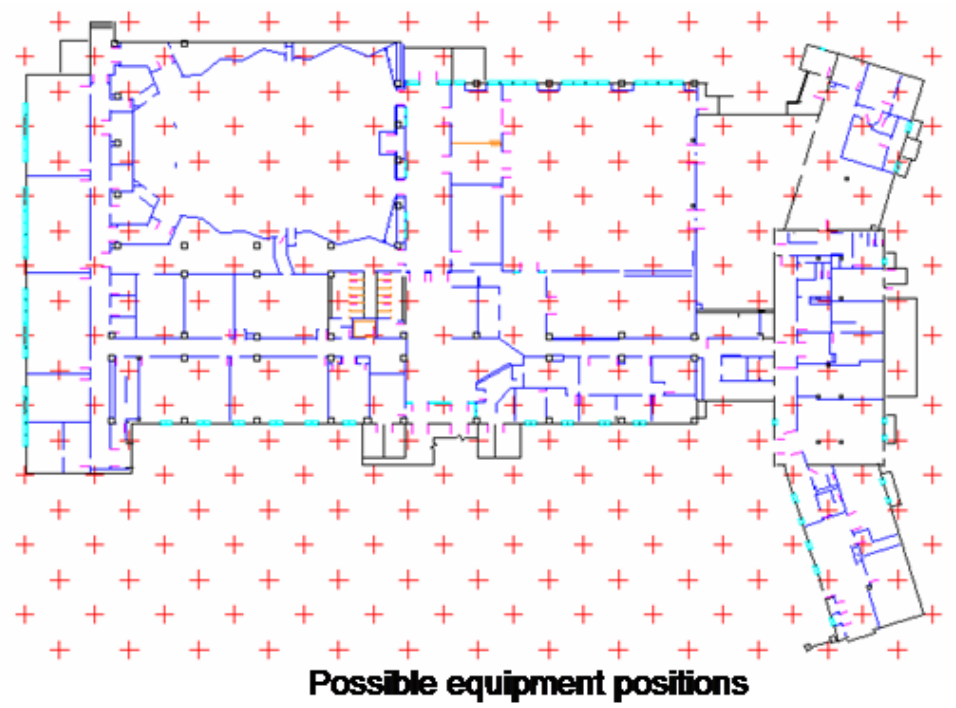

Figure 4.11: Screen capture from *SitePlanner*®from Wireless Valley Communications, Inc. Each point shown in the grid has been selected and input by the user to be considered as a position for equipment.

any other desired metrics, is selected by the user, along with the desired performance level. For example, the user may choose a desired performance metric of $-70.0dBm$ RSSI. The software will then iterate to attempt to guarantee this level of performance at all points within the indicated regions during the processing loop.

4.4.4 Processing Loop

The goal of the processing loop is to determine the preferred or optimal number (or cost) and placement of the selected equipment within the site-specific model that satisfies the desired performance level at all, or nearly all, points within the desired regions. This is a straightforward calculation loop that consolidates all of the concepts presented previously in this research. A site-specific model of the environment is utilized. The user may define

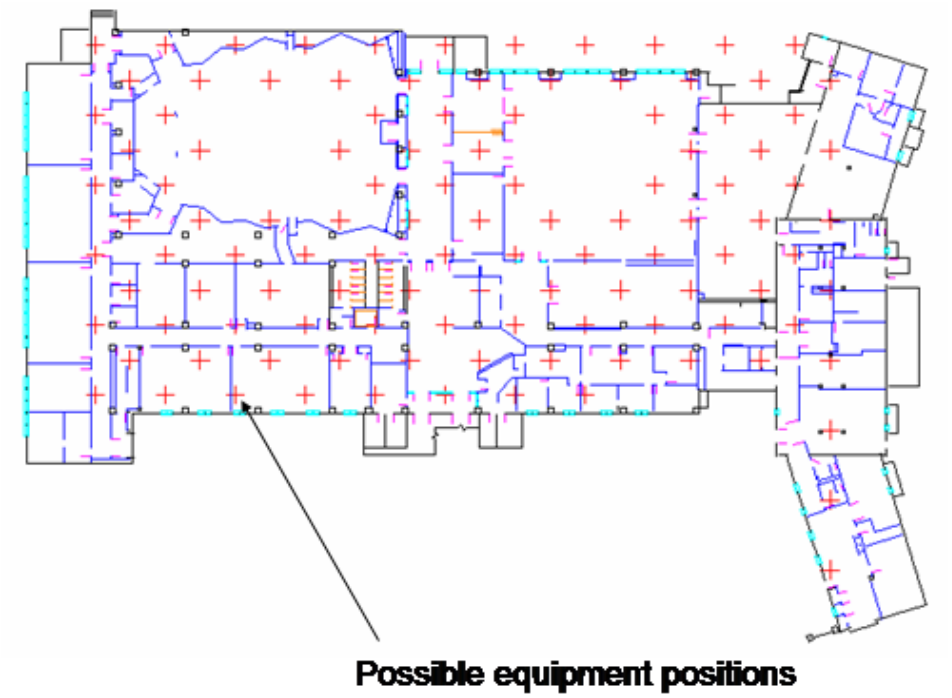

Figure 4.12: Screen capture from *SitePlanner*®from Wireless Valley Communications, Inc. Each point shown in the grid has been chosen by the user to be considered as a possible position for equipment. The user has selected and removed points from the grid to reduce the number of positions to consider for equipment placement.

preferred or desired metrics, or these metrics may be embedded within the software, and may assign weightings for various parameters so that the software may use different rules for determining optimal and preferred performance.

As described in Chapter 2, the site-specific model contains surfaces, where each surface represents the face of obstructions within the environment. Each surface has been associated with or embedded with data specifying its material and electromagnetic characteristics. Specific types and combinations of wireless network equipment have been modeled and modeled as described previously in this chapter. The ability to predict radio wave propagation using the ray tracing techniques presented in Chapter 3 has been implemented. Using ray tracing to predict the movement and interaction of electromagnetic waves within the site-specific model, the system is able to determine the performance of wireless transmitters positioned

within the site-specific model. As will be shown in the following chapter, the use of lookup tables and measurement data as given in Chapter 5, enables the software to translate the predicted electromagnetic wave interactions between different types of transmitter and receiver equipment types into a prediction of throughput or frame error rate performance.

The basic, brute-force approach to the processing loop described above is to position equipment at every possible location. However, this approach becomes computationally prohibitive as the size of the search space increases. Equipment is recursively removed and the predicted result is updated to determine whether or not that removal produces an undesirable result in terms of meeting the performance level. Through this process, a selected set of equipment types, placements, and design architectures can be determined that closely satisfies the desired performance goal. Thus, similar to automatic printed circuit board layout tools, this research has produced the first site-specific automatic wireless network layout tool, resulting in over thirty patents issued or pending through Wireless Valley.

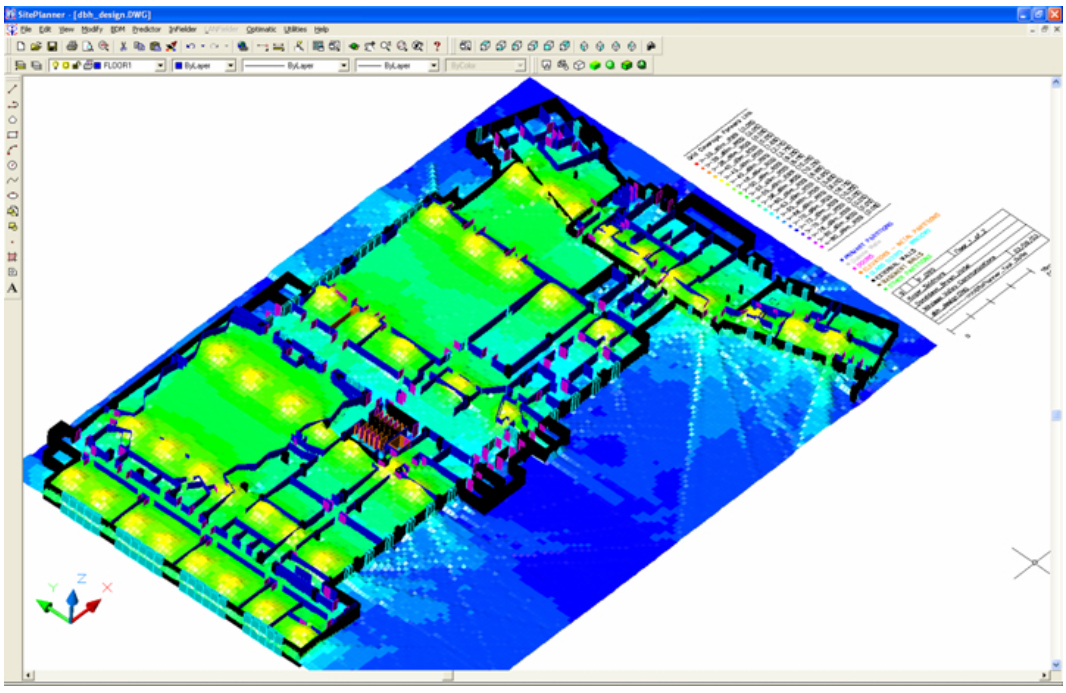

Figure 4.13: Screen capture from *SitePlanner*®from Wireless Valley Communications, Inc. showing predicted RSSI levels at the beginning of the automated equipment placement processing loop. Forty-two WLAN access points have been allowed to be placed at all possible locations within the region. Note the large number of very strong hot spots.

Figure 4.13 provides an example simulation output showing predicted RSSI levels throughout a single floor of a building for the case of equipment having allowable placements at all possible locations. Figure 4.14 provides the same building after the processing loop has completed. Note the reduced equipment usage.

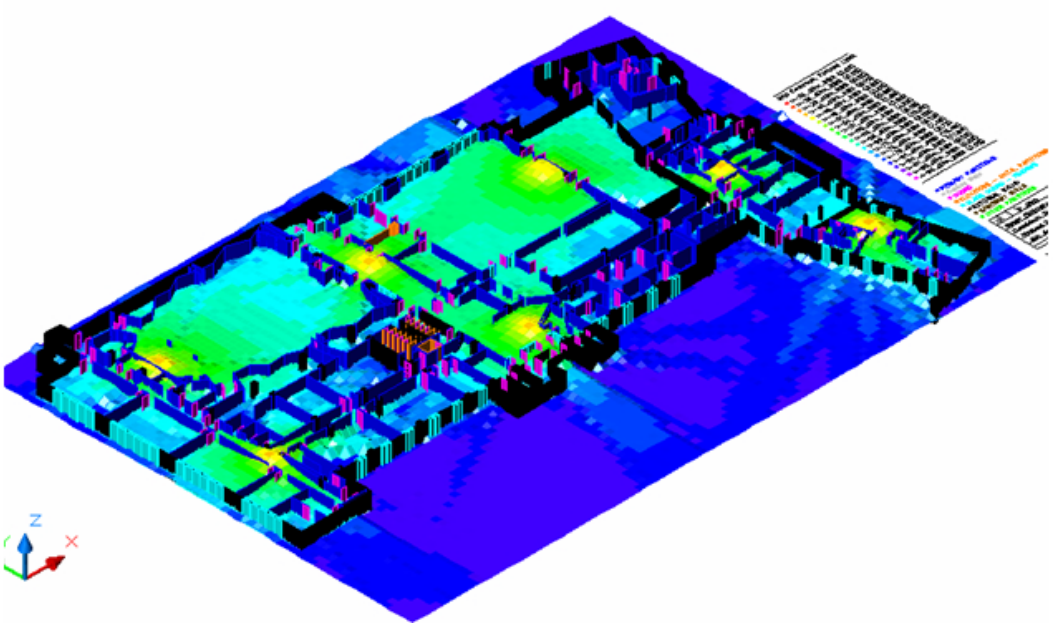

Figure 4.14: Screen capture from *SitePlanner*®from Wireless Valley Communications, Inc. showing predicted RSSI levels throughput the facility after the automated equipment placement processing loop. An optimal set of equipment placements has been identified which reduces the number of WLAN access points from Figure 4.13 but still satisfies the desired performance goal. This automatic design feature is a powerful capability for network deployment.

Additional research is underway to optimize the processing loop to dramatically reduce the overall calculation time, and to also analyze the possibility of utilizing multiple performance metrics as goals for the processing loop.

4.5 Conclusion

During the course of this research, a software system has been created that can accurately model any type of wireless network hardware and can represent both the placement and interconnection of wireless network infrastructure within a site-specific representation of the environment. An editable library of equipment types is maintained by the software, and individual pieces of equipment may be specified in terms of performance and aesthetic characteristics and budgetary status. The user may interactively select, place, and interconnect equipment from the library within a site-specific model of the environment. As this occurs, vital network performance information is displayed in real-time, enabling the user to make instant tradeoff decisions regarding the selection and use of specific equipment types and/or configurations. By tracking individual equipment performance characteristics along with the interconnections of the equipment within the wireless network, the impact of equipment choices on the overall network performance can be directly incorporated and reflected within the simulation engine. Finally, an automated method for determining equipment placement and configuration within a site-specific model based upon achieving desired performance criteria has been implemented.

Chapter 5

Network Performance Lookup Tables

5.1 Introduction

The design of wireless communications up to and including second generation technologies revolved around two factors: insuring a strong, reliable signal between transmitter and receiver, and ensuring adequate capacity. Equalizers or RAKE receivers built into air interfaces were assumed to mitigate multipath, leaving only coverage and interference as issues to be concerned with. Coverage with minimal interference was the critical factor in the design of such systems, and the evolution of performance predictive algorithms for wireless communication system design followed suit. The majority of the techniques that have emerged in the area of radio-wave propagation, as discussed in Chapter 3, have had as a goal the prediction of received signal strength given a known transmitter and receiver in some model of the physical environment.

Modern and emerging wireless communication systems require more sophisticated analysis [72, 141]. Data plays a significant role in all modern wireless communication networks. The ability to send and receive information in any form is a key factor in the design and development of next generation wireless protocols and technologies. Throughput, bit error rate (BER), packet error rate (PER, and/or frame error rate (FER) are considered reasonable metrics for the performance of data communication systems, although certainly not the method for quantifying performance. Such systems are dependent on more than just strong

signal between transmitter and receiver, being more limited by noise and interference [72, 141]. The performance of a wireless data communication system in terms of throughput, BER, PER, and/or FER may be approximated from the received signal strength intensity (RSSI), system noise (SNR), system interference (SIR), and delay spread levels [72, 158]. As the radio frequency (RF) channel characteristics are predictable using techniques discussed in Chapter 3, it becomes possible to predict the performance of a wireless data system using results presented in this chapter if there exists a reliable transform between the RF channel characteristics and end-user transport layer throughput characteristics.

Given knowledge of the received signal strength relative to the system noise and/or interference along with detailed information on the air interface standards, protocols, and/or the specific combinations of equipment involved, it is possible to predict the ideal throughput for a wireless communication system. However, many protocol standards are vague regarding specific guidelines for the physical and medium access layer [82, 158]. This allows for variability among wireless devices from different vendors. In fact, in [72], it is clear that different WLAN vendors make use of different traffic contention protocols with their respective access points. Thus, it is reasonable to conjecture, a wireless modem of a given standard from one manufacturer may provide for much different throughput and performance levels compared to a wireless modem from a separate manufacturer, even when the two modems are placed under the exact same conditions [72, 82]. As such, any attempt to accurately represent and predict the throughput, BER, PER, and/or FER of a wireless system must be capable of handling variations among separate vendor devices, as well as for variations in the types of services or number of users. One way to assure that a prediction method accurately models particular equipment from a given vendor is to use measurement data to fine tune the predictive solution, as shown in Section 5.6.0.1.

5.2 Determining Throughput and/or Frame Error Rate

Recent interest in wireless data communication systems has sparked research into techniques for deriving system throughput and/or frame error rate given information such as received signal strength, system noise levels, interference, number of users, and the type of service. To date, much of this work has revolved around the collection of measured performance

metrics (e.g., throughput, RSSI, SIR, SNR, etc.) and the creation of empirical models that can be used as lookup tables in order to derive throughput given signal-to-interference ratio (SIR), signal-to-noise ratio (SNR), and/or delay spread on a per technology basis [16, 23, 34, 38, 41, 72, 95, 158]. However, until this thesis, no one had ever combined a powerful site-specific design or measurement environment, a comprehensive method and system for predicting radio wave propagation, and the ability to completely model vendor-specific distribution system equipment and technology.

It should also be noted that empirical data can be used to derive an expected SIR, SNR, or delay spread given a specific throughput level as well. Methods that use empirical data and curve-fitting of empirical data to yield accurate predicted values are advantageous as they directly account for the performance differences among various vendor equipment under similar operating conditions [72]. A comparison of empirical data to the theoretical ideal performance (as specified by the vendor or the air interface standard) also provides the means to evaluate different vendor equipment against one another, the impact of varying numbers of users, and the introduction of users of varying priority class on a per technology basis.

The research presented in this thesis proposes a method for predicting throughput and/or FER in the manner of Equation 5.1 through the use of lookup tables. The use of lookup tables is in defining a mapping function from one or more input variables (in this case, RSSI, SIR, SNR, delay spread, and other parameters) to a single output variable (in this case, throughput, FER, PER, BER, or other value). This is depicted graphically in Figure 5.1.

One form for the transform function identified in Figure 5.1 for predicting throughput T is shown in Equation 5.1.

$$T = C_1[Ad + Bd^2 + C] + C_2[D(RSSI) + E(RSSI)^2 + F] + C_3 \sum_{i=1}^{M} (G_i P_i + K_i) \qquad (5.1)$$

In Equation 5.1, T is throughput, d is the distance in meters between transmitters and receivers (either through a straight linear path between transmitter and receiver or a traced path representing the route taken by radio waves passing through the site-specific model between the transmitter and receiver), $RSSI$ is the received signal strength intensity from one or more desirable or undesirable transmitters, M denotes either multipath components from one or more transmitters or a combination of important multipath components from

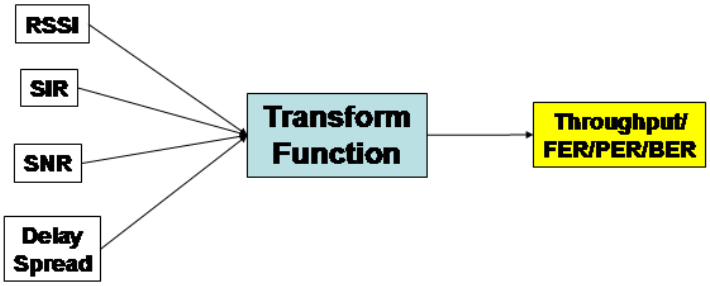

Figure 5.1: Graphical representation of the mapping of one or more input variables (e.g., RSSI, SIR, SNR, delay spread, etc.) to a single output variable (e.g., throughput, PER, BER, FER, etc.) through a transform function. The number and types of the inputs and outputs may vary, and multiple transmitters and receivers and their observed or predicted characteristics may be applied in a very broad fashion in Equation 5.1.

a collection of transmitters, G represents processing gains for each multipath component, P represents power levels for each multipath component, and A, B, C, C_1, C_2, C_3, D, E, F, and K are either constants, or linear or nonlinear functions of environment types, packet sizes, manufacturer equipment types, air interface standards, modulation schemes, physical or MAC layer parameters such as signal levels, interference levels, delay spreads, channel characteristics, or multipath characteristics from one or more transmitters or receivers, or other parameters. Equation 5.1 provides a general, comprehensive method for predicting throughput in any wireless data network. However, the type and value of each parameter or function used in Equation 5.1 may be specific to each combination of equipment types used for both the transmitter and receiver. It is also difficult to derive the proper types and values for each parameter in Equation 5.1 without empirical data. Therefore, a general method for automatically determining the parameters of Equation 5.1 from empirical data is highly desirable.

This thesis proposes a method that leads to some specific solutions of Equation 5.1 through the use of lookup tables, where the lookup tables are calibrated given empirical data whose transfer function, as depicted in Figure 5.1, is a simplified form of Equation 5.1. The approach described in this chapter is as follows. One-to-one lookup tables are created that correlate a single input variable (e.g., RSSI, SIR, SNR, delay spread, etc.) with a single output variable

(e.g., throughput, BER, PER, FER, etc.). The process for creating and expanding lookup tables given empirical data is described in Section 5.3. The data in the lookup tables may be interpolated through the use of one of several interpolation techniques (simplified versions of Equation 5.1), described in Section 5.3.2. By interpolating the measurement data, the lookup table may then be fully populated with any number of data points. The process of identifying an appropriate output from a lookup table given a valid input involves a simple search through the table to locate the table index that most closely matches the input value. Multiple lookup tables may then be combined as described in Section 5.5 to enable multiple input variables to be used to determine a single output value as depicted in Figure 5.1.

5.3 Performance Lookup Tables

By collecting empirical data for throughput, SIR, SNR, delay spread, and/or frame error rate, a chart can be created that correlates the readings on a one-to-one basis. Such a performance lookup table would then enable an observer to derive an expected throughput given a SIR or SNR ratio, or vice versa, by simply looking up the given value in the chart.

Table 5.3 lists example throughput and SNR readings provided for an IEEE 802.11b wireless local area network (WLAN) modem available from WaveLAN as specified in [72].

To utilize the performance lookup table, a wireless engineer can simply measure a SNR level and then locate the nearest SIR entry in the chart to determine the approximate throughput to expect. The more measurement data points that are collected, the more accurate and useful the data in the chart becomes [121]. Such tables can be collected and utilized for any wireless technology, providing a convenient reference for designers of any wireless communication system [41, 34, 95, 121, 158]. Thus, the specific location of users in an environment being serviced by a wireless data network can yield RSSI, SIR, and SNR values that can be used with lookup tables similar to Table 5.3 to determine expected throughput for the user.

Table 5.1: Example throughput measurements and the corresponding SNR measurements for a WaveLAN wireless LAN access point [72].

Throughput	SNR (dB)
490	4.5
1425	4.2
1410	4.35
1253	5.0
1180	7.2
1170	7.5
1165	7.9
1100	8.9
1110	9.8
1850	10.0
1501	15.0
1522	17.5
1902	17.0

5.3.1 Creating Lookup Tables

During the course of this research, software was written to facilitate the creation of performance lookup tables. Figure 5.2 shows a screen capture of the main software window allowing a user to create or edit performance lookup tables.

The performance table editor allows the user to create any type of performance relationship on a per technology, per transmitter type, and per receiver type basis. For example, a performance lookup table can be created that relates SIR to throughput for an IEEE 802.11b wireless network utilizing Cisco 340 access points and Lucent Orinoco PCMCIA WLAN modem cards and HP iPAQ handheld PDAs. The resulting table may look very different from one that is identical in every way except that the receiver may be a Dell Laptop PC.

As new table entries are entered, they are displayed graphically in a chart. Users may enter any number of chart points in any order. Once the user is satisfied with the lookup table, the table is associated with a given wireless standard using the available pull-down control. *SitePlanner* maintains a list of air interface standards, and each standard can have any number of different lookup tables associated with it.

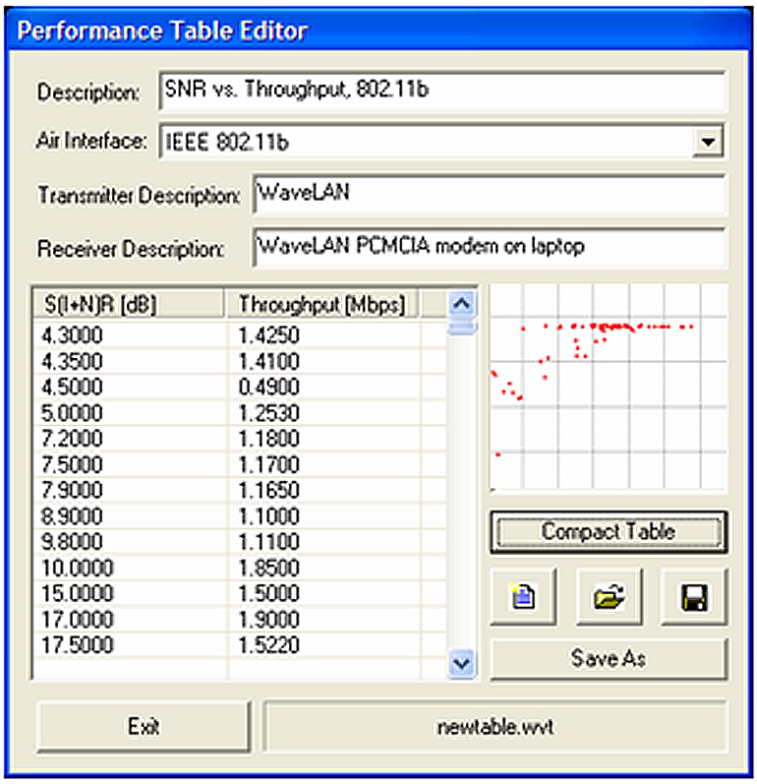

Figure 5.2: Sample dialog box implemented as a new feature to *SitePlanner* from Wireless Valley Communications that provides the means to input and edit throughput lookup tables on a per technology basis. This feature enables the entry of throughput lookup tables for any wireless communication standard. Table values currently shown are taken from [72].

As shown in Section 5.2, wireless equipment from different vendors, even if they were developed for the same wireless standard protocol, can have very different throughput levels while under the same environmental conditions. As a result, it is insufficient to simply associate a lookup table with an air interface. Instead, each lookup table must be associated with a hardware component, such as a wireless LAN access point or cellular base station, in order to properly account for the differences between individual pieces of hardware. *SitePlanner* becomes an ideal platform in which to incorporate this functionality, as *SitePlanner* is fully capable of modeling each piece of equipment that comprises a wireless network as described in Chapter 4. In addition to adding the capability to create and work with throughput lookup tables, functionality has been added to *SitePlanner* to enable a user to associate a specific lookup table with each transceiver positioned within a *SitePlanner* design.

5.3.2 Populating Performance Lookup Tables

During the course of this research, the site-specific measurement data collection software programs *LANFielder*®and *SiteSpy*®from Wireless Valley Communications were created in order to facilitate the use of empirical data to populate performance lookup tables[163]. *LANFielder* and *SiteSpy* both enable a user to simultaneously record throughput, RSSI, and channel noise site-specifically using any IEEE 802.11a or IEEE 802.11b compliant wireless LAN PCMCIA modems. Because *LANFielder*®and *SiteSpy*®function at the application level, the empirical results they record not only take into account the particular technology, receivers, and transmitters involved, but directly account for the mobile platform being used (e.g., handheld PDA, laptop PC, etc.). Other measurement receivers, such as spectrum analyzers or scanning receivers can also be used to collect RSSI or channel noise readings. The software editor shown in Figure 5.2 is capable of reading measurement log files from *LANFielder*®and *SiteSpy*®and automatically populating a performance table with their contents.

5.3.3 Interpolation Techniques

One drawback to the use of performance lookup tables involves the requirement for a large number of indices in order to achieve an accurate result. By definition, a lookup table attempts to create a one-to-one matching between an input metric and an output. The lookup mechanism implemented during the course of this research identifies the closest table index value to a given input value and returns the output value for that index. Therefore, if a lookup table is sparsely populated, the nearest index value for a given input may be distant and the returned output value skewed as a result.

In order to minimize this potential source of error and provide a mechanism whereby a sparsely populated lookup table could be easily expanded, various interpolation mechanisms were investigated. Three types of interpolations were analyzed during the course of this research: linear fit from Section 5.3.3.1, exponential fit from Section 5.3.3.2, and Bézier curve fit from Section 5.3.3.3. As can be seen from analyzing Figures 5.4, 5.5, and 5.6, the Bézier curve fit more closely follows the original distribution of data points in the table. In general, if more than three data points exist in the table, the Bézier curve fit presents

a closer approximation to the original data. As the number of measurement data points increases, the accuracy of the interpolation technique may not be a factor. For example, the *LANFielder* and *SiteSpy* software applications mentioned in Section 5.3.2 can collect thousands of empirical data points relating RSSI and SNR to throughput in under an hour. Note that RSSI values may be from desired or undesired users or sources. With the ready availability of large quantities of highly accurate measurement data, the value of applying an interpolation algorithm declines.

5.3.3.1 Linear Interpolation

Given measurement data within a chart as shown in Table 5.3, it is possible to derive a piecewise linear equation that attempts to describe the pattern formed by the data [72]. Figure 5.3 graphically represents the data given in Table 5.3.

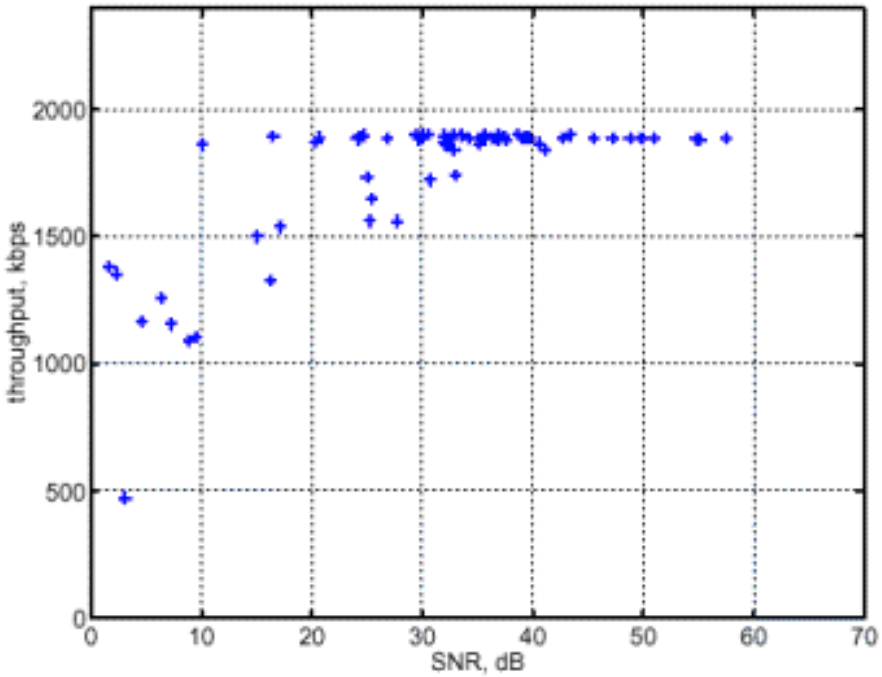

Figure 5.3: Throughput measurements graphed versus their corresponding SNR measurements [72].

Note that the data points more or less follow a piecewise linear path. This is due to a noted

trend of modern wireless LAN equipment to operate with a fairly steady throughput level until a particular SIR or SNR threshold level is reached, at which point the throughput performance drops off linearly [72]. Equation 5.2 is a very simple version of Equation 5.1 and provides a reasonable model for approximating throughput using a piecewise linear fit [72].

$$T = \begin{cases} T_{max} & : \quad SNR > SNR_c \\ A * SNR - T_0 & : \quad SNR <= SNR_c \end{cases} \tag{5.2}$$

In Equation 5.2, T_{max} is the maximum throughput of the wireless LAN equipment under ideal conditions; SNR_c is the signal-to-noise (or signal-to-interference) ratio at which the throughput of the wireless LAN deteriorates; T_0 is the throughput of the wireless LAN once the SNR (or SIR) reached 0 dB; and A is the slope of the line that closely fits the decaying throughput of the wireless LAN once the SNR_c threshold is surpassed. SNR_c can be derived from Equation 5.3 [72].

$$SNR_c = \frac{T_{max} + T_0}{A} \tag{5.3}$$

Note that Equation 5.2 is an exceedingly simplified version of Equation 5.1. All of the parameters in the equation are specific to wireless LAN equipment of different makes and models, although T_0 may be constrained to zero [72]. Figure 5.4 graphs the data from Table 5.3 with a fitted linear model overlaid onto it [72].

5.3.3.2 Exponential Interpolation

Given measurement data within a chart as shown in Table 5.3, it is possible to derive an exponential equation that attempts to describe the pattern formed by the data [72]. Equation 5.4 is a very simple version of Equation 5.1 and provides a reasonable model for approximating throughput using an exponential function [72].

$$T = T_{max} * (1 - \exp(-\alpha * (SNR - SNR_0))) \tag{5.4}$$

As with the linear model in Section 5.3.3.1, most of the parameters in the equation are

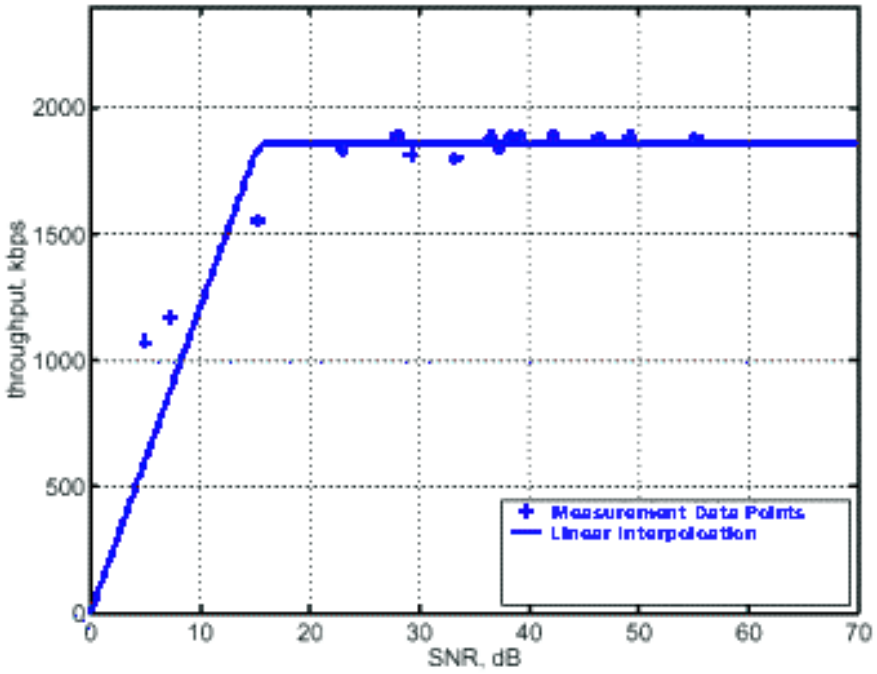

Figure 5.4: Piecewise linear equation developed to fit throughput measurements plotted versus their corresponding SNR measurements. The graph plots both the piecewise linear function and the measurement data points on the same axis [72].

specific to particular wireless LAN equipment types and vendors. In Equation 5.4, T_{max} is the maximum throughput of the wireless LAN under ideal conditions; α is the slope of the exponential curve; and SNR_0 is the signal-to-noise ratio level at which the throughput equals to zero. T_{max}, α, and SNR_0 are all equipment-specific characteristics, although SNR_0 can be constrained to zero [72]. Note that Equation 5.4 represents a simplified form of Equation 5.1. Figure 5.5 graphs the data from Table 5.3 with a fitted exponential model overlaid onto it [72].

5.3.3.3 Bézier Curve Interpolation

Given measurement data within a chart as shown in Table 5.3, it is possible to fit a spline to the measurement data. Bézier curves were chosen as an appropriate spline-fit method since Bézier curves are guaranteed to pass through the first and last control points and

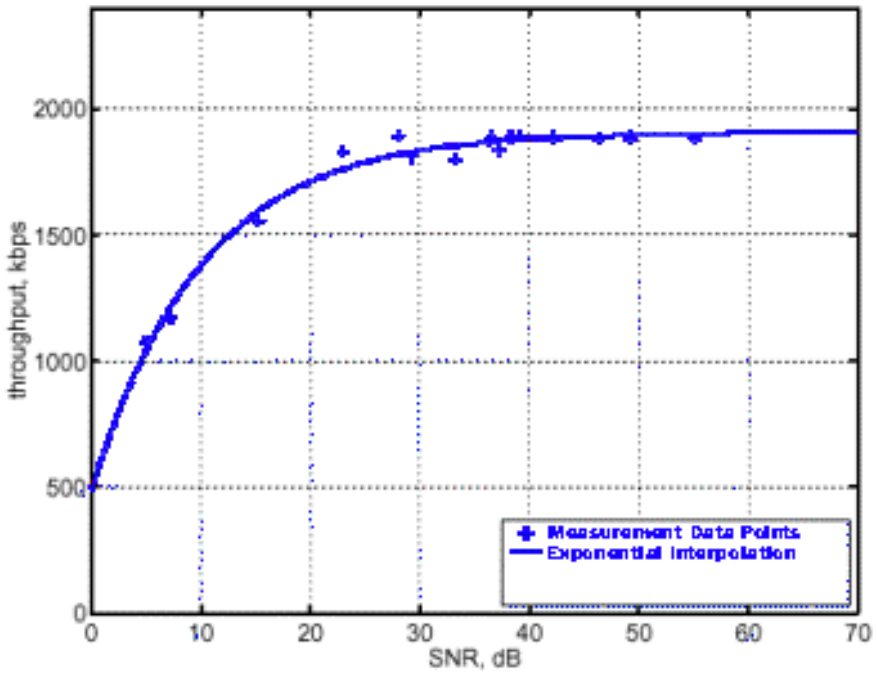

Figure 5.5: Exponential equation developed to fit throughput measurements plotted versus their corresponding SNR measurements. The graph plots both the exponential function and the measurement data points on the same axis [72].

are simplified versions of Equation 5.1 [151]. To fit a Bézier curve to our table values, the minimum and maximum possible throughput or FER levels are chosen to serve as the first and last control points for the curve respectively. The empirical data points are used for the other control points. A maximum of twenty (20) control points are used for the resulting Bézier curve. This results in a Bézier curve of polynomial degree $max(n + 1, 20)$, where n is the number of measurement points. If the number of measurement points exceeds 20, the measurement data points selected to be control points are randomly selected from the table.

To form the Bézier interpolation, we start with the set of measured data points. The minimum and maximum throughput or FER points are added to form a set of $n + 2$ total points. Each point P_k in the set takes the form of $P_k = (x_k, y_k)$, where x_k represents the index into the table (e.g., SIR, SNR, etc.), and y_k represents the throughput or FER. Each point P_k in the set is then used as a control point for the resulting Bézier curve. The control points are blended to produce a positioning vector $P(u)$ that describes the path of the Bézier curve.

[151]

$$P(u) = \sum_{k=0}^{n} P_k BEZ_{k,n}(u), 0 <= u <= 1 \tag{5.5}$$

In Equation 5.5, the *Bernstein polynomials* $BEZ_{k,n}(u)$ are calculated as [151]

$$BEZ_{k,n}(u) = C(n,k)u^k(1u)^{n-k} \tag{5.6}$$

where $C(n,k)$ is calculated as [151]:

$$C(n,k) = \frac{n!}{k!(n-k)!} \tag{5.7}$$

Thus, a mapping from any (x_k, y_k) pair to a corresponding point (x_b, y_b) on the curve fit may expressed as

$$x(u) = \sum_{k=0}^{n} x_k BEZ_{k,n}(u) y(u) = \sum_{k=0}^{n} y_k BEZ_{k,n}(u) \tag{5.8}$$

This process is used to populate the table with values which follow the Bézier curve. Note that this process is yet another form of the general solution given in Equation 5.1. Figure 5.6 graphs the data from Table 5.3 with a fitted Bézier curve overlaid onto it.

5.3.4 Types of Performance Lookup Tables

Lookup tables provide a correlation between two values. For the purposes of this research, a mechanism for creating, editing, and populating performance lookup tables was created. As a result, software was written to generation performance lookup tables that relate values of RSSI, SIR, SNR, or delay spread to values of throughput or frame error rate. Although this research focused on performance lookup tables of the aforementioned types, it is easy to extend the concept of performance lookup tables to apply to the correlation of two or more values of interest to a wireless network architect. For example, a performance lookup table can be generated and populated with values that correlate velocity with throughput, propagation distance with frame error rate, or position location and SNR to throughput.

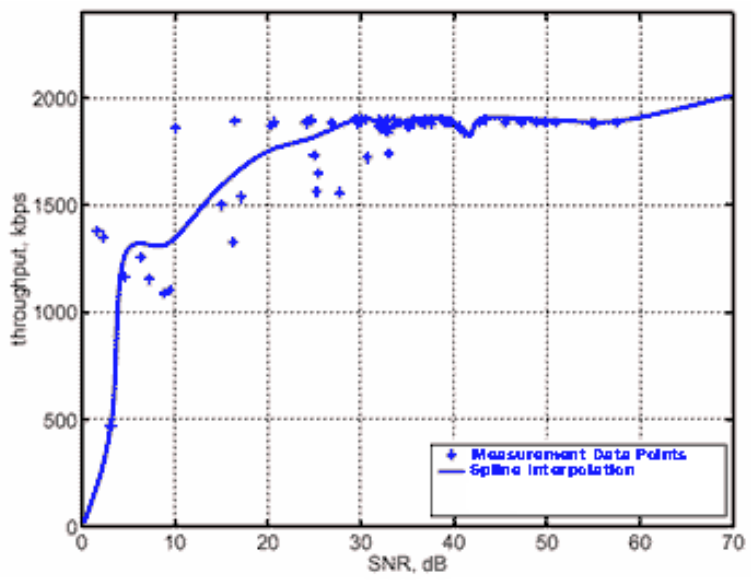

Figure 5.6: Bézier curve used to fit throughput measurements plotted versus their corresponding SNR measurements. The graph plots both the Bézier curve and the measurement data points on the same axis [72].

5.3.5 Lookup Table Reliability

It is important to consider the reliability of a given performance lookup table. The accuracy of a performance lookup table is directly related to the accuracy of the relationship between the values represented by the table. If a strong correlation does not exist between the tables input and output, the reliability of the performance lookup table may become questionable. For example, if a performance lookup table is constructed that attempts to correlate room temperature with the throughput of a particular wireless LAN access point, the resulting relationship may be questionable at best in its applicability to other access points. Likewise the accuracy of the empirical data used in constructing the performance lookup table can also introduce error into the relationship [72]. The use of the interpolation methods described in Section 5.3.3 can reduce the impact of a small number of erroneous data points.

5.4 Site-Specific Performance Prediction

In this section, the framework of a site-specific throughput and frame error rate prediction system is presented. This system was created by integrating new features into the *SitePlanner*®wireless system design software available from Wireless Valley Communications. *SitePlanner* already provides the means of predicting and displaying RSSI, SNR, and SIR for any site-specific environment using the techniques described in Chapter 3 [163]. Additional features have been integrated into the *SitePlanner*®software in order to extend that functionality to the prediction of throughput and FER through the incorporation of performance lookup tables. The basic process proceeds as described below.

First, the user develops a site-specific model of the environment as described in Chapter 2. Next, wireless transceivers are positioned within the site-specific model as described in Chapter 4. As shown in Figure 5.7, software dialogs have been created that enable a user to assign one or more performance tables to each transceiver modeled within the site-specific model.

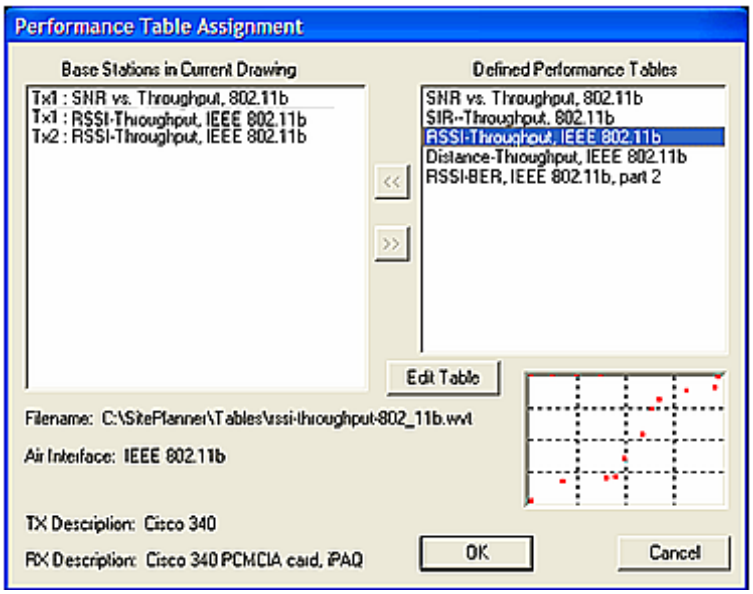

Figure 5.7: Screen capture from *SitePlanner* showing the dialog which allows the user to assign one or more performance lookup tables to transceivers placed within the site-specific environment.

The user selects which performance tables are proper and desirable to be assigned to each transceiver in the site-specific model. Next, a radio wave propagation model is used to predict RSSI, SIR, SNR, or delay spread at specific locations within the site-specific model as described in Chapter 3. The resulting predicted values at each location in the site-specific model are used as indices into the particular performance lookup tables assigned to each transceiver. The result is that a throughput or FER value can be determined at any point within the site-specific model of the environment for the wireless network. The resulting performance value can be displayed to the user in various ways. Figure 5.8 shows a screen capture from *SitePlanner* displaying predicted throughput within a building.

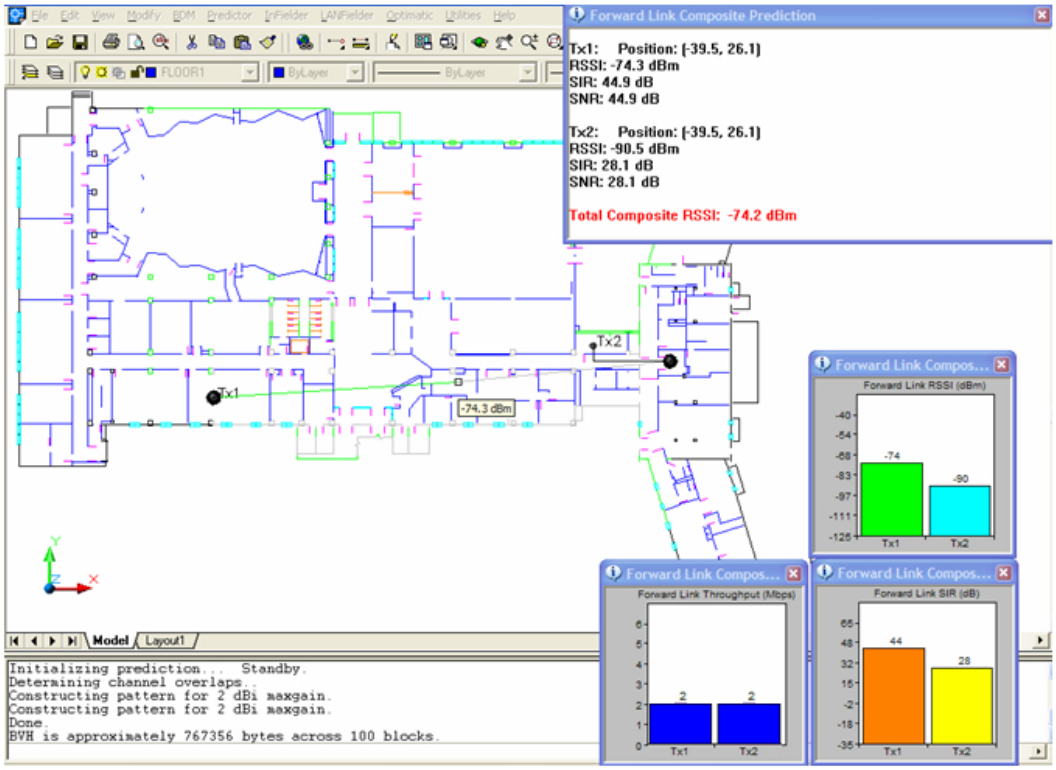

Figure 5.8: Throughput prediction performed using *SitePlanner* from Wireless Valley Communications following modifications to utilize lookup tables to approximate throughput given predicted SNR.

Using *SitePlanner*, the building environment of Durham Hall on the Virginia Tech campus was modeled, and wireless LAN access points representing Bay Networks BayStack 660 series access points in the building were positioned and associated with the throughput lookup table

given in Table 5.3. These values were initially chosen based upon empirical data presented in Section 5.6.0.1. A series of predictions were then performed, resulting in the output shown in Figure 5.9.

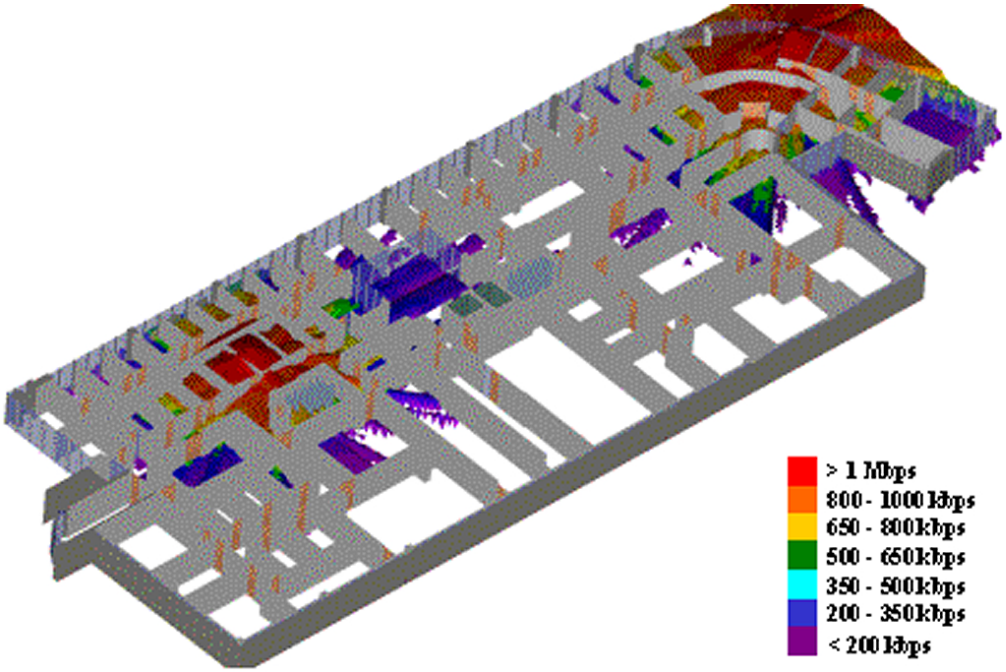

Figure 5.9: Throughput prediction performed using *SitePlanner* from Wireless Valley Communications following modifications to utilize lookup tables that approximate throughput given predicted SNR. Two access points are included in the prediction. A region of fluctuating height and color identifies the throughput levels for the two access points. The height of the region corresponds to predicted SNR levels, while the color corresponds to the predicted throughput from the lookup table.

5.5 Correlating Multiple Performance Lookup Tables

It is advantageous to correlate the data contained in multiple lookup tables. That is, using more than a single input value to determine throughput or FER can lead to a more accurate determination of network performance. For example, utilizing RSSI as a performance table lookup without also considering noise or interference levels is not sufficient for an accurate estimate of throughput or frame error rate [72], [121]. Likewise, utilizing a SIR or SNR

value as a performance table lookup without also considering if a sufficient level of RSSI is present can be just as inaccurate. Therefore, using a combination of RSSI, SIR, and/or SNR values as inputs into some form of multiple table lookup to determine network performance is highly desirable.

To facilitate this, software was written that enables multiple lookup tables to be used simultaneously to carry out network performance determination. The dialog box shown in Figure 5.7 depicts a transceiver with multiple performance tables assigned. No correlation need necessarily exist between the multiple performance tables assigned to a transceiver for the purposes of this research. The inputs provided to those tables generally RSSI, SIR, SNR, and/or delay spread values predicted to occur at a given location within a site-specific model for the transceiver are certainly related to one another. Additional research is required to determine the effect an existing correlation, or lack thereof, between multiple performance tables has on the accuracy of the predicted performance.

If multiple performance tables are assigned to a transceiver, the problem arises of no longer having a simple one-to-one relationship between inputs and outputs. Instead, multiple RSSI, SIR, SNR, and/or delay spread inputs must be mapped to a single throughput or frame error rate value. Three alternative methods for doing so were investigated and are summarized below. More research into the accuracy achieved by each method is required.

5.5.1 Average Output

The first method to consider is a simple linear averaging of the output values returned as a result of performing a lookup on each assigned table. In the simplest form of the method, the identified output values from each lookup table are summed and divided by the number of tables to determine a final output value.

While simple and straightforward, this method does not account for any possible relationship among the lookup tables or the input values used. In addition, it perhaps unfairly weights higher output values. For example, consider two throughput lookup tables assigned to a single transceiver. The first table relates SIR to throughput, while the second relates SNR to throughput. For the first table, a low SIR value returns *100 kbps*. For the second table, a high SNR value returns *4 Mbps*. It is possible for both a low SIR and a high SNR to exist

simultaneously, in which case the averaging method returns a throughput value of *2.1 Mbps* in this example. *2.1 Mbps* represents a 47.5 percent decline in the output value compared to the SNR lookup result alone, but represents a 2000 percent increase over the SIR lookup result respectively. Equation 5.9 presents the formula used to calculate the average output given n performance lookup tables, each with output O_i.

$$\text{Avg Output} = \sum_{i=1}^{n} \frac{O_i}{n} \tag{5.9}$$

5.5.2 Weighted Average Output

An alternative to the simple averaging method presented in Section 5.5.1 is to apply some form of weighting factor to the validity of each lookup table. In essence, a weighting factor is a measure of the relative importance of the parameter to which the weighting factor is applied. The application of weighting factors is very straightforward. A multiplier is assigned to each table. The larger the multiplier, the more important (more weighted) the specific lookup table results are to be considered. The weighting is applied as shown in Figure 5.10.

$$\text{Weighted Avg Output} = \frac{\sum_{i=1}^{n} O_i W_i}{\sum_{i=1}^{n} W_i}, W > 0 \tag{5.10}$$

In Equation 5.10, n is the number of lookup tables, O_i is the output value from a given lookup table, and W_i is the weighting factor applied to a given lookup table. For example, consider two throughput lookup tables assigned to a single transceiver. The first table relates SIR to throughput and is given a weighting of $W = 2$, while the second relates SNR to throughput and is given a weighting of $W = 1$. For the first table, a low SIR value returns *100 kbps*. For the second table, a high SNR value returns *4 Mbps*. It is possible for both a low SIR and a high SNR to exist simultaneously, in which case the weighted averaging method returns a throughput value of *1.4 Mbps* in this example.

5.5.3 Worst Case Output

One final method for resolving the issue of having multiple performance tables and multiple inputs is to simply identify the worst case output value from among the set of output values

produced by each lookup table. In this method, the output throughput or frame error rate value indexed by the input value given to each table is identified. Note that one output value will be identified for each lookup table. The worst output value from among the set of identified output values is chosen to be the predicted result. Of the three methods considered, the worst case output scenario is the easiest to apply, involves no calculation, and requires little or no user input or interaction.

At first glance, this may seem overly simplistic. However, the reasoning behind this method attempts to take advantage of the known relationship between the input values to the tables. For example, consider two throughput lookup tables assigned to a single transceiver. The first table relates SIR to throughput, while the second relates SNR to throughput. Given a SIR and a SNR value to input to the tables, two throughput values will be returned. If the throughput value corresponding to the given SIR input is less than the throughput value determined from the given SNR input, the implication is that although an adequate level of SNR exists, the interference levels are inadequate to sustain the same level of throughput. In the reverse case, if the throughput value corresponding to the given SIR input is greater than that for the SNR input, the implication is that although the SIR level is adequate, the noise floor is too high to sustain the same degree of throughput.

5.6 Verification of Predictions

The accuracy of the table lookup method is constrained due to the number and accuracy of the measurement information used to form the table and due to the accuracy of the site-specific predictive model(s) used to determine SNR or SIR. However, a significant advantage to using table lookup to determine throughput based upon predicted SNR or SIR is that the accuracy may be readily fine-tuned when accurate measurement data is provided. As more measurement information becomes available, the accuracy of the table lookup can continually be made more accurate. This is very attractive, as it enables any wireless engineer to develop highly accurate throughput tables on a per technology basis with little to know direct knowledge of the underlying protocols, air interface, or hardware. That is, it is unnecessary to have detailed information regarding the operating characteristics of a particular hardware device in order to develop an accurate means of predicting the performance of that device

in terms of data throughput. Instead, measurement data can be used to continually refine the predictive accuracy of the table lookup.

There are various ways of approaching the process of calibrating the table lookup parameters depending on the specific type of measurement data that is available. To collect site-specific measurement data for use in the calibration process, a transmitter of known location and operating characteristics must be available. A site-specific computer model of the physical environment in which the transmitter is located must be available. Such a model may be a simple raster image, a three-dimensional vector representation, or some form of hybrid. Different types of site-specific models are discussed in Chapter 2. A technique must be available for predicting SNR or SIR at any location within the computer model of the site-specific environment. Various prediction models are discussed in Chapter 3. Three such approaches are discussed below.

5.6.0.1 Calibration Using Site-Specific Measurements

A commercial application such as *LANFielder* from Wireless Valley Communications, Inc., can acquire and provide simultaneous throughput and SNR site-specific measurement information to a wireless engineer [163]. LANFielder can provide specific information on the actual throughput and SNR or SIR levels at any given location serviced by a transmitter. It is likely that this measured data will not precisely correspond to existing data in the table lookup due to variations within different physical environments that affect radio wave propagation [72]. However, the table lookup can provide a very good approximation that wireless engineers can use as a reference.

Given accurate measurement data relating SNR or SIR to throughput, the values in the lookup data can be updated in one of several ways. First, if an existing data point in the table corresponds to a measured data point (i.e., a measured SNR or SIR value corresponds to an existing SNR or SIR value in the table), the throughput value in the table may be averaged with the measured throughput value to form a replacement throughput value for the corresponding SNR or SIR, or the existing value in the table may simply be replaced by the new measured value. Additional research is required to determine which of these two approaches is more favorable. This process of averaging the throughput value in the table with the new measured throughput by simply adding the values and dividing by two

implies a linear relationship between throughput readings, and also greatly favors the newly recorded throughput value over previous measurement readings that were averaged to form the current value in the table. Further research will be required to properly quantify the impact this has on the accuracy of the resulting performance table.

If the measured SNR or SIR value does not already have a corresponding entry in the throughput lookup table, a new entry is simply added to the table as described in Section 5.3.2.

5.6.0.2 Calibration Using Site-Specific Throughput-Only Measurements

If site-specific throughput measurements are available, but corresponding SNR or SIR measurements are not, the data within throughput table may still be fine-tuned if one utilizes predicted SNR or SIR values. In this situation, the assumption is that the accuracy of the predicted SNR or SIR values is sufficient. With this assumption, SNR or SIR values may be acquired using some form of site-specific predictive technique from Chapter 3, and may be used in place of measured SNR or SIR values in order to provide the required SNR-to-throughput and/or SIR-to-throughput relationship necessary to fine-tune the prediction.

The accuracy of the predicted SNR or SIR values can be calibrated on the basis of measured RSSI data. If measured RSSI data is available, techniques discussed in [165] provide the means to calibrate site-specific predictive algorithms to provide results that closely match the measured RSSI values. By calibrating the site-specific model used to predict RSSI, SNR, and SIR using measured RSSI values, a wireless engineer can ensure that the predicted results are as accurate as possible [165]. This will ensure that the predicted SNR or SIR values used as indices into the throughput lookup table would match as closely as possible measured SNR or SIR values were they to be available.

By substituting measured SNR or SIR values with predicted values, the process of calibrating a throughput lookup table proceeds as discussed in Section 5.6.0.1.

5.6.1 Verifying the Calibration Process

In order to verify the validity of the performance table concept, a number of measurements of SNR and throughput were recorded and compared versus the predicted throughput levels. A measurement campaign was carried out in the Durham Hall academic building on the University of Virginia Tech campus. This campaign was carried out using five BayNetworks BayStack 660-series IEEE 802.11 access points as transmitters with a BayStack 660 PCMCIA WLAN card in a Windows Pentium II class pen tablet personal computer [166]. The access points (identified as *Bay1*, *Bay2*, *Bay3*, *Bay4*, and *Bay6* in Figure 5.10) were positioned on the fourth floor. Measurement data was collected on the fourth floor using *LANFielder*®, a software application developed at Wireless Valley Communications that is capable of measuring and site-specifically storing RSSI, SNR, throughput, packet error rate, rogue access points, and other crucial performance information within a computer model of a physical environment [163]. The measurement data was collected by powering on a single access point at a time, and then walking through floor four recording measurement readings using *LANFielder*. All data was collected during times when the building was minimally occupied, and the access points were isolated from the other networks within Durham Hall such that no other users were present. In addition, no known sources of interference were present during this empirical study. These measurement readings are indicated in Figure 5.10. Although Figure 5.10 only shows measured throughput levels, *LANFielder* can display any of the recorded performance metrics, such as SNR and packet error rate, in a similar fashion.

The empirical data collected within Durham Hall was used to populate the performance lookup tables to be used in predicting performance. This was done following the guidelines of Section 5.6.0.1 and utilizing the performance table editor introduced in Section 5.3.1. The resulting performance table is displayed in Figure 5.11. The newly calibrated performance tables were used to predict throughput for the given WLAN, the results of which may be seen in Figure 5.9. Additional throughput and SNR measurements were recorded on fourth floor Durham Hall, and the results were compared versus predicted throughput levels. Table5.6.1 provides details of the accuracy achieved for each access point. As can be seen from Table 5.6.1, the predicted throughput accuracy is quite high. Further analysis is required to confirm the accuracy under different network loading scenarios, and for situations where interference

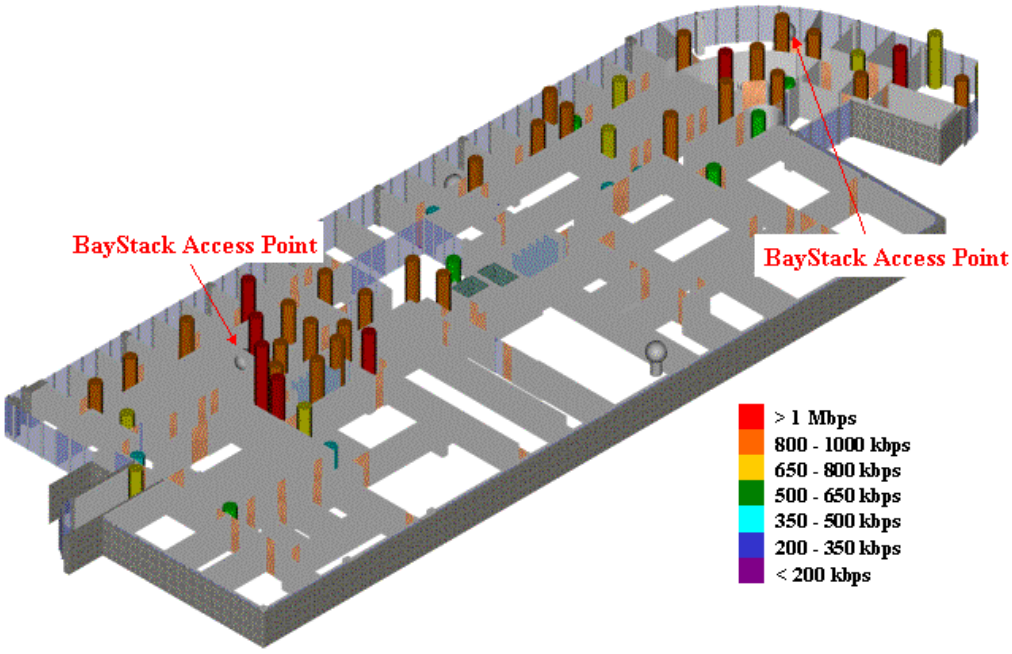

Figure 5.10: Screen capture from *SitePlanner* showing site-specific measured throughput data points collected on the fourth floor of Durham Hall on the Virginia Tech campus using *LANFielder* from Wireless Valley Communications. The cylinders shown in the floor plan identify measured throughput values for the five active Bay Networks BayStack 660 access points (Bay1, Bay2, Bay3, Bay4, and Bay6). Both the height and color of the cylinders correspond to the measured throughput levels at each location. [166]

exists.

5.7 Conclusion

In this chapter, a simple yet effective technique is presented for determining a prediction model to predict the throughput or frame error rate of a wireless communications network for any air interface standard, protocol usage, network loading, or mixture of transmitter and receiver equipment types. The technique makes use of lookup tables that correlate predictable performance metrics such as RSSI, SIR, SNR, and delay spread, which can all be

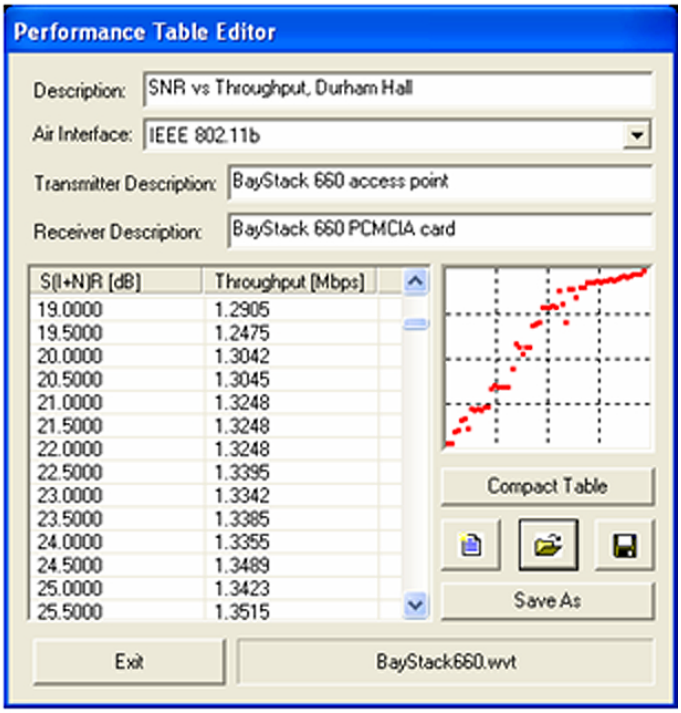

Figure 5.11: Performance lookup table created from measured SNR and throughput data collected using BayNetworks BayStack 660 WLAN access points and PCMCIA cards on the fourth floor of Durham Hall on the Virginia Tech campus.

generated using the predictive techniques outlined in Chapter 3 in this thesis, with observable performance metrics such as throughput and frame error rate. Software was written and presented that allows for the creation and of lookup tables, as well as the ability to calibrate the table contents with empirical data in order to perform excellent application-layer network performance prediction. A process is defined for using the lookup tables within the context of site-specific prediction of wireless communication system performance, and outputs from sample predictions are shown. This represents a powerful new way of allowing Information Technology (IT) staff to carry out wireless network designs without needing extensive knowledge regarding either the equipment, wireless standards, or underlying technology being deployed.

Table 5.2: Measured versus predicted throughput statistics for the simulation shown in Figure 3.14.

Access Point	Floor #	Maximum Throughput (kbps)	# Measurements	Mean Error (kbps)	Std. Dev. (kbps)
Bay1	4	1800	71	15.0	22.9
Bay2	4	1800	25	33.1	55.0
Bay3	4	1800	22	13.8	83.7
Bay4	4	1800	30	17.2	33.6
Bay6	4	1800	31	14.9	27.1

Chapter 6

Conclusion

6.1 Introduction

The ultimate goal of this research was to develop a practical yet comprehensive system and method for use in the design and deployment of next generation wireless communication systems. This has been successfully achieved and presented herein. This research has spawned nearly three dozen patent applications and, and the software system created by this research is already in use by more than two hundred corporate, government, and academic entities world-wide.

6.2 Accomplishments

In the area of site-specific databases, the accomplishments of this research include:

- Developed an efficient, automated method and system for the creation, editing, and management of two- or three-dimensional, integrated indoor-outdoor site-specific computer models of a physical environment suitable for use in predicting and simulating wireless communication system performance.

In the area of site-specific radio wave propagation prediction, the accomplishments of this research include:

- Designed and implemented an efficient, PC-based next generation reflection-based ray-tracing engine, combining the concepts of ray shooting, geodesic spheres for ray launching, and irregular spherical bounding volume hierarchies in a manual, semi-automatic, or fully automatic process for use in predicting radio wave propagation.
- Designed and implemented a unique method of tracking and storing ray-tracing simulation results in the form of horizontal and vertical reception lines/planes.
- Designed and implemented efficient techniques for incorporating equipment-specific effects into wireless network performance simulation, including details of equipment placement and interconnection.
- Designed and implement a process in software whereby optimal wireless network equipment placement and configuration can be carried out automatically on the basis of achieving a desired performance goal.

In the area of throughput, bit error rate, and frame error rate prediction for any wireless communication system, the accomplishments of this research include:

- Designed and implemented unique lookup tables capable of correlating RSSI, SIR, SNR, and delay spread to the vital end-user parameters of throughput, packet error rate, bit error rate, or frame error rate on a per technology and per equipment type basis.
- Designed and implemented the incorporation of the lookup tables into the ray-tracing simulation to enable direct prediction and display of throughput and frame error rate within a site-specific model.
- Designed and implemented the ability to create and/or calibrate lookup table values based on empirical results.
- Designed and implemented a technique to correlate multiple lookup tables in order to map multiple, different input criteria into a single output value.

6.3 Future Research

There is a need for continued research to build upon the results presented herein. The concept of utilizing reception places for organizing ray-tracing simulation results lends itself to the possibility of empirically tuning ray-tracing prediction parameters. This is vital to the future applicability of ray-tracing as a predictive technique for wireless network performance and appears doable. However, finding the optimal or preferred methods for optimizing or tuning ray tracing models based on measurements, especially measurements which do not include power delay profile data, is a fruitful area of research.

The ability to automatically position and configure wireless networking equipment site-specifically in order to achieve a desired performance goal has been demonstrated. Further study is warranted to improve the process in terms of computational efficiency and practicality through alternate algorithms. Current CAD technology provides the opportunity to extend the automated equipment placement method to include the determination of optimal cable placement and routing, and to incorporate unique equipment types such as radiating cable.

User experience with portions of the *SitePlanner*®and *LANPlanner*^{TM} software applications developed from this research will help quantify the true time savings of the results presented herein. Eventually, the techniques and processes described herein can be used to control hardware configuration remotely, automatic network performance monitoring and control, and be embedded within hardware equipment or directly into microprocessors, microcontrollers, or any other form of microchips. This research was accomplished at Wireless Valley Communications, Inc., with support from the Wireless Valley Bradley Industrial Scholars Fellowship program at Virginia Tech. Patents are pending on many of the key results presented here.

Bibliography

[1] N.S. Adawi, H.L. Bertoni, J.R. Child, W.A. Daniel, J.E. Dettra, R.P. Eckert, E.H. Flath, R.T. Forrest, W.C.Y. Lee, S.R. McConoughey, J.P. Murray, H. Sachs, G.L. Schrenk, N. H. Shepherd, and F.D. Shipley, "Coverage Prediction for Mobile Radio Systems Operating in the 800/900 MHz Frequency Range," *IEEE Transactions on Vehicular Technology*, vol. 37, no. 1, February 1988.

[2] Agilent, *www.agilent.com*, Palo Alto, CA, January 2002.

[3] S. Aguirre, L.H. Loew, and Lo Yeh, "Radio Propagation into Buildings at 912, 1920, and 5990 MHz Using Microcells," *Proceedings of 3rd IEEE ICUPC*, pp. 129-234, Oct. 1994.

[4] M. Ahmed, K. Blankenship, C. Carter, P. Koushik, W. Newhall, R. Skidmore, N. Zhang and T. S. Rappaport, *Use of Topographic Maps with Building Information to Determine Communication Component Placement for Radio Detection and Tracking in Urban Environments*, MPRG Technical Report MPRG-TR-95-19, Virginia Tech, Blacksburg, VA, November 1995.

[5] H.R. Anderson, "The Impact of Building Database Resolution on Predicted LMDS System Performance," *IEEE Transactions on Vehicular Technology*, pp. 81-84, July 1999.

[6] G.E. Athanasiadou, A.R. Nix, and J.P. McGeehan, "A Ray Tracing Algorithm for Microcellular and Indoor Propagation Modeling," *IEE Antennas and Propagation Conference Publications*, vol. 2, pp. 231-235, April 1995.

[7] G.E. Athanasiadou, A.R. Nix, and J.P. McGeehan, "Indoor 3-D Ray Tracing Predictions and Their Comparison with High Resolution Wideband Measurements," *IEEE VTS 46th Vehicular Technology Conference*, Atlanta GA, vol. 1, pp. 36-40, May 1996.

[8] G.E. Athanasiadou and A.R. Nix, "Investigation into the Sensitivity of the Power Predictions of a Microcellular Ray Tracing Propagation Model," *IEEE Transactions on Vehicular Technology*, vol. 49, pp. 1140-1151, July 2000.

[9] A. W. Y. Au and V. C. M. Leung, "Modeling and Analysis of Spread Spectrum Signaling with Multiple Receivers for Distributed Wireless In-Building Networks," *IEEE Pacific Rim Conference on Communications, Computers and Signal Processing*, vol. 2, pp. 694-697, 1993.

[10] Autodesk, Inc., *www.autodesk.com*, San Rafael, CA, January 2002.

[11] Bahl et al., Systems and methods for locating mobile computer users in a wireless network, U.S. Patent Application No. 20020095486, U.S. Patent and Trademark Office, Washington, D.C., 2001.

[12] C.A. Balanis, *Advanced Engineering Electromagnetics*, John Wiley & Sons, New York, 1989.

[13] M.A. Beach, E.K. Tameh, and A.R. Nix, "A 3-D Integrated Macro and Microcellular Propagation Model Based on the use of Photogrammetric Terrain and Building Data," *IEEE 47th Vehicular Technology Conference*, Phoenix AZ, vol. 3, pp. 1957-1961, May 1997.

[14] H.L. Bertoni, W. Honcharenko, L.R. Maciel, and H.H. Xia, "UHF Propagation Prediction for Wireless Personal Communications," *Proceedings of the IEEE*, vol. 82, no. 9, pp. 1333-1359, Sep. 1994.

[15] H.L. Bertoni, *Radio Propagation for Modern Wireless Systems*, Prentice Hall, New Jersey, 2000.

[16] B. Bing, "Measured Performance of the IEEE 802.11 Wireless LAN," *Local Computer Networks*, 1999.

[17] B. Bisceglia, G. Franceschetti, G. Mazzarella, I.M. Pinto, and C. Savarese, "Symbolic Code Approach to GTD Ray Tracing," *IEEE Transactions on Antennas and Propagation*, vol. 36, no. 10, pp. 1492-1495, Oct. 1988.

[18] K. L. Blackard, T. S. Rappaport, and C. W. Bostian, "Radio Frequency Noise Measurements and Models for Indoor Wireless Communications at 918 MHz, 2.44 GHz, and 4.0 GHz," *ICC 1991*, vol. 1, pp. 28 - 32, 1991.

[19] K. L. Blackard, T. S. Rappaport, and C. W. Bostian, "Measurements and Models of Radio Frequency Impulsive Noise for Indoor Wireless Communications," *IEEE Journal on Selected Areas in Communications*, vol. 11, no. 7, Sep. 1993.

[20] M. Born and W. Wolf, *Principles of Optics: Electromagnetic Theory of Propagation, Interference, and Diffraction of Light*, Pergamon Press, New York, 6th edition, 1980.

[21] R. A. Brickhouse and T. S. Rappaport, "Urban In-Building Cellular Frequency Reuse," *IEEE Globecom*, London, England, 1996.

[22] K. H. Brockel et al, *Apparatus and Processes for Realistic Simulation of Wireless Information Transport Systems*, US Patent 5,794,128, to United States of America as represented by the Secretary of the Army, Patent and Trademark Office, Washington, D.C., 1998.

[23] G. Bronson, *Performance Evaluation of Wireless LANs in the Indoor Environment*, masters thesis, Worcester Polytechnique Institute, Center for Wireless Information Network Studies, 1993.

[24] M. D. Casciato, *Radio Wave Diffraction and Scattering Models For Wireless Channel Simulation*, doctoral dissertation, University of Michigan, Department of Electrical Engineering, 2001.

[25] Celplan, *www.celplan.com*, Reston, Virginia, January 2002.

[26] K. K. Chawla et al, *Method and Apparatus for Wireless Communication System Organization*, US Patent 5,878,328, Patent and Trademark Office, Washington, D.C., 1999.

[27] Z. Chen and J.A. Guivara, "Systematic Selection of Very Important Point Algorithm from Digital Terrain Model for Constructing Triangular Irregular Networks," *Auto-Carto 8*, pp. 50-60, 1987.

[28] S. H. Chen and S.K. Jeng, "An SBR/Image Approach to Indoor Radio Wave Propagation Modeling," *IEE Antennas and Propagation Society International Symposium*, vol. 4, pp. 1952-1955, June 1995.

[29] S. H. Chen and S.K. Jeng, "An SBR/Image Approach to Indoor Radio Wave Propagation in Indoor Environments with Metallic Furniture," *IEEE Transactions on Antennas and Propagation*, vol. 45, no. 1, pp. 98-106, Jan. 1997.

[30] D. J. Cichon, T. Zwick, and J. Lahteenmaki, "Ray Optical Indoor Modeling in Multi-Floored Buildings: Simulations and Measurements," *IEE Antennas and Propagation Society International Symposium*, vol. 1, pp. 522-525, June 1995.

[31] D. J. Cichon, T.C. Becker, and M. Dottling, "Ray Optical Prediction of Outdoor and Indoor Coverage in Urban Macro- and Microcells," *IEEE VTS 46th Vehicular Technology Conference*, Atlanta GA, vol. 1, pp. 41-45, May 1996.

[32] R. Cohen et al, *Method for Laying out the Infrastructure of a Cellular Communications Network*, US Patent 5,465,390, Patent and Trademark Office, Washington, D.C., 1995.

[33] A. B. Cohoe et al, *SONET Network Element Simulator*, US Patent 6,108,309, Patent and Trademark Office, Washington, D.C., 2000.

[34] M. Coinchon, A. Salovaara, and J. Wagen, "The Impact of Radio Propagation Predictions on Urban UMTS Planning," Univ. of Applied Sciences of Western Switzerland, Technical Report, Fribourg, Switzerland, 2001.

[35] D. Cooper et al, *Automated Network Simulation and Optimization System*, US Patent 5,809,282, Patent and Trademark Office, Washington, D.C., 1998.

[36] S. Cornbleet, *Microwave and Geometrical Optics*, Harcourt Brace & Company, New York, 1994.

[37] L. DeFloriani, B. Falcedieno, C. Nagy, and C. Pienovi, "A Hierarchical Structure for Surface Approximation," *Computers and Graphics*, vol. 8, pp. 183-193, 1984.

[38] A. DeSimone, M. C. Chuah, and O. Yue, "Throughput Performance of TransportLayer Protocols over Wireless LANs", *IEEE Globecom*, 1993.

[39] D.M.J. Devasirvatham, R. R. Murray, H. W. Arnold, and D. C. Cox, "Four-Frequency CW Measurements in Residential Environments for Personal Communications," *Proceedings of 3rd IEEE ICUPC*, pp. 140-144, Oct. 1994.

[40] R. S. Drysdale et al, *Method and Apparatus for Performing Service Level Analysis of Communications Network Performance Metrics*, US Patent 6,058,102, Patent and Trademark Office, Washington, D.C., 2000.

[41] D. Duchamp and N. F. Reynolds, "Measured Performance of a Wireless LAN," *Proceedings of the 17th Conference on Local Computer Networks*, 1992.

[42] D. P. Dumarot et al, *System and Method for Optimizing Computer Software and Hardware*, US Patent 6,059,842, Patent and Trademark Office, Washington, D.C., 2000.

[43] G.D. Durgin, "Ray Tracing Applied to Radio Wave Propagation Prediction," *IEEE looking.forward*, vol. 5, no. 2, Summer 1997.

[44] G.D. Durgin, N. Patwari, and T.S. Rappaport, "Improved 3-D ray Launching Method for Wireless Propagation Prediction," *IEE Electronics Letters*, vol. 33, no. 16, pp. 1412-1413, July 1997.

[45] G.D. Durgin, H. Xu, and T. S. Rappaport, "Path Loss and Penetration Loss Measurements In and Around Homes and Trees at 5.85 GHz," MPRG Tech. Rep. MPRG TR-97-10, Virginia Tech, June 1997.

[46] G.D. Durgin, "The NII Band and Wireless Internet," *The Propagator*, vol. 8, no. 4, Fall 1997.

[47] G. Durgin, *Advanced Site-Specific Propagation Prediction Techniques*, master's thesis, Virginia Polytechnic Institute and State University, Bradley Department of Electrical and Computer Engineering, Blacksburg, VA, 1998.

[48] G. Durgin, T. S. Rappaport, and H. Xu, "Measurements and Models for Radio Path Loss and Penetration Loss In and Around Homes and Trees at 5.85 GHz," *IEEE Transactions on Communications*, vol. 46, no. 11, Nov. 1998.

[49] G.D. Durgin, T.S. Rappaport, and H. Xu, "5.85 GHz Radio Path Loss and Penetration Loss Measurements In and Around Homes and Trees," *IEEE Communications Letters*, vol. 40, no. 2, March 1998.

[50] S. Deffree, "WLAN Popularity Grows", Electronic News, www.e-insite.net, April 2003.

[51] A. Ephremides and D. Stamatelos, *Method and Device for Placement of Transmitters in Wireless Networks*, US Patent 5,987,328, Patent and Trademark Office, Washington, D.C., 1999.

[52] V. Erceg, A.J. Rustako Jr., and R.S. Roman, "Diffraction Around Corners and Its Effects on the Microcell Coverage Area in Urban and Suburban Environments at 900 MHz, 2 GHz, and 6 GHz," *IEEE Transactions on Vehicular Technology*, vol. 43, no. 3, pp. 762-766, Aug. 1994.

[53] ESRI, *www.esri.com*, Redlands, CA, January 2002.

[54] A. Falsafi, K. Pahlavan, and G. Yang, "Transmission Techniques for Radio LAN's – A Comparative Performance Evaluation Using Ray Tracing," *IEEE Journal on Selected Areas in Communications*, vol. 14, no. 3, pp. 477-491, April 1996.

[55] Federal Communications Commission, "Report and Order for NII Band Allocation," Tech. Rep. RM-8648 and RM-8653, Federal Communications Commission, 9 Jan. 1997.

[56] K. Feher, *Wireless Digital Communications: Modulation and Spread Spectrum Applications*, Prentice Hall, Upper Saddle River, N.J., 1995.

[57] F. Feisullin et al, *Prediction System for RF Power Distribution*, US Patent 5,949,988, to Lucent Technologies, Inc., Patent and Trademark Office, Washington, D.C., 1999.

[58] L. de Floriani, "A Pyramidal Data Structure for Triangle-Based Surface Description," *IEEE Computer Graphics and Applications*, March 1989, pp. 67-78.

[59] S.J. Fortune, D.M. Gay, B.W. Kernighan, O. Landron, R. A. Valenzuela, and M.H. Wright, "WiSE Design of Indoor Wireless Systems: Practical Computation and Optimization," *IEEE Computational Science and Engineering*, pp. 58-68, Spring 1996.

[60] S. Fortune, "Efficient Algorithms of Indoor Radio Propagation," *IEEE Vehicular Technology Conference*, vol. 1, pp. 572-576, 1998.

[61] S. Fortune, "Topological Beam Tracing," *SCG 1999*, Miami FL, pp. 59-68, 1999.

[62] R.J. Fowler and J.J. Little, "Automatic Extraction of Irregular Network Digital Terrain Models," *ACM*, vol. 4, pp. 1999-2000, 1979.

[63] J.E. Freehafer, *Geometrical Optics*, pp. 41-47, Dover Publications Inc., New York, 1951.

[64] R. Gahleitner and E. Bonek, "Radio Wave Penetration into Urban Buildings in Small Cells and Microcells," *IEEE 44th Vehicular Technology Conference*, Stockholm, pp. 887-891, July 1994.

[65] P. Gamba, B. Houshmand, and M. Saccani, "Detection and Extraction of Buildings from Interferometric SAR Data," *IEEE Transactions on Geoscience and Remote Sensing*, vol. 38, no. 1, pp. 611-618, Jan 2000.

[66] P. Gamba and B. Houshmand, "Digital Surface Models and Building Extraction: A Comparison of IFSAR and LIDAR Data," *IEEE Transactions on Geoscience and Remote Sensing*, vol. 38, no. 4, pp. 1959-1968, July 2000.

[67] J. Goldsmith and J. Salmon, "Automatic Creation of Object Hierarchies for Ray Tracing," *IEEE Computer Graphics and Applications*, May 1987.

[68] D.J. Goodman, "Trends in Cellular and Cordless Communications," *IEEE Communications Magazine*, pp. 31-39, June 1991.

[69] B.E. Gschwendtner and F.M. Landstorfer, "3-D Propagation Modeling in Microcells Including Terrain Effects," *6th IEEE Symposium on PIMRC*, vol. 2, pp. 532-536, 1995.

[70] M. Hata, "Empirical Formula for Propagation Loss in Land Mobile Radio Service," *IEEE Transactions on Vehicular Technology*, vol. 29, pp. 317-325, 1980.

[71] D. Hearn and M. P. Baker, *Computer Graphics*, Prentice Hall, Englewood Cliffs, New Jersey, 1994.

[72] B. Henty and T.S. Rappaport, *Throughput Measurements and Empirical Prediction Models for IEEE 802.11b Wireless LAN (WLAN) Installations*, master's thesis, Virginia Polytechnic Institute and State University, Blacksburg, VA, Bradley Department of Electrical and Computer Engineering, 2001.

[73] C.M.P. Ho, T.S. Rappaport, and M.P. Koushik, "Antenna Effects on Indoor Obstructed Wireless Channels and a Deterministic Image-Based Wide-Band Propagation Model for In-Building Personal Communication Systems," *International Journal of Wireless Information Networks*, vol. 1, no. 1, 1994.

[74] W. Honcharenko, H.L. Bertoni, J.L. Dailing, J. Qian, and H.D. Yee, "Mechanisms Governing UHF Propagation on Single Floors in Modern Office Buildings," *IEEE Transactions on Vehicular Technology*, vol. 41, no. 4, pp. 496-504, Nov. 1992.

[75] W. Honcharenko and H.L. Bertoni, "Prediction of RF Propagation Characteristics in Buildings Using 2-D Ray Tracing," *IEEE 45th Vehicular Technology Conference*, Chicago IL, pp. 429-433, July 1995.

[76] M. Hope and N. Linge, "Determining the Propagation Range of IEEE 802.11 Radio LAN's for Outdoor Applications," *Local Computer Networks*, 1999.

[77] R. Hoppe, P. Wertz, G. Wolfle, and F.M. Landstorfer, "Fast and Enhanced Ray Optical Propagation Modeling for Radio Network Planning in Urban and Indoor Scenarios," *Virginia Tech Symposium on Wireless Personal Communications*, vol. 10, June 2000.

[78] F. Ikegami, S. Yoshida, T. Takeuchi, and M. Umehira, "Propagation Factors Controlling Mean Field Strength on Urban Streets," *IEEE Transactions on Antennas and Propagation*, vol. 32, pp. 822-829, 1980.

[79] i-Cubed, *www.i3.com*, Fort Collins, CO, January 2002.

[80] Recommendation ITU-R P.1238-2, *Propagation Data and Prediction Methods for the Planning of Indoor RadioCommunication Systems and Radio Local Area Networks in the Frequency Range 900 MHz to 100 GHz*, Int'l Telecommunications Union, Geneva, 2001.

[81] J. Lee, "Assessing the Existing Methods for TIN Extraction," *Proceedings of International Symposium on Computer-Assisted Cartography, ACSM-ASPRS 1991*, vol. 1, pp. 194-203, 1991.

[82] A. Kamerman and G. Aben, "Throughput Performance of Wireless LANs Operating at 2.4 and 5 GHz," *IEEE 11th International Symposium of Personal, Indoor and Mobile Radio Communications*, vol. 1, p. 190-195, 2000.

[83] R. Kattenbach and H. Fruchting, "Wideband Measurements of Channel Characteristics in Deterministic Indoor Environments at 1.8 and 5.2 GHz," *IEEE PIMRC*, vol. 3, pp. 1166-1170, 1995.

[84] P. Kawas et al, *Computer Aided Design Method and Apparatus for Networks*, US Patent 6,058,262, Patent and Trademark Office, Washington, D.C., 2000.

[85] J.B. Keller, "Geometrical Theory of Diffraction," *Journal of the Optical Society of America*, vol. 52, no. 2, pp. 16-130, Feb. 1962.

[86] S.C. Kim, B.J. Guarino, Jr., T.M. Willis III, V. Erceg, S.J. Fortune, R.A. Valenzuela, L.W. Thomas, J. Ling, and J.D. Moore, "Radio Propagation Measurements and Prediction Using Three-Dimensional Ray Tracing in Urban Environments and 908 MHz and 1.9 GHz," *IEEE Transactions on Vehicular Technology*, vol. 48, pp. 931-946, May 1999.

[87] J. Kobielus, G. Somerville, and T. Baylor, "Optimizing In-Building Coverage," *Wireless Review*, vol. 15, no. 5, pp. 24-30, March 1998.

[88] P. M. Koushik, T. S. Rappaport, M. Ahmed, and N. Zhang, "SISP - A Software Tool for Propagation Prediction," *Advisory Group for Aerospace Research and Development, Conference Proceedings 574*,Athens, Greece, 1995.

[89] R.G. Kouyoumjian and P.H. Pathak, "A Uniform Geometrical Theory of Diffraction for an Edge in a Perfectly Conducting Surface," *Proceedings of the IEEE*, vol. 62, no. 11, pp. 1448-1461, Nov. 1974.

[90] P. Kreuzgruber, P. Unterberger, and R. Gahleitner, "A Ray Splitting Model for Indoor Radio Wave Propagation Associated with Complex Geometries," *IEEE 43rd Vehicular Technology Conference*, Secaucus NJ, vol. 1, pp. 227-230, May 1993.

[91] A.D. Kucar, "Mobile Radio: An Overview," *IEEE Communications Magazine*, pp. 72-85, Nov. 1991.

[92] T. Kurner, D.J. Cichon, and W. Wiesbeck, "Concepts and Results for 3-D Digital Terrain-Based Wave Propagation Models: An Overview," *IEEE Journal on Selected Areas in Communications*, vol. 11, no. 7, pp. 1002-1012, Sep. 1993.

[93] R.O. LaMaire, A. Krishna, P. Bhagwat, and J. Panian, "Wireless LANs and Mobile Networking: Standards and Future Directions," *IEEE Communications Magazines*, vol. 34, no. 8, pp. 86-94, Aug. 1996.

[94] G. Lampard and T. Vu-Dinh, "The Effect of Terrain on Radio Propagation in Urban Microcells," *IEEE Transactions on Vehicular Technology*, vol. 42, no. 3, pp. 314-317, Aug. 1993.

[95] J. Lansford, R. Nevo, and B. Monello, "Wi-Fi (802.11b) and Bluetooth Simultaneous Operation: Characterizing the Problem," white paper, www.mobilian.com, Hillsboro, OR, 2000.

[96] M.C. Lawton and J.P. McGeehan, "The Application of a Deterministic Ray Launching Algorithm for the Prediction of Radio Channel Characteristics in Small-Cell Environments," *IEEE Transactions on Vehicular Technology*, vol. 43, no. 4, pp. 955-969, Nov. 1994.

[97] M. Lebherz, W. Wiesbeck, and W. Krank, "A Versatile Wave Propagation Model for the VHF/UHF Range Considering Three-Dimensional Terrain," *IEEE Transactions on Antennas and Propagation*, vol. 40, no. 10, pp. 1121-1131, Oct. 1992.

[98] W.C.Y. Lee, "Elements of Cellular Mobile Radio Systems," *IEEE Transactions on Vehicular Technology*, vol. 35, no. 2, May 1986.

[99] W.C.Y. Lee, "Smaller Cells for Greater Performance," *IEEE Communications Magazine*, pp. 52-71, Nov. 1991.

[100] W.C.Y. Lee and D.J.Y. Lee, "Microcell Prediction by Street and Terrain Data", *IEEE Vehicular Technology Conference*, vol. 3, pp. 2167-2171, June 2000.

[101] B.A. Lewis and J.S. Robinson, "Triangulation of Planar Regions with Applications," *The Computer Journal*, vol. 21, no. 4, pp. 324-332, 1978.

[102] G. Liang and H.L. Bertoni, "A New Approach to 3-D Ray Tracing for Propagation Prediction in Cities," *IEEE Transactions on Antennas and Propagation*, vol. 46, pp. 853-863, June 1998.

[103] H. Ling, R.C. Chou, and S.W. Lee, "Shooting and Bouncing Rays: Calculating the RCS of an Arbitrary Shaped Cavity," *IEEE Transactions on Antennas and Propagation*, vol. 37, no. 2, pp. 194-205, Feb. 1989.

[104] W.J. Lipa et al, *Assessing Network Performance without Interference with Normal Network Operations*, US Patent 6,061,722, Patent and Trademark Office, Washington, D.C., 2000.

[105] M. Liron, *Method and Apparatus for Optimizing Computer Networks*, US Patent 5,598,532, to Optimal Networks, Patent and Trademark Office, Washington, D.C., 1998.

[106] A. Louzir, A. Aemamra, D. Harrison, and C. Howson, "Spatial Characterization of Single Room Indoor Propagation at 5.8 GHz," *IEEE Antennas and Propagation Society International Symposium Digest*, vol. 1, pp. 518-521, June 1995.

[107] R.J. Luebbers, "Finite Conductivity Uniform GTD Versus Knife Edge Diffraction in Prediction of Propagation Loss," *IEEE Transactions on Antennas and Propagation*, vol. 32, no. 1, pp. 70-76, Jan. 1984.

[108] R.J. Luebbers, "Propagation Prediction for Hilly Terrain Using GTD Wedge Diffraction," *IEEE Transactions on Antennas and Propagation*, vol. 32, no. 9, pp. 951-955, Sep 1984.

[109] R.J. Luebbers, W.A. Foose, and G. Reyner, "Comparison of GTD Propagation Model Wide-Band Path Loss Simulation with Measurements," *IEEE Transactions on Antennas and Propagation*, vol. 37, no. 4, pp. 499-505, April 1989.

[110] L.R. Maciel, H.L. Bertoni, and H.H. Xia, "Unified Approach to Prediction of Propagation Over Buildings for All Ranges of Base Station Antenna Height," *IEEE Transactions on Vehicular Technology*, vol. 42, no. 1, pp. 41-45, Feb. 1993.

[111] N. Maclinovsky, *Topographic Triangulation in Reduced Time*, U.S. Patent 6,075,541, to Trimble Navigation Ltd., Patent and Trademark Office, Washington, D.C. 2000.

[112] Y. Maeda, K. Takaya, and N. Kuwabara, "Experimental Investigation of Propagation Characteristics of 2.4 GHz ISM-Band Wireless LAN in Various Indoor Environments," *IEE Transactions in Communications*, vol. E82-B, no. 10, Oct. 1999.

[113] M. Makino, A. Ohsaki, S. Shinoda, and H. Shirai, "A Visual Simulation of Ray Propagation for Wireless Communication Systems," *IEEE TENCON 1999*, pp. 534-537, 1999.

[114] Mapinfo, *www.mapinfo.com*, Troy, New York, January 2002.

[115] Marconi, *www.marconi.com*, London, United Kingdom, January 2002.

[116] O. Markus, *Method and Apparatus for Planning a Cellular Radio Network by Creating a Model on a Digital Map Adding Properties and Optimizing Parameters, Based on Statistical Simulation Results*, US Patent 5,561,841, to Nokia Telecommunications, Patent and Trademark Office, Washington, D.C., 1996.

[117] H. Meng, P. Koushik, and T.S. Rappaport, "Comparative Study of Indoor and Outdoor Site-Specific Propagation Prediction Models," Tech. Rep. MPRG-TR-93-07, Virginia Tech, Feb. 1993.

[118] B. J. Menich et al, *Method and Apparatus for Mitigating Interference Produced by a Communication Unit in a Communication System*, US Patent 5,594,946, Patent and Trademark Office, Washington, D.C., 1997.

[119] A. Mirante and N. Weingarten, "Radial Sweep Algorithm for Constructing Triangular Irregular Networks," *IEEE Computer Graphics and Applications*, vol. 2, pp. 11-21, May 1983.

[120] R.D. Murch, J.H.M. Sau, and K.W. Cheung, "Improved Empirical Modeling for Indoor Propagation Predictions," *IEEE 45th Vehicular Technology Conference*, Chicago IL, pp. 439-443, July 1995.

[121] G. Nader, *Radio Link Performance of Third Generation (3G) Technologies for Wireless Networks*, master's thesis, Virginia Polytechnic Institute and State University, Blacksburg, VA, Bradley Department of Electrical and Computer Engineering, 2001.

[122] M.J. Neve and G.B. Rowe, "Mobile Radio Propagation Prediction in Irregular Cellular Topographies Using Ray Methods," *IEE Proceedings on Microwaves, Antennas, and Propagation*, vol. 142, no. 6, pp. 447-451, Dec. 1995.

[123] M. Nidd, S. Mann, and J. Black, "Using Ray Tracing for Site-Specific Indoor Radio Signal Strength Analysis," *IEEE 47th Vehicular Technology Conference*, Phoenix AZ, vol. 2, pp. 795-799, May 1997.

[124] P. Nobles, D. Ashworth, and F. Halsall, "Propagation Measurements in an Indoor Radio Environment at 2, 5, and 17 GHz," *IEE Colloquium on High Bit Rate UHF/SHF Channel Sounders – Technology and Measurements*, London UK, pp. 4//1-4//6, 1993.

[125] W.M. O'Brien, E.M. Kenny, and P.J. Cullen, "An Efficient Implementation of a Three-Dimensional Microcell Propagation Tool for Indoor and Outdoor Urban Environments," *IEEE Transactions on Vehicular Technology*, vol. 49, pp. 622-630, March 2000.

[126] M.A. Panjwani and A.L. Abbott, *An Interactive Site Modeling Tool for Estimating Coverage Regions for Wireless Communication Systems in Multifloored Indoor Environments*, master's thesis, Virginia Tech, Dept. Electrical and Computer Engineering, 1995.

[127] M.A. Panjwani, A.L. Abbott, and T.S. Rappaport, "Interactive Computation of Coverage Regions for Wireless Communications in Multifloored Indoor Environments," *IEEE Journal on Selected Areas in Communications*, vol. 14, no. 3, pp. 420-430, April 1996.

[128] L. Piazzi and H.L. Bertoni, "Effect of Terrain on Path Loss in Urban Environments for Wireless Applications," *IEEE Transactions on Antennas and Propagation*, vol. 46, pp. 1138-1147, Aug. 1998.

[129] L. Piazzi and H. L. Bertoni, "Achievable Accuracy of Site-Specific Path-Loss Predictions in Residential Environments," *IEEE Transactions on Vehicular Technology*, vol. 48, no. 3, May 1999.

[130] L. W. Pickering et al, *Cell Engineering Tool and Methods*, US Patent 5,491,644, to Georgia Tech Research Corporation, Patent and Trademark Office, Washington, D.C., 1996.

[131] M.F. Polis, and D.M. McKeown, Jr., "Iterative TIN Generation from Digital Elevation Models," *CVPR 1992*, pp. 787-790, 1992.

[132] A.R. Prasad, N.R. Prasad, A. Kamerman, H. Moelard, and A. Eikelenboom, "Indoor Wireless LANs Deployment," *IEEE 51st Vehicular Technology Conference Proceedings 2000*, Tokyo, Japan, vol. 2, pp. 1562-1566, 2000.

[133] N.R. Prasad, "IEEE 802.11 System Design," *IEEE International Conference on Personal Wireless Communications 2000*, pp. 490-494, 2000.

[134] C.S. Rajguru, *Applications of GIS in Propagation Predictions*, master's thesis, Virginia Polytechnic Institute and State University, Bradley Department of Electrical Engineering, Blacksburg, VA, 1992.

[135] T.S. Rappaport, "The Wireless Revolution," *IEEE Communications Magazine*, pp. 52-71, Nov. 1991.

[136] T. S. Rappaport and S. Sandhu, "Radio-Wave Propagation for Emerging Wireless Personal Communication Systems,", *IEEE Antennas and Propagation Magazine*, vol. 36, no. 5, Oct. 1994.

[137] T. S. Rappaport, M. P. Koushik, C. Carter, and M. Ahmed, "Radio Propagation Prediction Techniques and Computer-Aided Channel Modeling for Embedded Wireless Microsystems," MPRG Technical Report MPRG-TR-95-08, Virginia Tech, Blacksburg, VA, July 1995.

[138] T. S. Rappaport, M. P. Koushik, M. Ahmed, C. Carter, B. Newhall, and N. Zhang, "Use of Topographic Maps with Building Information to Determine Communication component Placements and GPS Satellite Coverage for Radio Detection and Tracking

in Urban Environments," MPRG Technical Report MPRG-TR-95-14, Virginia Tech, Blacksburg, VA, Sep. 1995.

[139] T.S. Rappaport et al, "Use of Topographic Maps with Building Information to Determine Antenna Placement for Radio Detection and Tracking in Urban Environments," MPRG Technical Report MPRG-TR-96-06, Virginia Tech, Blacksburg, VA, 1995.

[140] T.S. Rappaport, G.D. Durgin, and N. Patwari, "An Advanced 3-D Ray Launching Method for Wireless Propagation Prediction," *IEEE 47th Vehicular Technology Conference*, Phoenix AZ, vol. 2, pp. 785-789, May 1997.

[141] T.S. Rappaport, *Wireless Communications Principles and Practices*, Prentice Hall, Upper Saddle River, N.J., 2002.

[142] T.S. Rappaport, R.R. Skidmore, Method and system for managing a real time bill of materials, U.S. Patent No. 6,493,679, U.S. Patent and Trademark Office, Washington, D.C., 2002.

[143] T.S. Rappaport, R.R. Skidmore, Method and system for automated optimization of antenna positioning in 3-D, U.S. Patent No. 6,317,599, U.S. Patent and Trademark Office, Washington, D.C., 2001.

[144] T.S. Rappaport, R.R. Skidmore, System for the three-dimensional display of wireless communication system performance, U.S. Patent No. 6,499,006, U.S. Patent and Trademark Office, Washington, D.C., 2002.

[145] T.S. Rappaport, R.R. Skidmore, and P. Sheethalnath, Method and System for Modeling and Managing Terrain, Buildings, and Infrastructure, U.S. Patent Application Serial No. 20030023412, U.S. Patent and Trademark Office, Washington, D.C., 2001.

[146] T.S. Rappaport, R.R. Skidmore, and B. Henty, "Textual and Graphical Demarcation of Location, and Interpretation of Measurements," U.S. Patent Application Serial No. 20020077787, U.S. Patent and Trademark Office, Washington, D.C., 2002.

[147] T.S. Rappaport, R.R. Skidmore, "Method and System for Analysis, Design, and Optimization of Communication Networks," U.S. Patent Application Serial No. 20020006799, U.S. Patent and Trademark Office, Washington, D.C., 2002.

[148] D.O. Reudink, "Properties of Mobile Radio Propagation Above 400 MHz," *IEEE Transactions on Vehicular Technology*, Nov. 1974.

[149] K. Rizk, J.F. Wagen, and F. Gardiol, "Influence of Database Accuracy on Two-Dimensional Ray-Tracing Based Predictions in Urban Microcells," *IEEE Transactions on Vehicular Technology*, vol. 49, pp. 631-642, March 2000.

[150] Sage Research, "Wireless LAN Adoption: A Quantitative Analysis", Sage Research, Inc., *http://www.sageresearch.com*, Natick MA, June 2001.

[151] D. Salomon, *Computer Graphics & Geometric Modeling*, Springer NY, 1996.

[152] M.G. Sanchez, L. de Haro, A.G. Pino, and M. Calvo, "Exhaustive Ray Tracing Algorithm for Microcellular Propagation Prediction Models," *IEE Electronics Letters*, vol. 32, no. 7, pp. 624-625, March 1996.

[153] S. Sandhu, P. Koushik, and T. S. Rappaport, "Predicted Path Loss for Rosslyn, VA," MPRG Technical Report MPRG-TR-94-20, Virginia Tech, Blacksburg, VA, December 9, 1994.

[154] S. Sandhu, P. Koushik, and T. S. Rappaport , "Predicted Path Loss for Rosslyn, VA, Second set of predictions for ORD Project on Site Specific Propagation Prediction," MPRG Technical Report MPRG-TR-95-03, Virginia Tech, Blacksburg, VA, March 1995.

[155] K.R. Schaubach, N.J. Davis, and T.S. Rappaport, "A Ray Tracing Method for Predicting Path Loss and Delay Spread in Microcellular Environments," *IEEE 42nd Vehicular Technology Conference*, Denver Co, vol. 2, pp. 932-935, May 1992.

[156] S.Y. Seidel and T.S. Rappaport, "914 MHz Path Loss Prediction Models for Indoor Wireless Communications in Multifloored Buildings," *IEEE Transactions on Antennas and Propagation*, vol. 40, no. 2, pp. 207-217, Feb. 1992.

[157] S.Y. Seidel and T.S. Rappaport, "Site-Specific Propagation Prediction for Wireless In-Building Personal Communication System Design," *IEEE Transactions on Vehicular Technology*, vol. 43, no. 4, pp. 879-891, Nov. 1994.

[158] T. Sexton, *Channel Modeling and High Speed Data Transmission Preformance for the Indoor Radio Channel*, doctoral dissertation, Worcester Polytechnique Institute, Center for Wireless Information Network Studies, 1989.

[159] P. T. Sheethalnath, *Novel Site-Specific Techniques for Predicting Radio Wave Propagation*, master's thesis, Virginia Tech, Dept. of Electrical and Computer Engineering, Blacksburg, VA, 2001.

[160] H. D. Sherali, C. M. Pendyala, and T. S. Rappaport, "Optimal Location of Transmitters for Micro-Cellular Radio Communication System Design," *IEEE Journal on Selected Areas in Communications*, vol. 14, no. 4, May 1996.

[161] R. Shuh, "Comparing Active and Passive Solutions for Distributed Antenna Systems in a 3G Environment," *IIR In-Building Coverage 2001*, Marbella, Spain, June 2001.

[162] *SIRCIM®2001 for Windows 95/98/NT/2000 User's Manual*, Wireless Valley Communications, Inc., Blacksburg, VA 2001.

[163] *SitePlanner®2001 for Windows 95/98/NT/2000 User's Manual*, Wireless Valley Communications, Inc., Blacksburg, VA, 2001.

[164] R. R. Skidmore, T. S. Rappaport, and A. L. Abbott, "Interactive Coverage Region and System Design Simulation for Wireless Communication Systems in Multifloored Indoor Environments: SMT Plus," *IEEE International Conference on Universal Personal Communications*, vol. 2, pp. 646-650, 1996.

[165] R. R. Skidmore and T. S. Rappaport, *A Comprehensive In-Building and Microcellular Wireless Communications System Design Tool*, master's thesis, Virginia Tech, Dept. Electrical and Computer Engineering, Blacksburg, VA, 1997. Privacy protected and unpublished for three years by VTIP, Inc.

[166] R. R. Skidmore, "Relating Coverage Area and Throughput in Wireless Local Area Networks," final project report, ECPE 6504, available from the web, 2000.

[167] R. R. Skidmore and T.S. Rappaport, System for creating a computer model and measurement database of a wireless communication network, U.S. Patent No. 6,442,507, U.S. Patent and Trademark Office, Washington, D.C., 2002.

[168] *SMRCIM®2001 for Windows 95/98/NT/2000 User's Manual*, Wireless Valley Communications, Inc., Blacksburg, VA 2001.

[169] H. W. Son and N.H. Myung, "A Deterministic Ray Tube Method for Microcellular Wave Propagation Prediction Model," *IEEE Transactions on Antennas and Propagation*, vol. 47, no. 8, pp. 1344-1350, Aug. 1999.

[170] G. Stratis et al, *Method and Apparatus for Predicting Signal Characteristics in a Wireless Communication System*, US Patent 5,953,669, to Motorola, Inc., Patent and Trademark Office, Washington, D.C., 1999.

[171] W.L. Stutzman and G.A. Thiele, *Antenna Theory and Design*, Wiley, New York, 1981.

[172] W.K. Tam and V.N. Tran, "Multi-Ray Propagation Model for Indoor Wireless Communications," *IEE Electronics Letters*, vol. 32, no. 2, pp. 135-137, Jan. 1996.

[173] S.Y. Tan and H.S. Tan, "UTD Propagation Model in an Urban Street Scene for Microcellular Communications," *IEEE Transactions on Electromagnetic Compatibility*, vol. 35, no. 4, pp. 423-428, Nov. 1993.

[174] S.Y. Tan and H.S. Tan, "Propagation Model for Microcellular Communication Applied to Path Loss Measurement in Ottawa City Streets," *IEEE Transactions on Vehicular Technologies*, vol. 44, no. 2, pp. 313-316, May 1995.

[175] S.Y. Tan and H.S. Tan, "Improved Three-Dimensional Ray Tracing Technique for Microcellular Propagation Models," *IEE Electronic Letters*, vol. 31, no. 17, pp. 1503-1505, Aug. 1995.

[176] S.Y. Tan and H.S. Tan, "Modeling and Measurements of Channel Impulse Response for an Indoor Wireless Communication System," *IEE Proceedings on Microwave, Antennas, and Propagation*, vol. 142, no. 6, pp. 405-410, Oct. 1995.

[177] Y. Tang and J.D. Reed, *Method for Wireless Communication System Planning*, U.S. Patent 5,828,960, to Motorola, Inc., Patent and Trademark Office, Washington, D.C., 1998.

[178] W.J. Tanis II and G.J. Pilato, "Building Penetration Characteristics of 880 MHz and 1922 MHz Radio Waves," *IEEE 43rd Vehicular Technology Conference*, Secaucus NJ, pp. 206-209, May 1993.

[179] A.F. de Toledo and A.M.D. Turmani, "Propagation Into and Within Buildings at 900, 1800, and 2300 MHz," *IEEE 42nd Vehicular Technology Conference*, Denver CO, vol. 2, pp. 633-635, May 1992.

[180] D.L. Tonelli et al, *Computer Method for Updating a Network Design*, US Patent 5,821,937, Patent and Trademark Office, Washington, D.C., 1998.

[181] D.L. Tonelli et al, *Designing Networks*, US Patent 5,831,610, Patent and Trademark Office, Washington, D.C., 1998.

[182] *The United States Census 2000*, The U.S. Census Bureau, *http://www.census.gov*, Washington, D.C., January 2002.

[183] United States Geological Survey, *www.usgs.com*, Washington, D.C., January 2002.

[184] R.A. Valenzuela, "A Ray Tracing Approach to Predicting Indoor Wireless Transmission," *IEEE 43rd Vehicular Technology Conference*, Secaucus NJ, vol. 1, pp. 214-217, May 1993.

[185] IEEE Vehicular Technology Society Committee on Radio Propagation, "Coverage Prediction for Mobile Radio Systems Operating in the 800/900 MHz Frequency Range," *IEEE Transactions on Vehicular Technology*, vol. 37, no. 1, Feb. 1988.

[186] J. Walfish and H.L. Bertoni, "A Theoretical Model of UHF Propagation in Urban Environments," *IEEE Transactions on Antennas and Propagation*, vol. 36, pp. 1788-1796, 1998.

[187] E.H. Walker, "Penetration of Radio Signals into Buildings in the Cellular Radio Environment," *The Bell System Technical Journal*, vol. 62, no. 9, pp. 2719-2734, Nov. 1983.

[188] D.S. Watkins, *Fundamentals of Matrix Computations*, John Wiley & Sons, New York, 1991.

[189] M. Wittmann, J. Marti, and T. Kurner, "Impact of the Power Delay Profile Shape on the Bit Error Rate in Mobile Radio Systems," *IEEE Transactions on Vehicular Technology*, vol. 24, no. 2, pp. 329-339, May 1997.

[190] H. Xu, T.S. Rappaport, R.J. Boyle, and J.H. Schaffner, "Measurement and Models for 38-GHz Point-to-Multipoint Radiowave Propagation," *IEEE Journal on Selected Areas in Communications*, vol. 18, no. 3, pp. 310-321, March 2000.

Author's Biographical Sketch

Roger R. Skidmore was born on May 9, 1972 in Pennington Gap, Virginia. He received his B.S. degree in computer and electrical engineering from Virginia Tech in 1995. During the course of his undergraduate degree, he participated in the cooperative education program, spending three semesters working with Ericsson in Lynchburg, VA. From 1995 to the present, he has worked as a graduate research assistant for the Mobile and Portable Radio Research Group at Virginia Tech. He received his Master's degree in 1997, and shortly thereafter joined Wireless Valley Communications, Inc., as its first employee. He now serves as President of Wireless Valley, and pursued his doctoral degree at Virginia Tech through the support of the Wireless Valley Industrial Fellowship program. His research focuses on in-building and microcellular wireless communication systems, including wireless LAN, wireless PBX, and wireless local loops. He has co-authored in excess of thirty patents pending both domestically and internationally.